Role of the cancer-associated fibroblasts on the radiation response of solid tumors

Inaugural-Dissertation
zur
Erlangung des Doktorgrades

Dr. rer. nat.

der Fakultät für
Biologie

an der

Universität Duisburg-Essen

vorgelegt von

Alizée Steer
aus Le Havre, Frankreich

Februar 2019

Die der vorliegenden Arbeit zugrunde liegenden Experimente wurden am Institut für Zellbiologie (Tumorforschung) in der Abteilung für Molekular Zellbiologie am der Universitätklinikum Essen, der Universität Duisburg-Essen durchgeführt.

1. Gutachter: Prof. Verena Jendrossek
2. Gutachter: Prof. Jens Siveke

Vorsitzender des Prüfungsausschusses:

Tag der mündlichen Prüfung: 04. July 2019

DOI: 10.17185/duepublico/70276
URN: urn:nbn:de:hbz:464-20200805-074717-9

Presented work was conducted as part of the Innovative Training Network RADIATE. The RADIATE project has received funding from the European Union's Horizon 2020 Research and Innovation Program under the Marie Skłodowska-Curie grant agreement No. 642623.

« Many of life's failures are people who did not realize how close they were to success when they gave up », Thomas Edison

« *Nothing in life is to be feared, it is only to be understood. Now is the time to understand more, so that we may fear less* », Maria Skłodowska-Curie

Table of contents

I. SUMMARY

The heterogeneous tumor stroma can support therapy resistance at multiple levels. Critical components of the stroma are here the fibroblasts and in particularly cancer-associated fibroblasts (CAFs). The aim of the present study was to investigate if and how fibroblasts alter the radiation response of cancer cells. Therefore, a general approach was used where cells from different tumor types in combination with different fibroblasts were analyzed for their behavior upon radiation. The influence of the cells on each other (tumor promoting versus suppressing) was also analyzed *in vitro* and *in vivo.*

First, *in vitro* experiments aimed to determine the influence of fibroblasts on the tumor cell survival, cell death, and proliferation after irradiation using indirect (transwell) and direct cell co-culture (3D model) of different fibroblasts/cancer cells combinations. In indirect co-culture, paracrine signals from embryonic NIH-3T3 fibroblasts promoted MPR31.4 prostate cancer cell proliferation and clonogenic survival whereas it impaired the proliferation and favored cell death of B16F10 melanoma cancer cells after radiation. Moreover, paracrine signals from L929 skin fibroblasts induced higher levels of apoptosis in irradiated MPR31.4 cells, although these cells promoted proliferation and clonogenic survival of irradiated Py8119 cells. Direct and indirect co-culture of cancer cells and fibroblasts resulted in different effects depending on the respective cell sets used. NIH-3T3 co-cultured with MPR31.4 and L929 with Py8119 revealed a tumor-promoting and radio-resistance effect whereas L929 co-cultured with MPR31.4 and NIH-3T3 with B16F10 revealed a tumor-suppressive effect.

The results could be confirmed *in vivo.* Co-implantation of MPR31.4 cells and NIH-3T3 fibroblasts or Py8119 cells and L929 fibroblasts led to increased tumor growth and reduced radiation-induced tumor growth delay when compared to tumors without fibroblasts. In contrast, co-implantation of MPR31.4 cells with L929 fibroblasts had neither an effect on tumor growth nor radiation-induced tumor growth delay. NIH-3T3 induced MPR31.4 prostate cancer cell radio-resistance and L929 induced Py8119 breast cancer cell radio-resistance whereas L929 had no effect on MPR31.4 radiation response.

Thus, the impact of fibroblasts on cancer cell behavior and radiation response largely depends on the combinations of the respective cell types used as they either exert a pro-tumorigenic effect, an anti-tumorigenic effect or no effect. The plasticity of CAFs ranging from tumor stimulation/radio-resistance to tumor inhibition/radio-sensitivity, which is largely influenced by paracrine communications with the cancer cells, allows for such a broad spectrum of activities by the same fibroblast-type.

Das heterogene Tumorstroma kann die Therapieresistenz auf mehreren Ebenen unterstützen. Kritische Bestandteile des Stromas sind hier die Fibroblasten und insbesondere Tumor-assoziierte Fibroblasten (CAFs). Ziel der vorliegenden Studie war es zu untersuchen, ob und wie Fibroblasten die Strahlenantwort von Tumorzellen beeinflussen. Dafür wurde ein Screening-Ansatz verwendet, bei dem etablierte Zelllinien unterschiedlicher Tumorntitäten in Kombination mit verschiedenen Fibroblasten-Zelllinien hinsichtlich ihres Verhaltens nach Bestrahlung analysiert wurden. Der Einfluss der Zellen aufeinander (Tumor- bzw./ Radioresistenz-fördernde oder -hemmende Wirkung) wurde *in vitro* und *in vivo* analysiert.

Die In-vitro-Experimente zielten darauf ab, den Einfluss verschiedener Fibroblasten in indirekter (Transwell) bzw. direkter Zell-Co-Kultur (3D-Modell) auf das Überleben, die Proliferation und den Zelltod der Tumorzellen nach Bestrahlung in verschiedenen Kombinationen zu bestimmen. In der indirekten Co-Kultur förderten parakrine Signale von embryonalen NIH-3T3-Fibroblasten die Proliferation von MPR31.4-Prostatakrebszellen und das klonogene Überleben, während sie die Proliferation von B16F10-Melanomzellen beeinträchtigten und deren Zelltod nach Bestrahlung begünstigten. Darüber hinaus induzierten parakrine Signale von L929-Hautfibroblasten in bestrahlten MPR31.4-Zellen höhere Apoptosewerte, obwohl diese Zellen die Proliferation und das klonogene Überleben von bestrahlten Py8119-Zellen förderten. Die direkte Co-Kultur von Krebszellen und Fibroblasten führte ebenfalls zu unterschiedlichen Wirkungen, abhängig von den jeweiligen verwendeten Zellkombinationen. MPR31.4 in Kombination mit NIH-3T3 und Py8119 mit L929 zeigten eine überlebensfördernde Wirkung, während L929 in Ko-kultur mit MPR31.4 Zellen sowie NIH-3T3 mit B16F10, das Überleben der bestrahlten Tumorzellen verminderten.

Die Ergebnisse konnten *in vivo* bestätigt werden. Die Co-Implantation von MPR31.4-Zellen und NIH-3T3-Fibroblasten oder Py8119-Zellen und L929-Fibroblasten führte im Vergleich zu Tumoren ohne Fibroblasten zu erhöhtem Tumorwachstum und verringerter strahlungsinduzierter Tumorwachstumsverzögerung. Im Gegensatz dazu hatte die Co-Implantation von MPR31.4-Zellen mit L929-Fibroblasten weder Einfluss auf das Tumorwachstum noch die durch Strahlung verursachte Verzögerung des Tumorwachstums. NIH-3T3 steigerte die Radioresistenz von MPR31.4-Prostatakarzinomzellen und L929 die Radioresistenz von Py8119 Brustkrebszellen, während L929 keinen Einfluss auf die Strahlenantwort subkutaner Tumoren von MPR31.4-Zellen hatte.

Der Einfluss von Fibroblasten auf das Verhalten von Krebszellen und die Strahlenreaktion hängt von den Kombinationen der jeweils verwendeten Zelltypen ab, da diese entweder einen pro-tumorigenen bzw. resistenzfördernden Effekt, einen

antitumorigenen Effekt bzw. radiosensitivitätsfördernden oder keinen Effekt ausübten. Die Plastizität der CAFs erlaubt es Tumorzellen in Richtung Tumorwachstum / Radio-Resistenz bis zu Tumorhemmung / Strahlenempfindlichkeit zu beeinflussen, Diese Effekte werden weitgehend durch parakrine Kommunikation mit den Krebszellen vermittelt, die ein breites Spektrum an Aktivitäten durch denselben Fibroblasten-Typ ermöglicht.

Les résistances aux traitements antitumorals peuvent être soutenu par les cellules non cancéreuses hétérogènes du microenvironnement tumoral (TME) ou stroma à différents niveaux. Les composants critiques du stroma sont ici les fibroblastes et en particulier les fibroblastes associés au cancer (FACs). Le but de ce projet était d'étudier comment les fibroblastes influencent la réponse tumorale à la radiothérapie. Par conséquent, une approche générale a été utilisée. Différents types de cellules cancéreuses en présence de différents fibroblastes ont été analysées pour déterminer leur comportement après irradiation. L'influence des cellules les unes sur les autres (promotion versus suppression des cellules cancéreuses) a également été analysée *in vitro* et *in vivo*.

Premièrement, les expériences *in vitro* visaient à déterminer l'influence des fibroblastes sur la survie, la mort et la prolifération des cellules cancéreuses après radiation. La co-culture de différentes combinaisons de fibroblastes et de cellules cancéreuses a été établis de façon indirecte (transwell) et directe (modèle 3D). En co-culture indirecte, les signaux paracrines des fibroblastes embryonnaires, NIH-3T3 ont favorisé la prolifération et la survie clonogénique des cellules cancéreuses de la prostate, MPR31.4 (confirmé également en co-culture tri-dimensionnelle direct) bien qu'ils aient altéré la prolifération des cellules cancéreuses du mélanome, B16F10 et aient favorisé leurs morts après irradiation. De plus, les signaux paracrines des fibroblastes cutanés L929 ont induit une augmentation de l'apoptose des cellules MPR31.4 alors qu'ils ont favorisé la prolifération et la survie clonogénique des cellules cancéreuses du sein, Py8119 après irradiation. La co-culture de cellules cancéreuses et de fibroblastes a eu des effets différents selon l'origine et le type des cellules utilisés. La co-culture des fibroblastes NIH-3T3 avec les cellules MPR31.4 et des fibroblastes L929 avec les cellules Py8119 a révélé un effet promoteur de tumeur via induction de la résistance tumorale à la radiothérapie alors que les fibroblastes L929 co-cultivée avec les cellules MPR31.4 et les fibroblastes NIH-3T3 avec les cellules B16F10 a révélé un effet suppresseur de tumeur avec induction de sensitivité tumorale à la radiothérapie.

Ces résultats ont pu être confirmés *in vivo*. La co-implantation des cellules MPR31.4 avec les fibroblastes NIH-3T3 et des cellules Py8119 avec les fibroblastes L929 ont entraîné une croissance accrue de la tumeur et une réduction du retard de croissance de la tumeur induite par les radiations par rapport aux tumeurs implantées sans fibroblastes. En revanche, la co-implantation des cellules MPR31.4 avec les fibroblastes L929 n'a eu aucun effet sur la croissance tumorale ni sur le retard de croissance tumorale induite par les radiations. La radiorésistance des cellules cancéreuses de la prostate MPR31.4 est donc induite par les

fibroblastes NIH-3T3 et celles des cellules Py8119 par les fibroblastes L929 bien que les fibroblastes L929 n'ont pas d'effet sur la réponse tumorale des cellules MPR31.4 à la radiothérapie.

L'impact des fibroblastes sur la progression des cellules cancéreuses et la réponse tumorale à la radiothérapie dépend en grande partie des combinaisons des types de cellules respectifs utilisés, car elles exercent soit un effet pro-tumorigène, soit un effet anti-tumorigène ou aucun effet. La plasticité des FAC allant de la stimulation et radiorésistance tumorale à l'inhibition et radiosensibilité tumorale, est largement influencée par les communications paracrines avec les cellules cancéreuses. Cette plasticité permet un large spectre d'activités d'un même fibroblaste.

II. INTRODUCTION

A. Cancer incidence and mortality

Cancer is the second leading cause of death in the world[1]. According to the GLOBOCAN data base, 18.1 million new cancer cases and 9.6 million cancer death were estimated in 2018[2]. Cancer incidence and mortality are rapidly growing worldwide. Among the different cancer types lung, breast (female), colorectal and prostate (male) cancers explain one-third of cancer incidence and mortality worldwide and are the respective top 4 cancers in terms of incidence and within the top 8 in terms of mortality (Figure II.1).

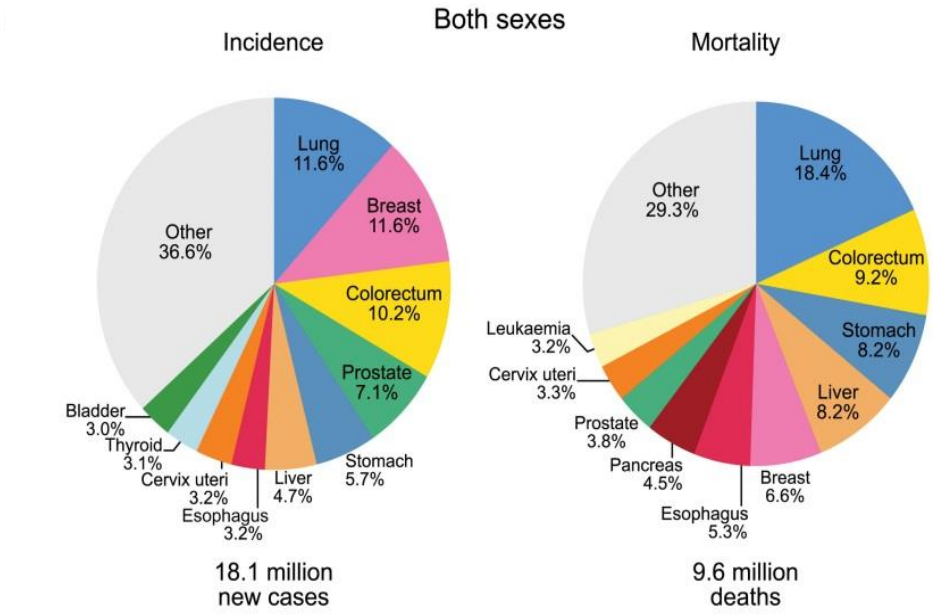

Figure II.1: **Distribution of cases and deaths for the 10 most common cancers in 2018 (both sex).** Worldwide in 2018, there were about 2.1 million newly diagnosed female breast cancer cases, accounting for almost 1 in 4 cancer cases among women. There were also almost 1.3 million new cases of prostate cancer and 359,000 associated deaths worldwide in 2018, ranking as the second most frequent cancer and the fifth leading cause of cancer death in men. Source: GLOBOCAN 2018[2].

These high numbers strongly recommend expanding cancer research aiming at a better understanding for the mechanisms underlying tumor development, aggressiveness, and therapy resistance.

B. Microenvironment

Genetic and cell-biology studies indicate that tumor growth is not just determined by malignant cancer cells themselves, but it is also supported by the tumor microenvironment, also termed tumor stroma[3]. Tumor cells do not act in isolation, but preferably survive in a rich microenvironment[3]. Under physiological conditions, the stroma is an important barrier to malignant transformation of cells. However, during neoplastic transformation the role of the stroma becomes changed with the potential to foster cancer cell invasiveness, progression, and potentially therapy resistance[4,5]. As the tumor evolves, the microenvironment progresses into an activated state by continuous paracrine tumor-stroma-cell communication which in turn synergistically supports and augments the tumor growth potential by creating a dynamic signaling exchange[6,7]. Many of the hallmarks of cancer as defined by Hanahan and Weinberg are provided or supported by various stromal components[3] (Figure II.2).

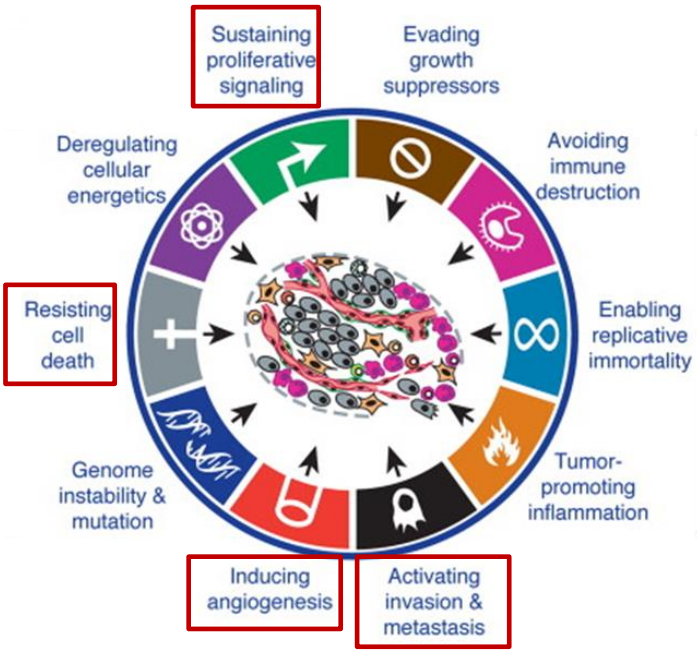

Figure II.2: **The Hallmarks of Cancer: Next generation,** the catalog of cancer cell capacities is a manifestation of ten essential alterations in cell physiology that collectively induce malignant growth[5].

1. Stromal composition

In solid tumors, the stroma includes various cells types. Apart from cancer cells, the tumor microenvironment contains cells of the immune system, the tumor vasculature (endothelial cells), fibroblasts, mesenchymal stem cells, as well as pericytes, sometimes adipocytes and non-cellular stroma, the extracellular matrix. (ECM) (Figure II.3).

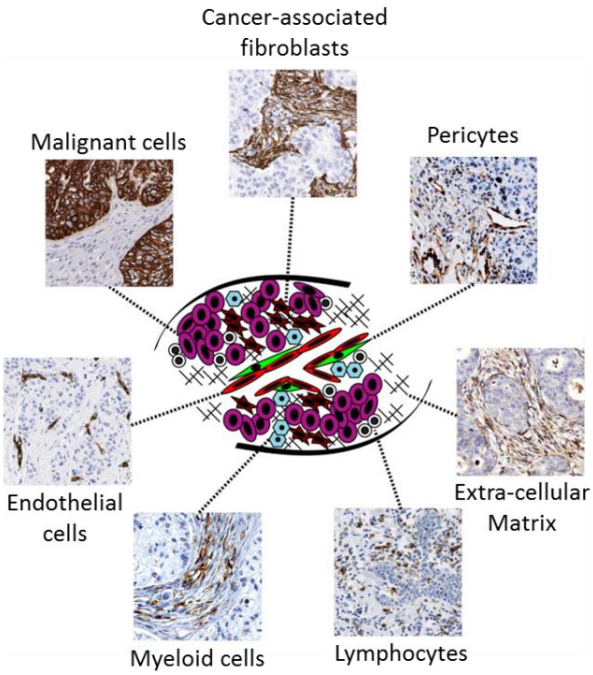

Figure II.3: **Stroma cells,** surrounded by immuno-histochemical pictures from breast carcinomas illustrating staining of representative markers for each compartment. The cancer-associated fibroblasts are shown with α-SMA staining, the pericytes with PDGF receptor-β staining, the extracellular matrix with collagen-1a1 staining, the lymphocytes with CD45 staining, the myeloid cells with CD11c staining, the endothelial cells with CD34 staining and to finish the malignant cells with cytokeratin 14 staining. Source: Hallmarks of cancer: Interactions with the tumor stroma[3].

Numerous immune cells can infiltrate tumor tissue and adopt tumor promoting or suppressing activities, which indicates a functional plasticity of stromal immune cells[8–10]. Pericytes, endothelial, smooth muscle cells and vessels provide nutrients and oxygen to the tumor by building up tumor blood vessels. Fibroblasts have been identified as one of the most active cell types of the tumor stroma[11–13]. In the microenvironment, fibroblasts are transformed into activated myofibroblasts, also termed cancer-associated fibroblasts (CAFs) through transforming growth factor beta (TGF-β) and interleukin (IL)-1 beta signaling[14,15]. CAFs were supposed to be the most important and most numerous cells in the stroma[12,16–18]. They are found in almost all solid cancers, but their relative abundance differs. Breast, prostate, and pancreatic cancers contain high numbers of CAFs, whereas brain, renal, and ovarian cancers were shown to contain less CAF numbers [19,20]. There is evidence that the interaction between the cancer cells and stromal cells of the microenvironment is bi-

directional and dynamic[21–24]. Neoplastic cells can secrete factors that recruit and activate stromal cells into the tumor microenvironment in a paracrine fashion. Stromal cells that have been recruited and activated can then release factors into the extracellular milieu that can stimulate or inhibit tumor growth.

Indeed, stromal cells provide signals to support tumor cell survival and tumor growth[3]. For example, CAFs were shown to express many factors such as hepatocyte growth factor (HGF), fibroblasts growth factor (FGF) or cytokines such as interleukin-6 (IL-6)[25] which -acting in isolation- are sufficient to induce transformation of epithelial cells[26]. In addition, part of the ability of tumor cells to evade programmed cell death is derived from survival signals supplied by the stromal compartment. For example, CAFs are known to produce insulin-like growth factors 1 and 2 (IGF-1 and 2)[27,28] which are known to pass on survival signals. Stromal cells also support angiogenesis. Major pro-angiogenic factors (e.g. VEGF, prostaglandin E2, (PGE2)) expressed within the tumor were shown to be produced principally by stromal cells[29]. For example, paracrine activation of PDFG-β receptor signaling in CAFs induces the expression of pro-angiogenic FGF-2 and the epithelial cell growth factor FGF-7[30]. Moreover, stromal cells are also involved in cancer cell invasion and metastasis. Indeed, CAFs contribute to this process by inducing epithelial-to-mesenchymal transition (EMT) of tumor cells e.g. through secretion of TGF-β and HGF[25]. In addition, CAFs remodel the extracellular matrix (ECM) by secreted proteases which lead to enhance tumor invasion and metastasis by cleaving the adhesion between tumor cells and adjacent cells or matrix[31].

2. Fibroblast transition: from healthy function to tumor stroma

Fibroblasts were first described in the late 19th century, based on their location and their microscopic appearance[32,33]. Fibroblasts are non-vascular, non-epithelial, and non-inflammatory cells, and are the principal cellular component of the connective tissue [34]. In a healthy context, fibroblasts are in an inactive quiescent state and can become activated during wound healing or fibrosis[35] (Figure II.4). Herein, fibroblasts can differentiate into contractile and secretory myofibroblasts that have a role in tissue repair and contribute to wound closure[36].

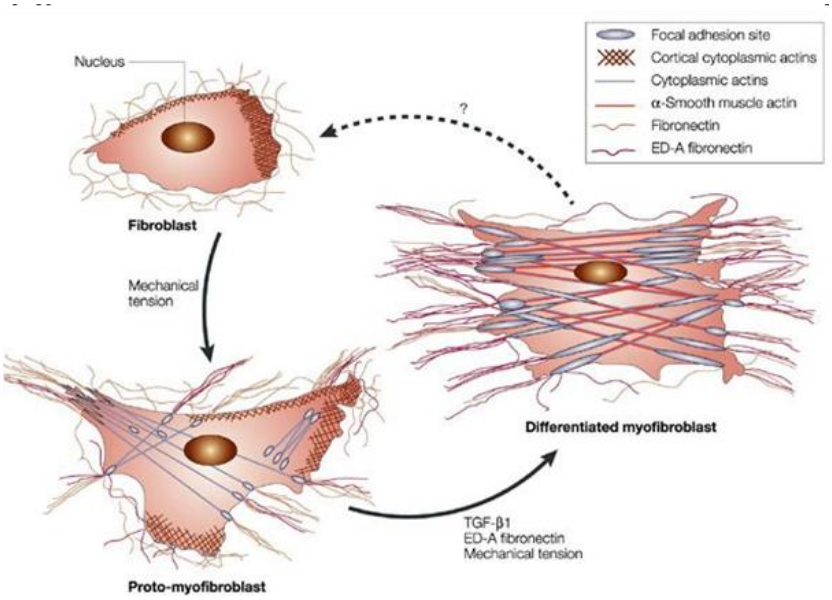

Figure II.4: **Model of myofibroblasts differentiation.** Quiescent fibroblasts don't show fiber stress or complexes adhesion with the ECM. But under mechanical stress, fibroblasts will differentiate into proto-myofibroblasts which form cytoplasmic stress fibers. Functionally, these cells can generate contractile force. Under TGF-β and fibronectin (ED-A) stimulation, in addition of mechanism stress, proto-myofibroblasts are modulated into differentiated myofibroblasts that are characterized by the expression of α-smooth muscle actin (α-SMA) and of a strong stress fibers development. Functionally, differentiated myofibroblasts generate greater contractile force than proto-myofibroblasts. Source: Tomasek and *al*, 2002[33]

After tissue damage, they can be activated by cytokines (TGF-β, IL-1) locally released from inflammatory and resident cells[37] or from malignant cells[10]. Fibroblasts can further migrate into the injured tissue and synthesize extracellular matrix components[38]. They can attract immune cells which participate in tissue homeostasis and contribute to ECM remodelling[39] (Figure II.5)[40].

In addition, fibroblasts can support and maintain the tissues' and organs' architecture[41].

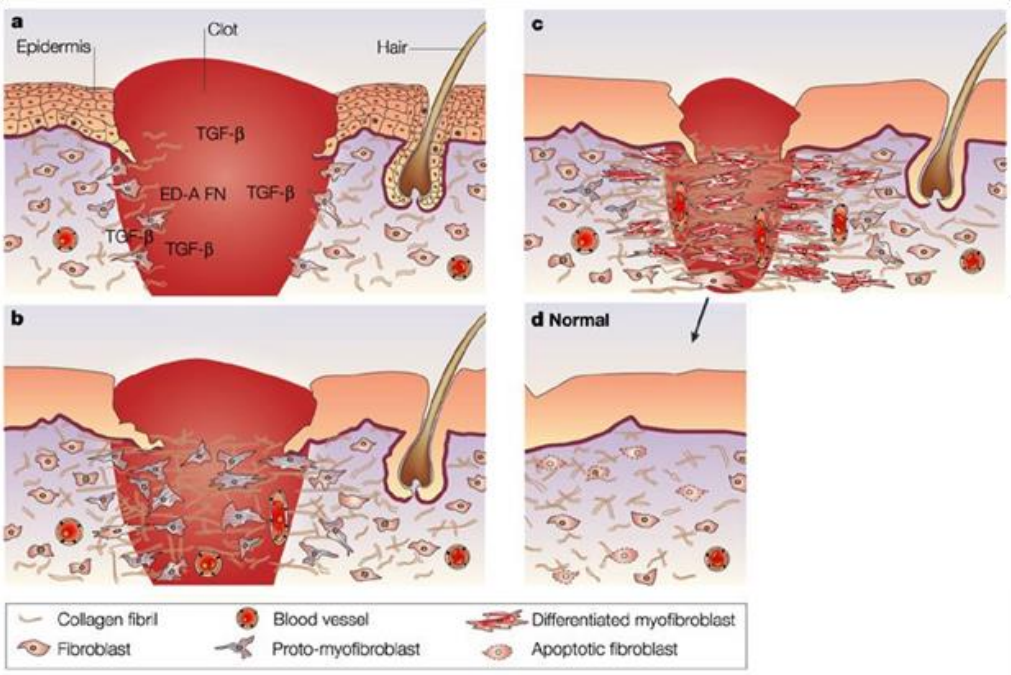

Figure II.5: **Model of the role of myofibroblasts during wound healing**. When a wound is filled by a fibrin clot, fibroblasts are stimulated to produce fibronectin extra-domain-A (ED-A) (a). They acquire the proto-myofibroblast phenotype. Proto-myofibroblasts are stimulated to secrete TGF-β1 and increased levels of fibronectin, ED-A (b). Proto-myofibroblasts become differentiated myofibroblasts by synthesizing α-SMA and increasing contractile force (c). When a healing wound closes, myofibroblasts disappear by apoptosis and a scar is formed (d) Source: adapted from Tomasek and *al*, 2002[33]

In tumors, cancer cells are able to hijack the normal function of fibroblasts. At the early stage, fibroblasts can prevent cancer progression by GAP junction between themselves[42,43]. GAP junctions are specialized intercellular connections. Fibroblasts form fibroblast-fibroblast connections and can physically prevent cancer progression (like three-dimensional network). Resident/normal fibroblasts can exert diverse suppressive functions against cancer initiation and progression via direct cell-cell contact, paracrine signaling by soluble factors (e.g. tumor necrosis factor α (TNFα), IL-6), and ECM stability[44]. Tumors are described as wounds that do not heal[45]. At later stages however, cancer cells reprogram and activate these cells towards CAFs[46]. Indeed, it is known since decades that TGF-β, produced by cancer cells, plays an important role in myofibroblast differentiation by regulating the expression of α-SMA which is an important constituent of CAFs[47,48].

C. Cancer–associated fibroblasts

At the tumor site, continuous exposition of fibroblasts with different stimuli promotes unique characteristics. Fibroblasts acquire excessive and specific secretory and ECM remodeling phenotypes, and thereby turn into CAFs. CAFs then can acquire an increased autocrine signaling ability and proliferative efficiency[44,49].

1. Stable genome

CAFs have stable karyotype and a lack of genetic alterations[50–53]. Thus, these cells are genetically stable and do not cause the disease. Their functions seem to depend on the presence of adjacent tumor cells[54]. Epigenetic modifications are required to switch normal fibroblasts into tumor invasion and growth-promoting CAFs[44,55]. Unlike wound healing, the fibroblasts in the tumor remain perpetually activated. Emerging data suggest that the irreversible activation of fibroblasts might be directed by epigenetic alterations[56–58].

2. Origin of CAFs

Even though, the resident fibroblasts are often admitted as the main source of CAFs[48], their low proliferative capacity challenges the model of local fibroblast activation as unique CAF-source. The origin of CAFs is manifold: CAFs were shown to be derived from different precursor cells: When a cancer appears in an organ, it includes the expansion of resident quiescent fibroblasts[59]. Nevertheless, CAFs can be recruited from another source such as the bone marrow with bone marrow-derived mesenchymal and hematopoietic stem cells[54,60,61]. Additionally, they might derive from other stromal cells as a result of trans-differentiation of pericytes, endothelial[62], epithelial cells[63] or adipocytes (Figure II.6).

For example, endothelial cells can suppress their CD31 expression and up-regulate the expression of fibroblast specific protein 1 (FSP-1) via the endothelial-mesenchymal transition (EndoMT) process. As explained in the paper of Dr. Zeisberg et *al.*, 2007[62], TGF-β can induce proliferating endothelial cells to undertake a phenotypic conversion into fibroblast-like cells. Such EndoMT is associated with the emergence of the mesenchymal marker FSP-1 and a down-regulation of CD31.

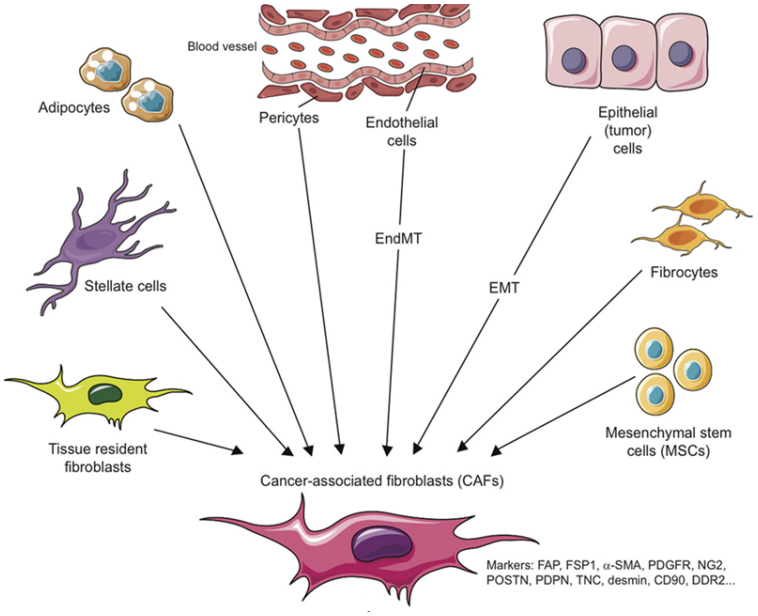

Figure II.6: **CAFs precursors.** CAFs can originate from diverse cell populations through different mechanisms and depending on the tissue analyzed. Source: adapted from Ziani, L., and *al*, 2018[56].

Likewise, epithelial cells can differentiate into fibroblasts-like phenotype via epithelial-mesenchymal transition (EMT) in inflammation and cancer[63]. Fibrocytes from the bone marrow can also be recruited and differentiate into myofibroblasts. However, due to the absence of specific fibroblast/CAF markers, the precise identification of their biological origin is difficult[64].

3. CAF Markers and heterogeneity

CAFs share several markers with other stromal cells, such as epithelial cells, endothelial cells, muscle cells, and mesenchymal stem cells[12,65]. Thus, the identification and characterization of a CAF phenotype remains challenging. Due to the lack of reliable and specific molecular fibroblast markers, detection of CAFs within the tumor requires combination of several markers. CAFs produce mesenchyme-specific proteins, illustrating their activation state, such as fibroblast activated protein (FAP), FSP-1, also known as S100A4), vimentin and alpha-smooth-muscle actin (α-SMA), all typical markers for myofibroblasts[65]. CAF also express receptors such as platelet-derived growth factor receptor β (PDGFRβ) that are involved in autocrine signaling loops. CAFs generate in addition a variety of matrix-components and matrix-remodeling enzymes such as the chondroitin sulfate proteoglycan NG2, (Neuron-Glial Antigen-2; NG2), tenascin C (TN-C), and fibronectin[66]. Moreover, those

markers are expressed differently from one CAFs to another (e.g. from different tissue) which indicates the existence of several sub-populations of CAFs, which are able to exert distinct tumorigenic effects[65].

4. CAF Functions

Fibroblasts and cancer cells communicate by paracrine signals and secretion of several signaling molecules like growth factors, chemokines and cytokines[67–69]. Vice-versa cytokines including TGF-β, PDGF, IL-4, IL-6 or again PGE have been reported to induce CAF differentiation[70,71] When tumor cells reroute fibroblasts into CAFs, interactions between CAFs and cancer cells were characterized as bi-directional and promote tumor growth, cancer invasion, angiogenesis and metastasis[72,73] (Figure II.7).

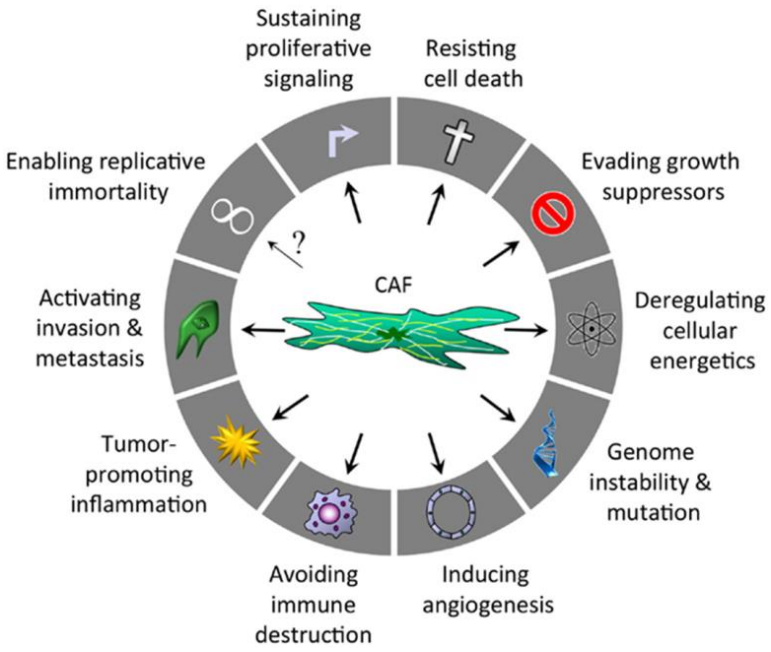

Figure II.7: **CAFs functions;** Hallmarks of cancer regulated by CAFs after Hanahan and Weinberg. E.g. Multiple CAF-derived factors maintain proliferative signaling, cell death resistance of cancer cells. Metabolic connection occurs between catabolic fibroblasts and anabolic cancer cells. CAFs fuel tumor growth through energy and biomass transfer. CAFs can also induce angiogenesis and avoid cancer cells immune destruction. Many of the hallmarks identified by Hanahan and Weiberg required for normal tissue to become cancerous are interconnected with the CAFs role and functions. Source: Tommelein, J. et al, 2015[65].

For example, Orimo et al shown that CAFs can promote tumor growth through their ability to secrete stromal cell-derived factor 1 (SDF-1)[67]. SDF-1

secreted by CAFs can act indirectly by recruiting endothelial progenitor cells to promote angiogenesis or by direct paracrine stimulation of cancer cells expressing the CXCR4 receptor. CAFs induce also tumor-promoting inflammation or immune suppression[45]. They can also remodel the extracellular matrix by secreting ECM components. These properties of CAFs support the malignant progression of tumors[54,74] (Figure II.7)[75].

D. Radiation and microenvironment

1. Importance of radiotherapy for cancer treatment

There are many types of cancer treatment: surgery, radiotherapy chemotherapy, immunotherapy, or targeted therapy, [76]. Nowadays, the majority of the patients will receive combinations of treatment to achieve best tumor control and quality of life[77]. Radiotherapy is recognized as an essential part of an effective cancer care procedure throughout the world, regardless of countries' economic status[78] (Figure II.8).

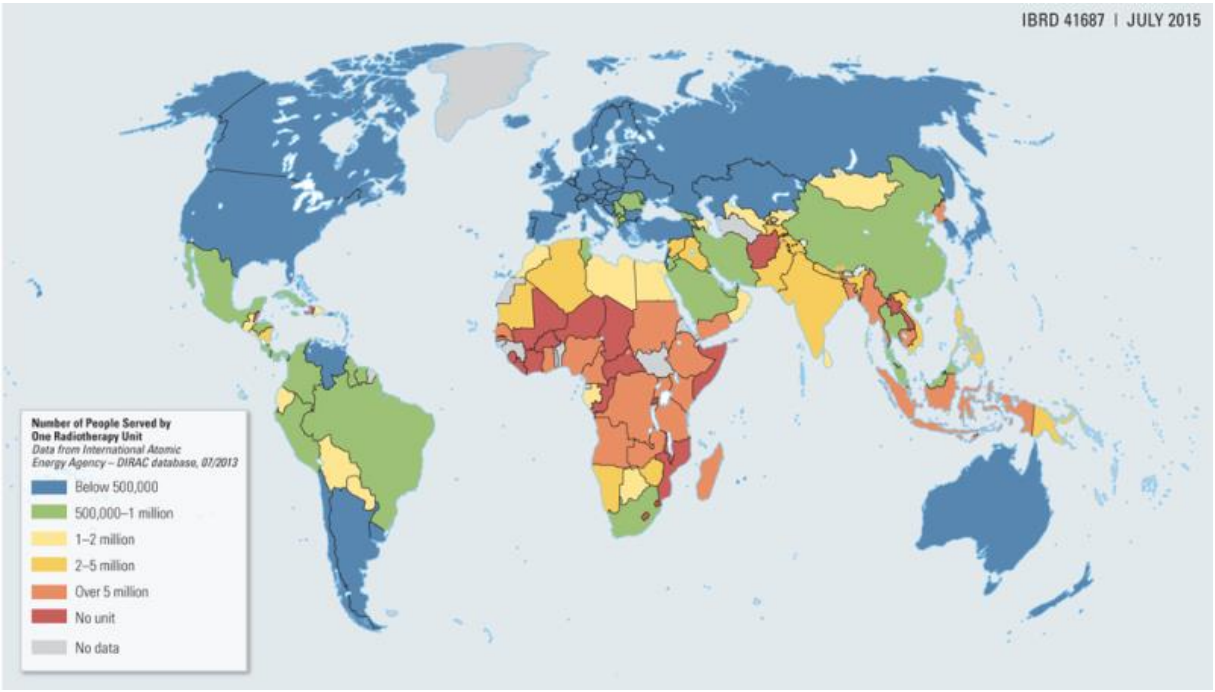

Figure II.8: **Number of People Served by One Radiotherapy Unit.** Source: Jaffray, D. A. & Gospodarowicz, M. K. Radiation Therapy for Cancer[68].

However, the global population's life expectancy is increasing. So cancer incidence rates are expected to expand[79]. Structural improvement of radiotherapy availability is one of the requirements to reduce cancer mortality

worldwide. The second requirements to reduce cancer related premature death is to explore more about the mechanisms of malignant transformation, tumor progression, and especially therapy resistance in order to improve treatment options. Indeed, today 50 to 60% of patients receive radiotherapy (RT) in their treatment schedules although radio-resistance still occurs.

2. Principle of radiation therapy

Radiation therapy works by damaging tumor cells' DNA. DNA damage is caused by photons (x or y-rays; discovered by Marie Skłodowska-Curie) or charged particles (e.g. protons, electrons…)[80].

If biological tissues absorb any form of radiation, there is a possibility that it will interact directly with critical targets in the cells such as proteins, RNA, DNA, enzymes. But the most biologic effects of radiation result principally from DNA damage through the indirect effect[81], through free radicals. Ionized water molecules in the cells produce free radicals that in turn bond with a DNA molecule, changing its structure. These free radicals can cause further damage to the cells resulting in a cellular stress response or cell death[80,82] (Figure II.9). Indeed, radiotherapy lead to create especially DNA double strand breaks which are much more difficult to repair for the cell[83]

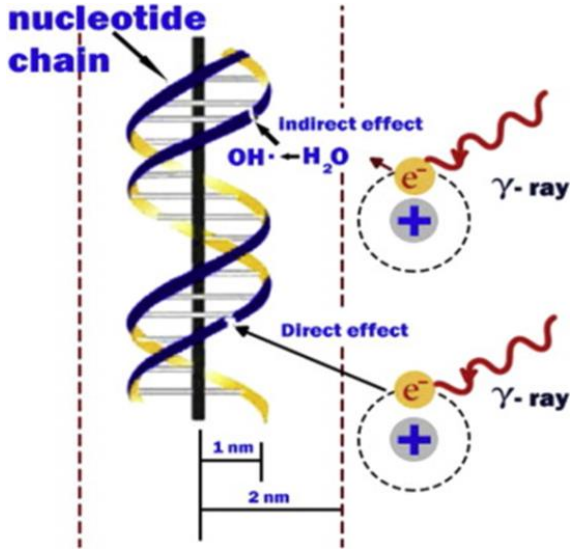

Figure II.9: **Direct and indirect actions of radiation**. (Modified from Hall & Giaccia, 2011) Source: Desouky, O and al. Targeted and non-targeted effects of ionizing radiation. J. Radiat. Res. Appl. Sci. 8, 247–254 (2015).

Cancer radiotherapy has two important aims: killing cancer cells while sparing normal tissues. The tolerance of most normal tissues to the toxic effects of ionizing radiation is higher than the sensitivity of the tumor cells[81]. In the normal tissue, cells proliferate not much and are highly differentiated. In contrast in tumors, cells are highly proliferative and less differentiated. Most healthy tissues bear generally more differentiated cells than tumors.

3. Microenvironment and radio-resistance

Over the past two decades, the radiobiologists view changed and recognized that the tumor microenvironment is of central importance for the radiotherapy response[84–86]. The clinical relevance of the tumor microenvironment in modulating the response of solid tumors to chemotherapy and radiotherapy has been documented[87–89].

Thus, the identification of molecules and pathways driving stroma-mediated resistance and more specifically CAFs-mediated resistance at advanced tumor stages may provide a molecular basis for the development of novel and effective strategies to target therapy resistance and improve treatment outcome[90,91]. Indeed, some studies tend to demonstrate the relevance of this type of investigation. For example, in the paper of Dr. Dauer et *al.*, inactivation of CAF via the inhibition of the TGF-β signaling pathway promoted regression of pancreatic cancer cells[91]. In addition, other studies investigated the role of an anti-fibroblast activation protein (FAP)-treatment to target stromal fibroblast function[92,93]. Previous work in our lab revealed that radiation resistance of prostate cancer cells can be linked to the membrane protein caveolin-1 (Cav1) in the stromal compartment. These observations suggested that some factors derived from the microenvironment may be involved in mediating radiation resistance whereas they were supposed to be tumor suppressive in the healthy situation. Though it had been shown that RT can promote the activation of fibroblasts in normal tissues and at the tumor margins towards a CAF-like phenotype and modulate the behavior of resident CAFs the role of fibroblasts/CAFs in modulating the response to radiotherapy required further definition.

E. Aim of the project

The impact of CAFs on the outcome of radiotherapy was still poorly understood. The central hypothesis of this work was that CAFs modulate the radiation response of tumors among others by altering the cancer cell phenotype as well as by modulating the tumor vasculature and/or tumor-promoting immune changes. Moreover, it was postulated that exposure to ionizing radiation might enhance the growth- and resistance-promoting properties of fibroblasts/CAFs.

Thus, the aims of the present PhD project were to determine and specify (1) if and how fibroblasts/CAFs modulate the radiation response of tumor cells from different tumor entities *in vitro* and *in vivo* and (2) to define how cancer cells impact the phenotype of stromal fibroblasts without and with irradiation (Figure II.10).

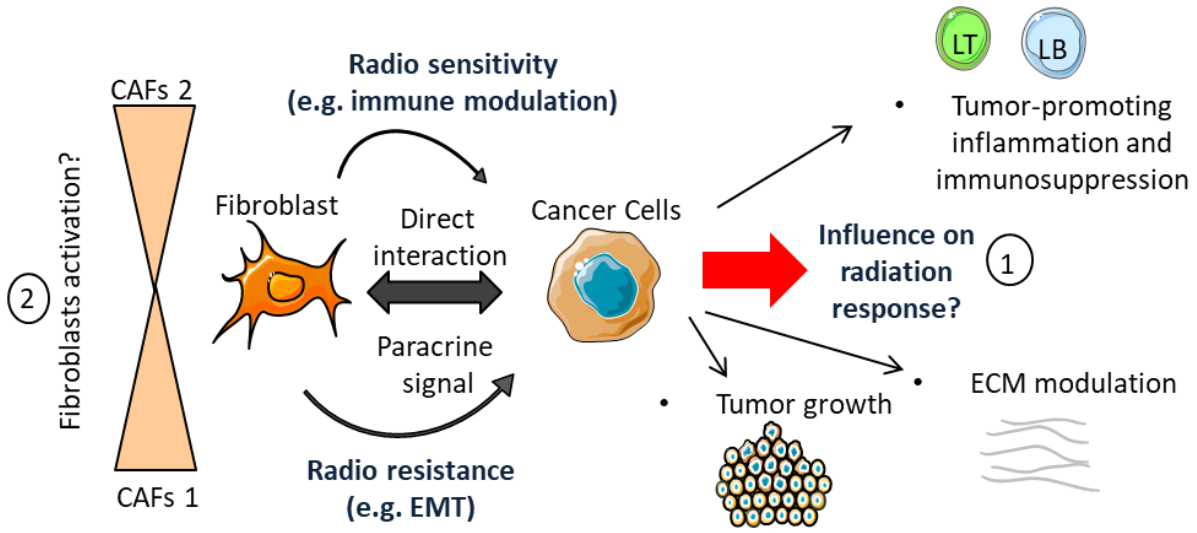

Figure II.10**: Hypothesis of the study**. CAFs modulate cancer radiation response by factors secretion, e.g. cytokines or growth factors. Depending on the type of signals, fibroblasts induce different cancer radiation responses either enhancing tumor radio-resistance (e.g. by inducing tumor EMT) or increasing tumor radio-sensitivity (e.g by modulating tumor immune infiltration). Vice-versa, cancer cells induce different fibroblast activation states with pro-tumorigenic, radiation resistance-promoting CAF1 and tumor-suppressive, radio-sensitivity-promoting CAF2 phenotypes being the two extreme activation states.

III. Materials and methods

A. Materials

1. Technical equipment

Table III.1: Applied technical equipment

Device	Manufacturer
-20°C freezer	Liebherr AG, Bulle, Switzerland
4°C Refrigerator	Liebherr AG, Bulle, Switzerland
-80°C Freezer **MDF**-U55V	Panasonic GmbH, Hamburg, Deutschland
ABI 7900HT Real-Time PCR System	Thermo Fisher Scientific
Biological irradiator X-RAD 320	Precision X-Ray
Centrifuge 5417 R	Eppendorf
Centrifuge Avanti JXN-26	Beckman Coulter, Brea, CA, USA
Centrifuge Jouan CR422	Thermo Scientific, Dreieich, Germany
Embedding station Shandon HistocentreTM	Thermo Scientific, Dreieich, Germany
Flow cytometer BD Accuri™ C6	Becton Dickinson Bioscience
Flow cytometers FACS CaliburTM	Becton Dickinson, Heidelberg, Germany
Fluorescence microscope Axio Observer Z1, ApoTome	Carl Zeiss, Jena, Germany
GelCount™ colony counter	Oxphord Optronix
Incubator C200	Labotect
Inverted light microscope Diavert	Ernst Leitz
Laminar-flow bench	BDK
Micro-plate shaker	Oehmen, Essen, Germany
AxioObserver.Z1 Inverted Microscope with ApoTome Optical Sectioning and a Live Cell Imaging System	Carl Zeiss, Jena, Germany
Microtome RM2235, water bath, flattening table	Leica, Wetzlar, Germany
Orbital shaker MTS 2/4	IKA-Werke
pH electrode edge®	Hanna Instruments
Photometer Nanodrop™ ND-1000	Thermo Fisher Scientific
Pipette controller ErgoOne® FAST	STARLAB
Pipette PIPETMAN® Classic	Gilson
RS 320 cabinet irradiator	XStrahl Limited
ThermoMixer® comfort	Eppendorf
Vortexer Reax 2000	Heidolph
Water bath	GFL

2. Consumables

Table III.2: Consumable material

item	Manufacturer
6-well plates	Eppendorf
96-well plates	TPP
Cell culture dishes	Sarstedt
Cell culture flasks	Sarstedt
Centrifuge tubes	Sarstedt
Combitips advanced®	Eppendorf
Cryo tubes	Sarstedt
Flow cytometry tubes	BD Falcon
Injection needles	Becton Dickinson Diagnostics
Pasteur pipettes	Brand
Pipette tips	Starlab
Plastic syringes	Becton Dickinson Diagnostics
qPCR seal	4titude
Reaction tubes	Sarstedt
Serological pipettes	Sarstedt
Barrier pen hydrophobic	Dako, Glostrup, Denmark
Coverslips	Engelbrecht, Edermuende, Germany
Disposable filters CellTrics (30, 50 µm)	Partec, Görlitz, Germany
Disposable scalpels	Mediware Servoprax, Wesel, Germany
Embedding cassettes	RotiLab Roth, Karlsruhe, Germany
Micropipettes	Gilson, Middleton, USA
Microscope slides	Engelbrecht, Edermuende, Germany
Microscope slides Superfrost Plus	R. Langenbrinck, Teningen, Germany
Objective slides	Engelbrecht, Edermuende, Germany
Surgical tools	B Braun, Melsungen, Germany
Millicell Hanging Cell Culture Insert, PET 0.4um, 6-well	Merck Millipore
0.45 µm filter	Sartorius

3. Kits

Table III.3: Utilized commercial kits

Kits	Manufacturer
Pierce™ BCA Protein Assay Kit	Thermo Fisher Scientific
qPCR MasterMix for SYBR® Green I	Eurogentec
QuantiTect® Reverse Transcription Kit	Qiagen
RNeasy® Mini Kit	Qiagen

4. General chemicals

Table III.4: Utilized chemicals

Chemical	Manufacturer
Acetic acid	Sigma-Aldrich
Ammonium chloride (NH4Cl)	Merck, Darmstadt, Germany
Bovine serum albumin (BSA)	Carl Roth
Coomassie brilliant blue	Sigma-Aldrich
Detection systems DAB+ chromogen DAB+ substrate buffer	Dako, Glostrup, Denmark
Dimethyl sulfoxide (DMSO)	Dimethyl sulfoxide (DMSO)
Ethanol	Carl Roth
Ethylendiaminetetraacetic acid (EDTA)	Sigma-Aldrich
Formaldehyde	Sigma-Aldrich
Glycerol	Carl Roth
Glycine	Merck Millipore
Isoflurane	Sigma-Aldrich
Paraformaldehyde	Sigma-Aldrich
Phenylmethanesulfonyl fluoride	Sigma-Aldrich
Propidium iodide (PI)	Carl Roth
Sodium chloride (NaCl)	Merck Millipore
Sodium citrate	Carl Roth
Sodium fluoride	Sigma-Aldrich
Sodium orthovanadate	Sigma-Aldrich
Sodium pyrophosphate	Sigma-Aldrich
Tris(hydroxymethyl)aminomethane (Tris)	Carl Roth
Triton X-100	Sigma-Aldrich
β-mercaptoathanol	Merck Millipore

5. Media, reagents and commercial buffers

Table III.5: Utilized media, reagents, and commercial buffers

Medium/Reagent/Buffer	Manufacturer
Agarose, BioReagent, for molecular biology, low EEO	Sigma-Aldrich, A9539-50G
Cell culture media DMEM RPMI 1640	Gibco, Karlsruhe, Germany
Fetal calf serum (FCS)	Biochrom AG, Berlin, Germany
Hoechst 33342	Thermo Fisher Scientific
Matrigel® Matrix (HC)	Corning
Opti-MEM™	Gibco Thermo Fisher
Page Ruler™ Pre-Stained Protein Ladder	Fermentas
Phosphate Buffered Saline (PBS)	Gibco
Trypsin-EDTA (0.05 %)	Biochrom AG, Berlin, Germany
G418 (Geneticin)	Biochrom AG, Berlin, Germany
Penicillin/Streptomycin100x (Pen/Strep)	Biochrom AG, Berlin, Germany
Eosin G	Roth, Karlsruhe, Germany
Masson-Goldner-Trichrome kit	Roth, Karlsruhe, Germany
Mayer´s hematoxylin	Roth, Karlsruhe, Germany
Mounting medium Roti Histokitt II	Roth, Karlsruhe, Germany

6. Buffers and solutions

Table III.6: Composition of staining solutions for flow cytometric analyses and cell survival assays

Staining solution	Component	Amount/Concentration
Coomassie brilliant blue staining solution	Coomassie brilliant blue Methanol Acetic acid	0.05 % (w/v) 20 % (v/v) 7.5 % (v/v)
Nicoletti	Sodium citrate Triton X-100 Propidium iodide *in PBS*	0.1 % (w/v) 0.1 % (v/v) 50 µg/mL
PI exclusion	Propidium iodide *in complete medium*	10 µg/mL

7. Antibodies

Table III.7: Antibodies applied for ImmunoHistology

Antibody	Origin	Dilution	Manufacturer
Alpha Smooth Muscle isoform	Mouse	1/50	Millipore, CBL171
Anti-mouse (HRP-conjugated)	Goat	1/500	Cell Signaling Technologies
Anti-rat IgGHRP linked	Goat	1/500	Novex/Thermo fischer, A18865

PCNA	Mouse	1/500	Genetex, GTX20029
Purified anti-mouse CD45	Rat	1/100	Biolegend, 103101

8. qRT-PCR Primers

All primers were produced by Metabion.

Table III.8: qRT-PCR mouse primer sequences

Primer		Sequence (5'-3')
pdgfr-β	Forward	CCTGTGCAGTTGCCTTACGA
pdgfr-β	Reverse	TCTCGCTACTTCTGGCTGTC
ng2/Cspg4 pair 2	Forward	GCTGTGCGTCGTTTGAGTTT
ng2/Cspg4 pair 2	Reverse	CAACAAACAGCCCATCTGCC
α-sma	Forward	ACGGCCGCCTCCTCTTCCTC
α-sma	Reverse	GCCCAGCTTCGTCGTATTCC
tgf-β	Forward	GAACCAAGGAGACGGAATACAG
tgf-β	Reverse	AACCCAGGTCCTTCCTAAAGTC
snai-1	Forward	TCAACTGCAAATATTGTAACAAGGA
snai-1	Reverse	CTGGCACTGGTATCTCTTCACA
snai-2	Forward	TCCTTCCTGGTCAAGAAACATT
snai-2	Reverse	TGTGATCCTTGGATGAAGTGTC
β-actin	Forward	CCAGAGCAAGAGAGGTATCC
β-actin	Reverse	CTGTGGTGGTGAAGCTGTAG

9. Eucaryotic cell lines

The mouse prostate epithelial cell line MPR31.4 was a kind gift of TC Thompson, Scott (Department of Urology, Baylor College of Medicine, Houston, USA)[94,95]. The mouse breast cancer cell line Py8119, the melanoma cell line B16F10, the prostate cancer cell line TrampC1, and the skin and embryonic fibroblasts cell lines L929, NIH-3T3 were purchased from ATCC (Manassas, VA).

10. Software and tools

Table III.9: Applied software and tools

Software	Manufacturer
BD Accuri™ C6	Becton Dickinson Biosciences
GelCount™ 1.4	Oxford Optronix
GraphPad Prism 6	GraphPad Software
Primer-BLAST	National Center for Biotechnology Information (NCBI)

SDS 2.2	Thermo Fisher Scientific
SparkControl™	Tecan Trading
CellQuestTM	Becton Dickinson, Heidelberg, Deutschland
ZEN lite	Carl Zeiss AG, Oberkochen, Deutschland
AxioVision	Carl Zeiss AG, Oberkochen, Deutschland
FlowJo®	Flow Jo
TotalLab Quant	TotalLab, Newcastle, USA
ImageJ	Wayne Rasband, NIH, Bethesda, MD, USA

B. Methods

1. Indirect (transwell) co-culture

Cancer cells were plated in 6 wells plates ensuring that after 72h the cells were not over-confluent. Transwells were added on the top of the cancer cells and fibroblasts were plated into the transwell either at the same cell concentration (ratio 1/1) or two times more (ratio 1/2).

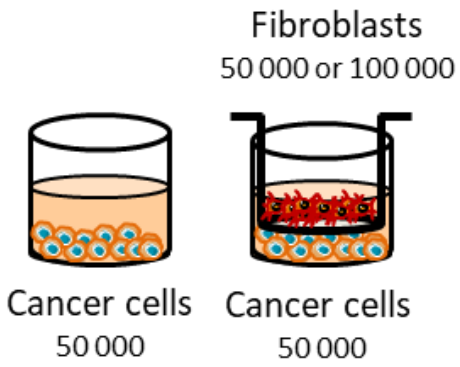

Figure III.1: Scheme of indirect co-culture set up between fibroblasts and cancer cells through a transwell.

2. Irradiation of cell cultures

Radiation with indicated doses (0–10 Gray (Gy)) was performed using the Isovolt-320-X-ray machine (Seifert–Pantak, East Haven, CT) at 320 kV, 10 mA with a 1.65-mm aluminum filter, and a distance of about 500 mm to the object being irradiated[96]. The effective photon energy was about 90 kV, and the dose rate about 3Gy/min.

3. Cell viability assay/proliferation

The number of living cells, dead cells and total cells were determined upon staining of the cells with the vital dye trypan blue. For this, cells were harvested with Trypsin-

EDTA, re-suspended in fresh medium, diluted with trypan blue, and counted employing a Neubauer chamber.

4. Scratch assay/migration

Cells' migration was observed by time-lapse microscopy for 72h after IR. Therefore, cells were grown to confluence, irradiated, and a thin wound was introduced by scratching with a 10 µl pipette tip. Wound closure was determined upon the different treatments by measuring the migration distance at different time points after scratching using ImageJ 1.47t (Wayne Rasband, National Institutes of Health, US states).

5. Flow cytometry cell death/proliferation (propidium iodide staining)

For quantification of apoptotic DNA-fragmentation (sub-G1 population), cells were incubated for 15–30 min with a staining solution containing 0.1% (w/v) sodium citrate, 50µg/ml PI, and 0.05% (v/v) Triton X-100 (v/v) and subsequently analyzed by flow cytometry (FACS Calibur, Becton Dickinson, Heidelberg, Germany; FL-2)[97].

6. Colony formation assay 2D

Clonogenic cell survival was tested in response to ionizing radiation with radiation doses between 0 Gy (control) and 10Gy. Exponentially grown cancer cells were seeded in 6-well plates and fibroblasts in transwell chambers. Cells were irradiated 24 h after seeding (5, 7.5, 10Gy) and further incubated under standard culturing conditions. Plates were incubated for a total of 7 days to allow growth of single colonies. For determination of colony formation cells were fixed in 3.7% formaldehyde and 70% ethanol, stained with 0.05% Coomassie Brillant blue. Colonies of at least 50 cells were counted.

7. qPCR/primer

RNA was reverse transcribed with the QuantiTect Reverse Transcription Kit (Qiagen), and quantitative PCR (qPCR) was carried out using specific oligonucleotide primers: β-actin (Actβ), PDGRFβ/ CD140b, NG2/Cspg4, α-SMA/ACTA2, Snai1, Snai2, TGF-β using qPCR Master Mix for SYBR Assay Rox (Eurogentec, Cologne, Germany)

according to the manufacturer's instructions. Gene expression levels were normalized to β-actin.

8. Generation of labeled cells

Transfection mixtures containing plasmid pEGFP-N1 (Addgene) or pTagRFP-N (Evrogen) (figure II.2) (kindly obtain from the lab of Nils Cordes) and lipofectamine in OptiMEM were incubated 1h at 37°C on MPR31.4, Py8119 and NIH-3T3 cells. Then, the cells were sorted by flow cytometry and selected with G418 antibiotics.

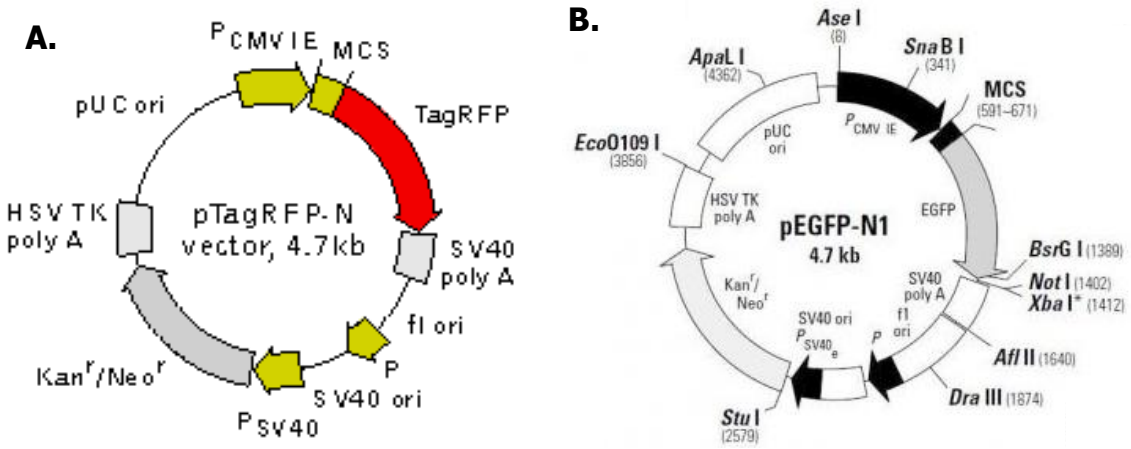

Figure III.2: **Plasmid vectors map A.** pTagRFP-N vector map encoding red fluorescence protein tagRFP. The vector allowed TagRFP expression alone in mammalian cells. pTagRFP-N vector encodes for neomycin (G418) for eukaryotic selection. **B.** pEGFP-N1 vector map encoding green fluorescence protein GFPmut1 variant. The vector allowed GFP expression alone in mammalian cells. pEGFP-N1 vector encodes for neomycin (G418) for eukaryotic selection.

9. 3D colony formation assay

Measurement of 3D cell survival was accomplished as reported before. In brief, single cancer cells alone or with fibroblasts were co-plated into a mixture of 1 mg/ml high concentration extracellular matrix (Corning® Matrigel® Basement Membrane Matrix High Concentration (HC), *LDEV-free, Product Number 354248) in 96-well plates. The cells were irradiated (0, 3, 6 and 9Gy) 24h after seeding and colonies (>50 cells) were microscopically counted 7 days after IR (2.5 magnification). In addition, colonies picture were taken by fluorescence microscopy (RFP, GFP, bright light) at 10 magnifications to determine the composition of the colonies[98].

10. Mouse tumor model

C57BL/6 wild-type (WT) mice were bred and housed under specific-pathogen-free conditions in the animal facilities laboratory of the University Hospital Essen. Food and drinking water were provided ad libitum. All protocols were approved by the universities' animal protection boards in conjunction with the legal authority (LANUV Düsseldorf) according to German animal welfare regulations and by the Committee on the Ethics of Animal Experiments of the responsible authorities [Landesamt für Natur, Umwelt und Verbraucherschutz (LANUV), Regierungspräsidium Düsseldorf Az.84-02.04.2014.A244; Az.84-02.04.2015.A586; Az.81-02.04.2018.A158; Az. 81-02.04.2018.A267]. Mouse xenograft tumors were generated by subcutaneous injection of 0.25 x 10^6 or 0.125 x 10^6 cancer cells (MPR31.4 or Py8119) either alone or mixed with 0.25 x 10^6 or 0.125 x 10^6 fibroblasts cells (NIH-3T3 or L929) into the hind limb of mice (total volume 50 µl) as previously described[96]. Up to 20 animals of each experimental group received a single subcutaneous injection of 0.5 x 10^6 or 0.25 x 10^6 viable cells.

11. Tumor irradiation

Mice were anesthetized with 2% isoflurane and irradiated in 0.8% isoflurane with either a single dose of 0Gy (sham control treatment) or with 10Gy ±5% in 5mm tissue depth (~1.53Gy/min, 300kV, filter: 0.5mm Cu, 10mA, focus distance: 60cm) using a collimated beam with a XStrahl RS 320 cabinet irradiator (XStrahl Limited, Camberly, Surrey, Great Britain)[99]. Mice were humanely sacrificed with CO_2 inhalation at indicated time points, and tumor tissue was isolated for respective downstream analysis.

12. Preparation of tumor for paraffin sections and cryosections

Tumors were fixed overnight at 4°C in 4% PFA in PBS, pH 7.2 and placed in embedding cassettes. After, dehydration in 70% ethanol, PFA-fixed tumors were processed using automated standard procedures and subsequently embedded in paraffin. Five µm tissues sections obtained with Leica microtome were mounted on coated microscope slides.

13. Immunohistochemistry

Paraffin-embedded tissue sections were hydrated using a descending alcohol series, incubated for 10–20 min in target retrieval solution (Dako, Glostrup, Denmark) and incubated with blocking solution (2% fetal calf serum/phosphate-buffered saline). After permeabilization, sections were incubated with primary antibodies over night at 4°C. Antigen was detected with a peroxidase-conjugated secondary antibody (1/250) and DAB staining (Dako). Nuclei were counterstained using hematoxylin.

14. Hematoxylin and eosin staining

Tumor sections were stained with hematoxylin and eosin (H&E). H&E is commonly used for identification of tissue structures. Hematoxylin stains cell nuclei purplish blue. Eosin stains cytoplasmic proteins and connective tissue fibers in different shades of pink and red. Paraffin-embedded tissue sections were hydrated using a descending alcohol series, stained 5 minutes in Mayer's hematoxylin and 3 minutes in 0.5% eosin G.

15. Masson Goldner Trichrome

Tumor sections were stained with Masson Goldner Trichrome (TC; Carl Roth Karlsruhe). TC is commonly used to selectively identify connective tissue, muscle and collagen fibers. Paraffin-embedded tissue sections were hydrated using a descending alcohol series subsequently stained for 5 minutes in a 1:1 solution of Weigert's hematoxylin components A and B. The slides were then stained with the solutions Goldner I (ponceau – acid fuchsin), Goldner II (phosphotungstic – orange) and Goldner III (light green), alternating the staining steps with 30 seconds washes in 1% acetic acid solution to remove the stain in excess.

16. Statistical Analysis

If not otherwise indicated, data were obtained from 3 independent experiments with at least 5 mice each. Statistical significance was evaluated by 1-way ANOVA followed by Tukey's comparisons post-test and set at the level of $p \leq 0.05$. Data analysis was performed with Prism 5.0 software (GraphPad, La Jolla, California).

IV. RESULTS

To investigate whether fibroblasts and more specifically CAFs modulate the radiation response of malignant tumors, different types of cancer cells and fibroblasts were used in this study (Table IV.1). Fibroblasts and cancer cells from different tissue's origins were selected with regard to the knowledge that breast, and prostate tumors contain a high number of CAFs and skin a high number of fibroblasts.

Name	Cell lines	Origin
MPR 31.4	Bone metastasis of adenocarcinoma	Prostate epithelial
Py8119	Adenocarcinoma	Mammary gland
B16F10	Melanoma	Skin
TrampC1	Adenocarcinoma	Prostate epithelial
NIH 3T3	Fibroblast	Embryo
L929	Fibroblast	Subcutaneous connective tissues

Table IV.1: **Name and origin of the different cell lines used.**

The different fibroblast-tumor cell combinations investigated in the present thesis revealed differences in the tumor radiation response. The impact of fibroblasts on tumor cells radiation response largely depended on the fibroblast and tumor cell type. Fibroblasts exerted either a tumor-suppressing effect or tumor-promoting effect. Therefore, the results were presented distinctly depending on the effect observed on the tumor.

A. Fibroblasts exert tumor-suppressing effects

1. Fibroblasts increased cancer cell death after radiation in short-term assays via a paracrine mechanism of action.

In order to gain insight into the effect of fibroblasts on the cancer cell radiation response, in vitro experiments with different sets of cancer cells (here MPR31.4 and B16F10) and fibroblasts (L929 and NIH-3T3) were performed. First, cancer cells and fibroblasts were co-cultured in a self-established indirect co-culture system (Transwell) to investigate the influence of factors secreted by the fibroblasts on the respective cancer cells. Cancer cell proliferation and apoptosis were measured

after 72h of fibroblasts-cancer cell co-culture in a ratio of one to one (Figure IV.1A, 1E).

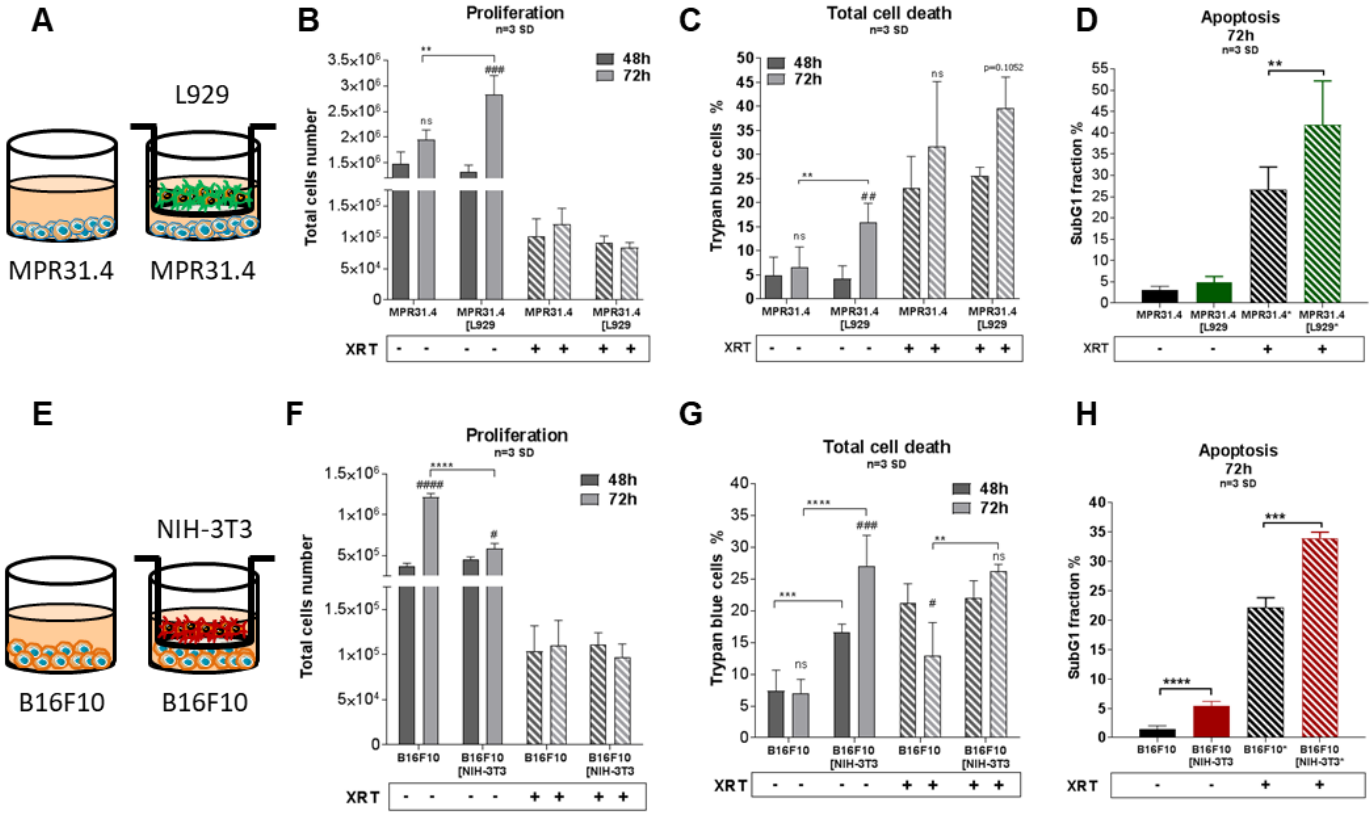

Figure IV.1: **Stromal fibroblasts were able to induce an increase of prostate and melanoma cancer cell death while cell proliferation was not affected after radiation.** MPR31.4 or B16F10 cancer cells alone or together with stromal fibroblasts (in indirect co-culture) were cultured for 24h prior irradiation with 0 or 10Gy (ratio 1-1, **A-E**). After 48h and 72h, total cell numbers as well as dead cells were counted by trypan blue (**B-F, C-G)**. "ns" present for no significant, **p<0.01, *** p<0.001 and ****p<0.0001, analyzed by two-way ANOVA test followed by Tukey's test, compared cancer cells with fibroblasts to cancer cells cultured alone. "ns" present for no significant, $^{\#}$p<0.5, $^{\#\#}$p<0.01, $^{\#\#\#}$p<0.001 and $^{\#\#\#\#}$p<0.0001 analyzed by two-way ANOVA test followed by Tukey's test, compared 72h to 48h. SubG1 fractions were measured by Nicoletti staining[85], 72h after irradiation **(D-H).** **p<0.01, *** p<0.001 and ****p<0.0001 analyzed by one-way ANOVA test followed by Tukey's test.

In the indirect co-culture, L929 fibroblasts-derived signals increased the proliferation of MPR31.4 prostate cancer cells, as they were able to enhance the number of total cancer cells from 1.3±0.1 x10^6 cells at 48h to 2.8±0.4 x10^6 total cells at 72h whereas under control conditions, no increase in cell numbers could be observed (Figure IV.1B). Instead NIH-3T3 fibroblasts-derived signals induced a

decrease of B16F10 melanoma total cell numbers at 72h, from 1.2±0.4 $x10^6$ cells in control condition to 0.6±0.06 $x10^6$ cells when indirectly co-cultured with NIH-3T3 fibroblasts (Figure IV.1F).

As expected, cancer cell proliferation decreased after radiation, only 1.21±0.25 $x10^5$ and 1.10±0.28 $x10^5$ MPR31.4 and B16F10 total cells were present in the well (Figure IV.1B and F). Fibroblast-derived signals had no influence on the total numbers of irradiated cancer cells, neither on MPR31.4 or B16F10 proliferation. (0.84±0.08 $x10^5$ MPR31.4 cells and 0.97±0.14 $x10^5$ B16F10 cells, 72h after XRT when co-cultured with L929 and NIH-3T3, respectively) (Figure IV.1B and 1F). In addition, fibroblasts were able to induce an increase in cancer cell death after 72h in both cell lines. MPR31.4 and B16F10 cell death levels increased from 6.7%±4.1 and 6.9%±2.2 to 15.9%±3.9 and 27%±4.8, respectively (Figure IV.1C, 1G). After IR, fibroblasts-derived signals resulted in enhanced apoptosis induction. Co-culturing with L929 fibroblasts resulted in 41.8%±10.3 of MPR31.4 cancer cells apoptosis as compared to MPR31.4 when cultured alone (26.6%±5.3 apoptosis) (Figure IV.1D). NIH-3T3-derived signals induced 33.9%±1.0 of B16F10 cancer cell apoptosis, as compared to 22.1%±1.7 when B16F10 were cultured alone (Figure IV.1H)

Taken together in indirect co-culture L929 were able to increase MPR31.4 cell death and NIH-3T3 increased B16F10 cell death as well as radiation-induced cell death suggesting a radio-sensitizing effect whereas proliferation was not affected.

2. Fibroblasts did not influence cancer cell long-term survival after radiation.

The indirect co-culture system was further used to study the long-term survival of respective cancer cells using standard 2D colony formation assay (CFA).

No effect of fibroblasts was observed (Figure IV.2) on the MPR31.4 and B16F10 long-term survival. Indeed, after counting the colonies (figure IV.2B, 2F) and calculating the cancer cell survival (Figure IV.2A, 2C, 2D and 2E). There was no significant difference between the survival fraction of the cancer cells cultured alone compared to the survival fraction of the cancer cells co-cultured indirectly with the fibroblasts.

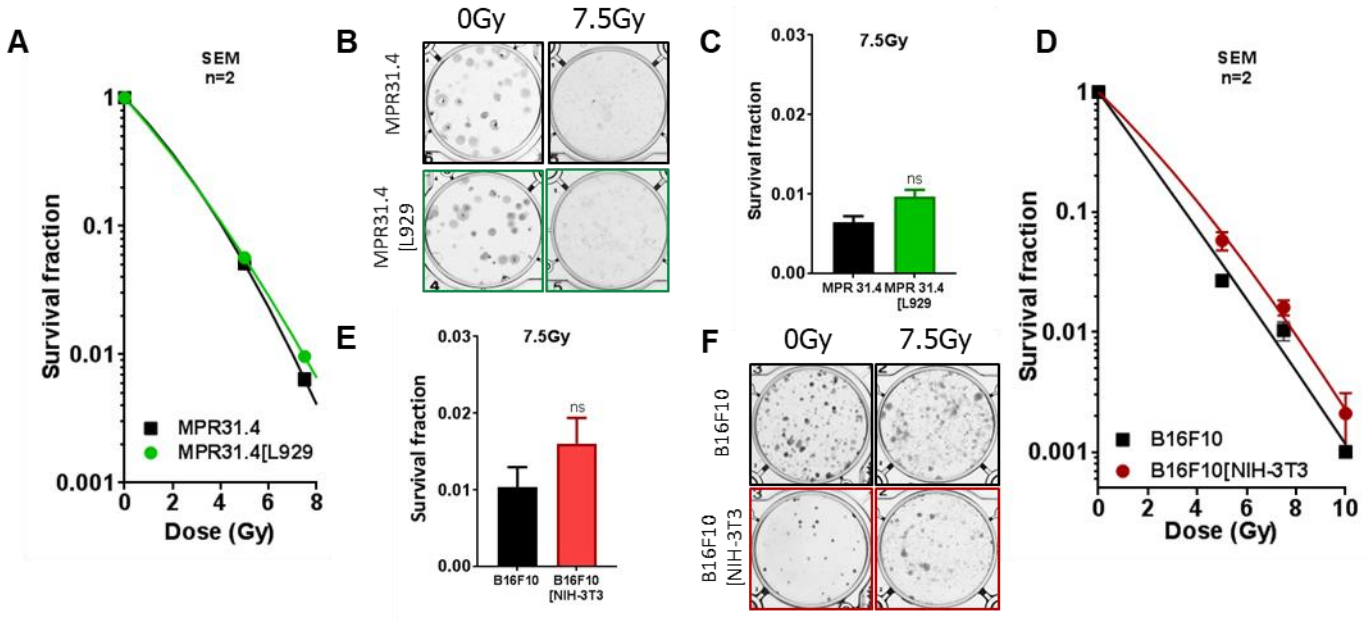

Figure IV.2: **L929 and NIH-3T3 fibroblasts did not alter the clonogenic survival of MPR31.4 and B16F10 cancer cells.** MPR31.4 or B16F10, cancer cells were plated alone or together with stromal fibroblasts for 24h prior to irradiation with 0 or 10Gy (ratio 1-1) and further incubated for additional 7 days after irradiation. Graphs depict the surviving fractions from two independent experiments measured in sextuplet each (means ± SEM) **(A-D, C-E)**. Plates were scanned, colonies were counted, and survival fraction was calculated **(B-F)**. "ns" present for no significant analyzed by one-way ANOVA test followed by Tukey's test.

However, B16F10 co-cultured with NIH-3T3 fibroblasts showed less plating efficiency compared to B16F10 culture alone (Figure IV.3). NIH-3T3 fibroblasts had an impact on B16F10 colonies formation but not on the radiation survival fraction.

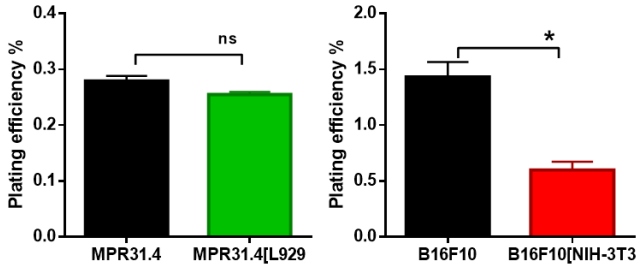

Figure IV.3: **NIH-3T3 fibroblasts induced a decrease of B16F10 colonies formation in indirect co-culture whereas L929 had no effect on MPR31.4 plating efficiency.** Plating efficiency of previous colony formation assay were calculated by dividing number of plating cells per the number of colonies formed. "ns" present for no significant and *p<0.05 analyzed by t-test.

3. L929 fibroblasts had no influence on the growth and the radiation response of subcutaneous MPR31.4 prostate tumors *in vivo*.

To investigate a potential relevance of the *in vitro* findings, MPR31.4 prostate cancer cells were implanted subcutaneously either alone or in combination with stromal L929 fibroblasts onto immune competent C57BL/6 mice. Tumor growth and growth retardation upon radiation were determined by measuring tumor size every day until the end of the experiment (Figure IV.4).

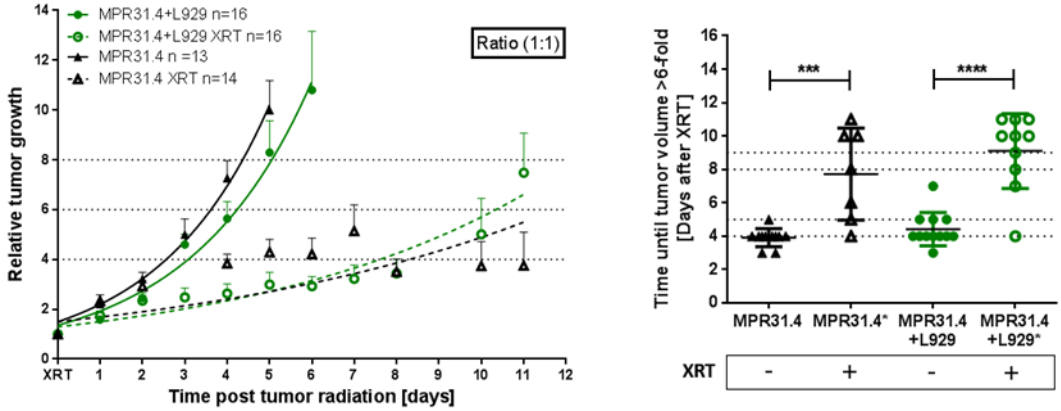

Figure IV.4: **Stromal L929 fibroblasts did not affect tumor growth and the radiation response of prostate tumors.** MPR31.4 prostate cancer cells alone or together with L929 skin fibroblasts (ratio of (1:1)) were subcutaneously co-implanted onto the hint leg of C57BL/6 mice. When tumor volumes of ~100 mm^3 were reached, one group received a single radiation dose of 10Gy to the tumor. The tumor volume was determined at indicated time points (left diagram). Data were represented as mean ± SEM from 2-3 independent experiments (in total 13 to 16 mice). Tumor growth and respective tumor growth delay were determined as time (days) until the 6-fold volume was reached (right diagram). ***p<0.001, ****p<0.0001 by one-way ANOVA followed by Tukey's test.

Tumors generated by co-implantation of MPR31.4 together with L929 cells and MPR31.4 alone reached a 6-fold volume after 4.42±1 days and 3.91±0.54 days, respectively, while irradiated tumors reached 6-fold volume after 9.1±2.23 and 7.71±2.75 days, respectively. Thus, co-implantation with L929 fibroblasts had no significant effect on the tumor growth since both tumors generated with MPR31.4 or MPR31.4 together with L929 had a comparable growth delay of respectively 3.81 and 4.68 days (Figure IV.4).

At the end of the experiments, to evaluate the tumors cell proliferation states into the different tumors, tumors were isolated and subjected to IHC for proliferating cell nuclear antigen (PCNA) (brown staining) (Figure IV.5).

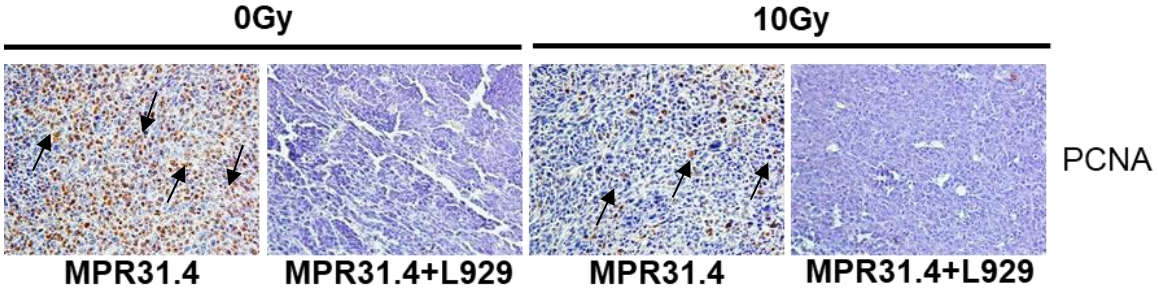

Figure IV.5: **Stromal fibroblasts, L929 induced a decline of the proliferation into the prostate tumor, MPR.31.4.** MPR31.4 prostate cancer cells alone or together with L929 skin fibroblasts (ratio of (1:1)) were subcutaneously co-implanted in C57BL/6 mice's right leg. When tumor volumes reached a critical size (5–12 days after tumor irradiation) tumors were isolated and subjected to IHC. Sections were stained for Proliferating Cell Nuclear Antigen (PCNA). Representatives' pictures were shown from 2-3 experiments (5 mice in total).

MPR31.4 tumors co-implanted with L929 fibroblasts expressed less PCNA than MPR31.4 tumor generated alone (Figure IV.5) pointing to inhibitory effects of L929 stromal fibroblasts on proliferation of prostate MPR31.4 tumor cells *in vivo*.

Taken together, fibroblast-derived signals increased cancer cell death in short-term experiments *in vitro* and reduced MPR31.4 tumor cell proliferation *in vivo*. Even though, fibroblasts did not impact cancer cell long-term survival, tumor growth and radiation response (Table IV.2). Overall, in this set of experiments the fibroblasts seemed to have more tumor-suppressive effects.

Cancer cells	Fibroblasts	Indirect co-culture					In vivo		Effect
		Short-term				Long-term	Growth delay	Proliferation	
		Proliferation		Cell death		CFA			
		0Gy	10Gy	0Gy	10Gy				
MPR31.4	L929	↗	-	↗	↗	-	-	↘	Tumor suppressive
B16F10	NIH-3T3	↘	-	↗	↗	-	n.d.	n.d.	Tumor suppressive

Table IV.2: L929 and NIH-3T3 induced an increase of MPR31.4 and Py8119 cell death (↗). L929 were shown to reduce MPR31.4 tumor proliferation. These results suggested a radiosentizing effect of the fibroblasts on the cancer cells. Minus (-) stand for "no effect" and "n.d" for "not determined".

B. Fibroblasts exert a tumor-promoting effect

1. Fibroblasts can increase cancer cell proliferation and reduce radiation-induced cancer cell death *in vitro* via a paracrine mechanism of action.

The indirect co-culture system was further used with other cancer cell/fibroblast combinations. MPR31.4 were co-cultured with NIH-3T3 fibroblasts and Py8119 breast cancer cells with L929 fibroblasts (Figure IV.6A, 6E). The combination of these fibroblasts cultured together with these cancer cells resulted in increased resistance of MPR31.4 and B16F10 to IR.

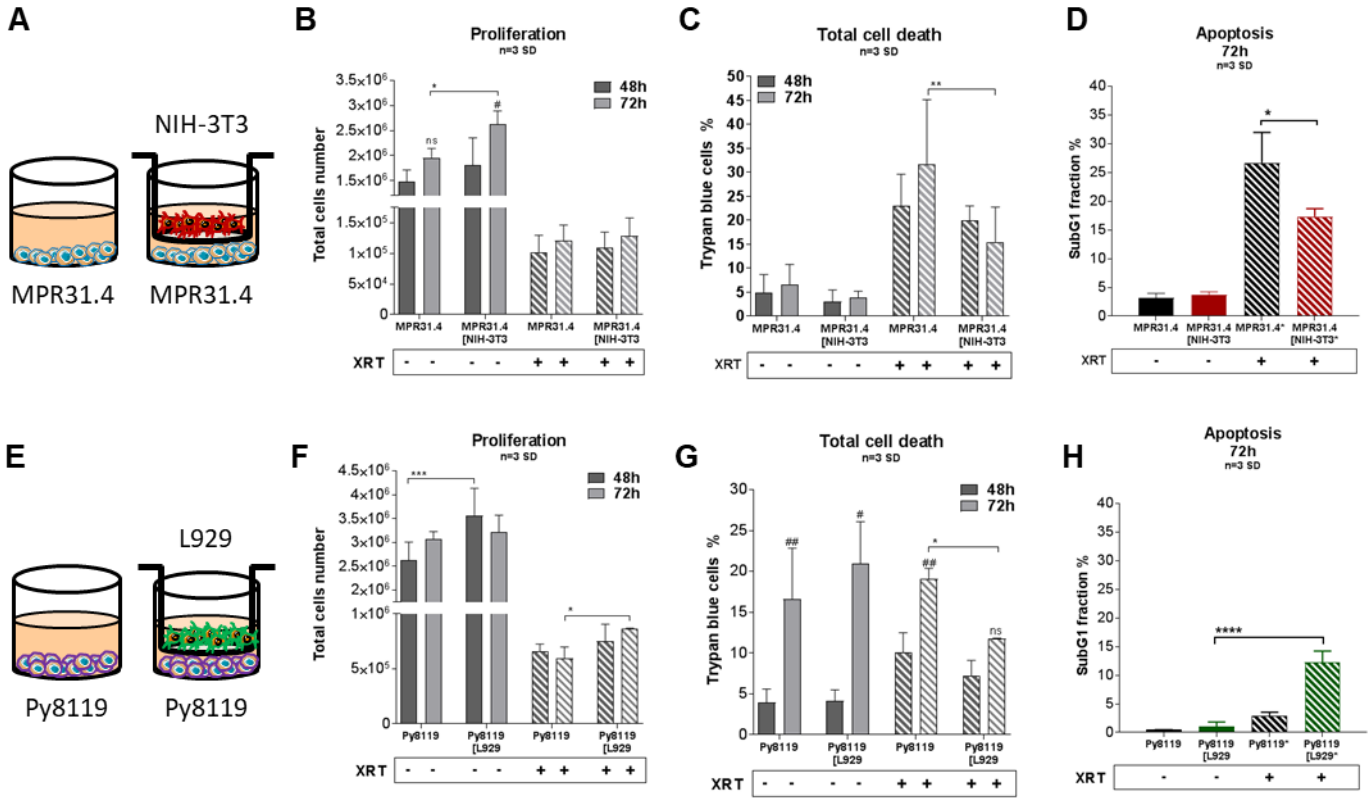

Figure IV.6: **Fibroblasts increased proliferation and reduced radiation-induced cell death of prostate and breast cancer cells.** MPR31.4 or Py8119 cancer cells were cultured alone or together with stromal fibroblasts (in indirect co-culture) for 24h prior to irradiation with 0 or 10Gy (ratio 1-1, **A-E**). After 48h and 72h, total cell numbers as well as dead cells were counted by trypan blue (**B-F, C-G)**. *p<0.05, **p<0.01 and ***p<0.001 analyzed by two-way ANOVA test followed by Tukey's test, compared cancer cells with fibroblasts to cancer cells cultured alone. "ns" present for no significant, $^{\#}$p<0.5 and $^{\#\#}$p<0.01 analyzed by two-way ANOVA test followed by Tukey's test, compared 72h to 48h. SubG1 fractions were measured by Nicoletti staining[85], 72h after irradiation **(D-H).** *p<0.05 and ****p<0.0001 analyzed by one-way ANOVA test followed by Tukey's test.

NIH-3T3-derived paracrine signals induced an increase of MPR31.4 proliferation and a decrease of MPR31.4 cells death after radiation. L929-derived signals induced an increase as well of Py8119 proliferation and a decrease of cells death after radiation (Figure IV.6).

After 72h of co-culture, MPR31.4 cultured together with NIH-3T3 fibroblasts showed 2.6±0.3 $x10^6$ cells numbers whereas MPR31.4 cells cultured alone showed a lower cell numbers of 1.9±0.2 $x10^6$ cell (Figure IV.6B). After radiation, the numbers of total Py8119 co-cultured together with L929 fibroblasts were 0.8±0.004 $x10^6$ cells whereas Py8119 cells cultured alone reached only 0.6±0.1 $x10^6$cells (Figure IV.6F). Respective fibroblasts affected cancer cell proliferation even after radiation (for Py8119 co-cultured with L929).

Cancer cells indirectly co-cultured with fibroblasts showed less cell death 72h after irradiation compared to the cancer cells cultured alone. Indeed, after IR, MPR31.4 cells showed 32.9±11.7% and Py8119 19.1±1.3% cell death. When indirectly co-cultured with NIH-3T3, MPR31.4 cell death was only 15.5±7.3% (Figure IV.6C) and Py8119 cell death was only 11.7±0.07%, respectively (Figure IV.6G). Moreover, irradiated MPR31.4 cells underwent less apoptosis when indirectly co-cultured with NIH-3T3 cells (17.3±1.4%) as compared to MPR31.4 cultured alone (Figure IV.6D).

In addition, it could be observed, that fibroblast-derived signals altered cancer cells migration after radiation. For this, a scratch was induced in the middle of the cell layers after IR (Supplementary figure VII.1A). In the Py8119 cultured alone, the scratch was reduced by 58.67±21.46µm after 72h, whereas when co-cultured with L929 fibroblasts, the scratch was reduced approximately by 180.32±54.89µm (supplementary figure VII.1B). After radiation, Py8119 cells co-cultured indirectly with L929 fibroblasts, closed the wound faster than Py8119 cultured alone.

In summary, in these cell combinations fibroblast-derived signals were shown to increase proliferation and to reduce cancer cell death after IR. Moreover, the fibroblasts may also influence cancer cell migration.

2. Fibroblasts improved MPR31.4 prostate and B16F10, breast cancer cell long-term survival in indirect co-culture

In the presence of NIH-3T3 or L929 fibroblasts the long-term survival of MPR31.4 and Py8119 cancer cells, respectively was significantly improved (indirect (transwell co-culture system) (figure IV.7)

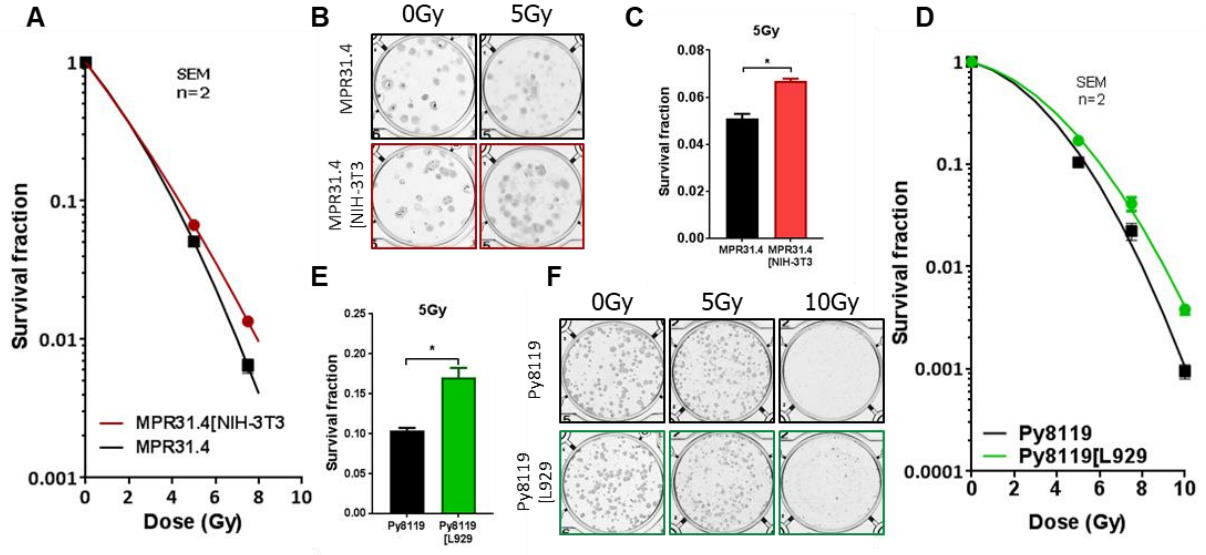

Figure IV.7: **NIH-3T3 fibroblasts increased clonogenic survival after radiation of MPR31.4 cells and L929 fibroblasts increased clonogenic survival of Py8119 breast cancer cells.** MPR31.4 or Py8119 cells were plated alone or together with stromal fibroblasts for 24h prior irradiation with 0 or 10Gy (ratio 1-1) and subsequently further incubated for additional 7 days. Graphs depict the surviving fractions from two independent experiments measured in sextuplet each (means ± SEM) **(A-D, C-E)**. Plates were scanned, colonies were counted, and survival fraction was calculated **(B-F)**. *p<0.05 analyzed by one-way ANOVA test followed by Tukey's test.

After quantification of the colonies (figure IV.7), the survival fraction of MPR31.4 cells cultured alone was lower than the survival fraction of MPR31.4 indirectly co-cultured with NIH-3T3 fibroblasts. The survival fraction of Py8119 cells was also improved when co-cultured with L929 fibroblasts compared to the Py8119 cells alone. The survival fraction of MPR31.4 and Py8119 alone was 0.051±0.003 and 0.104±0.003 after 5Gy IR. When indirectly co-cultured with the respective fibroblasts, the survival fractions of MPR31.4 and Py8119 significantly improved to 0.067±0.001 and 0.171±0.001, respectively.

However, no significant difference was observed in the cells plating efficiency between cancer cells cultured alone or together with fibroblasts (data not shown).

3. Fibroblasts improved prostate cancer long-term survival in 3D direct co-culture

Earlier work has revealed that fibroblasts/CAFs were shown to communicate with cancer cells by paracrine signal via small molecules like cytokines but also by direct cell-to-cell interaction[44]. To extend the effects observed in indirect co-culture, the direct interactions between stromal fibroblasts and cancer cells were investigated in addition using a 3D co-culture system. To allow discrimination of cancer cells and fibroblasts in these co-cultures MPR31.4 cancer cells were transfected with a pEGF-N1 vector encoding GFP whereas NIH-3T3 fibroblasts were labeled with a pTagRFP-N vector encoding RFP, sorted by flow cytometry for fluorescence-positive cells and subsequently additionally selected with G418 antibiotics for vector-integrated cells. MPR31.4 GFP-tagged cells were then cultured alone or in presence of NIH-3T3-RFP fibroblasts in a self-established 3D Matrigel co-culture system. Therefore 1000 of cancer cells were plated alone or together with 1000 fibroblasts in highly concentrated Matrigel. Colonies were observed by bright field and fluorescence microscopy 7 days after XRT (Figure IV.8B, 8C).

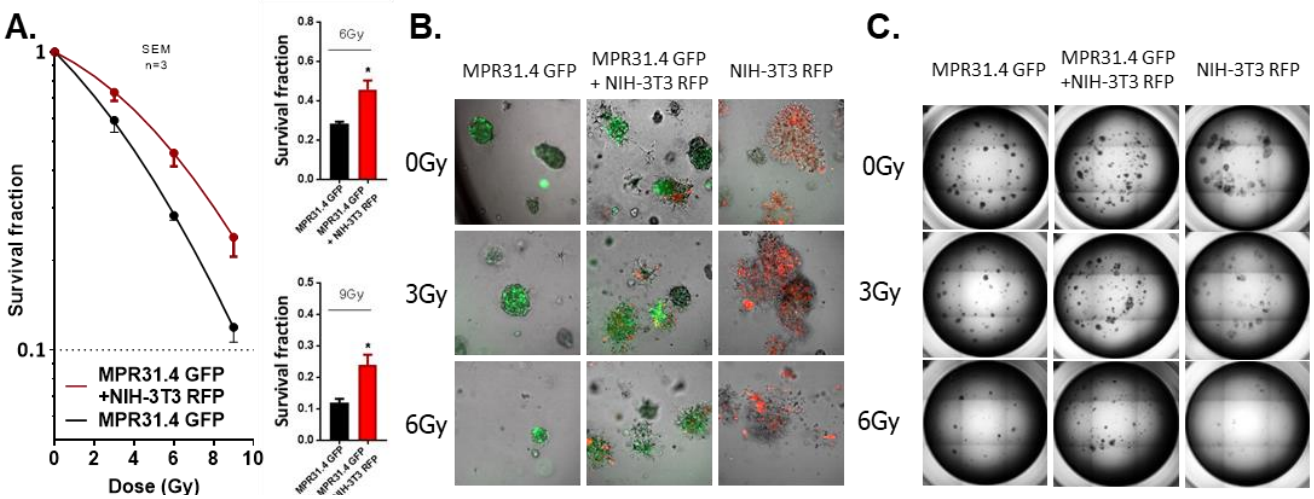

Figure IV.8: **Stromal fibroblasts increased clonogenic survival after radiation of the MPR31.4 cancer cells in direct 3D culture.** MPR31.4 cancer cells were plated for colony formation assay alone or together with NIH-3T3 fibroblasts (ratio (1/1)) in a 3D Matrigel system, irradiated with indicated doses (0–9Gy) and subsequently further incubated for additional 7 days. Surviving fractions from three experiments measured in quintuplet each were shown (means ± SEM). **A-C** the colonies were counted, and the survival fraction calculated. **B-D** Phase contrast pictures at 25x magnifications. **E-F** Representative fluorescent at 100x magnifications. Fibroblasts were stably transfected with RFP (red) and cancer cells with GFP (green). *p<0.5, by two-way ANOVA test followed by Tukey's test.

Formed colonies were quantified and cancer cell clonogenic survival was calculated (Figure IV.8A, 8C). Co-culture with NIH-3T3 fibroblasts enhanced clonogenic survival of MPR31.4 cells compared to MPR31.4 cells alone.

The survival fraction of MPR31.4-GFP alone was 0.283±0.017 after 6Gy IR while when co-cultured with NIH-3T3 fibroblasts, the survival fraction increased to 0.458±0.078, that indicates an increase of radiation resistance of the MPR31.4 cancer cells. In addition, cell plating efficiency were calculating for all conditions. NIH-3T3 enhanced the MPR31.4 formation of colonies compared to MPR31.4 cultured alone (Figure IV.9).

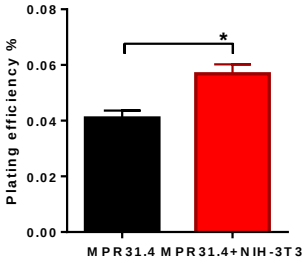

Figure IV.9: **NIH-3T3 fibroblasts increased MPR31.4 colonies formation in 3D direct co-culture.** Plating efficiency of previous colony formation assay was calculated by dividing number of plating cells per the number of colonies formed. *p<0.05 analyzed by t-test.

To exclude colonies composed only of fibroblasts in the co-cultures; the composition of the colonies was evaluated by fluorescence microscopy (Figure III.7B). In the direct co-culture conditions, colonies were composed either of a mixture of MPR31.4 cells and fibroblasts (GFP and RFP signal) or only of cancer cells (GFP). Colonies composed only of fibroblasts (RFP signal) were not found. Of note, fibroblasts cultured alone (figure IV.8B, 8C, right column) did not form regular colonies.

In summary, the direct interaction of NIH-3T3 fibroblasts with MPR31.4 prostate cancer cells promoted the long-term survival of the irradiated cancer cells in 3D co-culture *in vitro*.

4. CAFs induced radiation-resistance *in vivo* using prostate and breast cancer xenografts

To further validate the previous observations, *in vivo* experiments were performed using the MPR31.4 and Py8119 cancer cells implanted subcutaneously

either alone or in combination with stromal NIH-3T3 and L929 fibroblasts onto C57BL/6 mice.

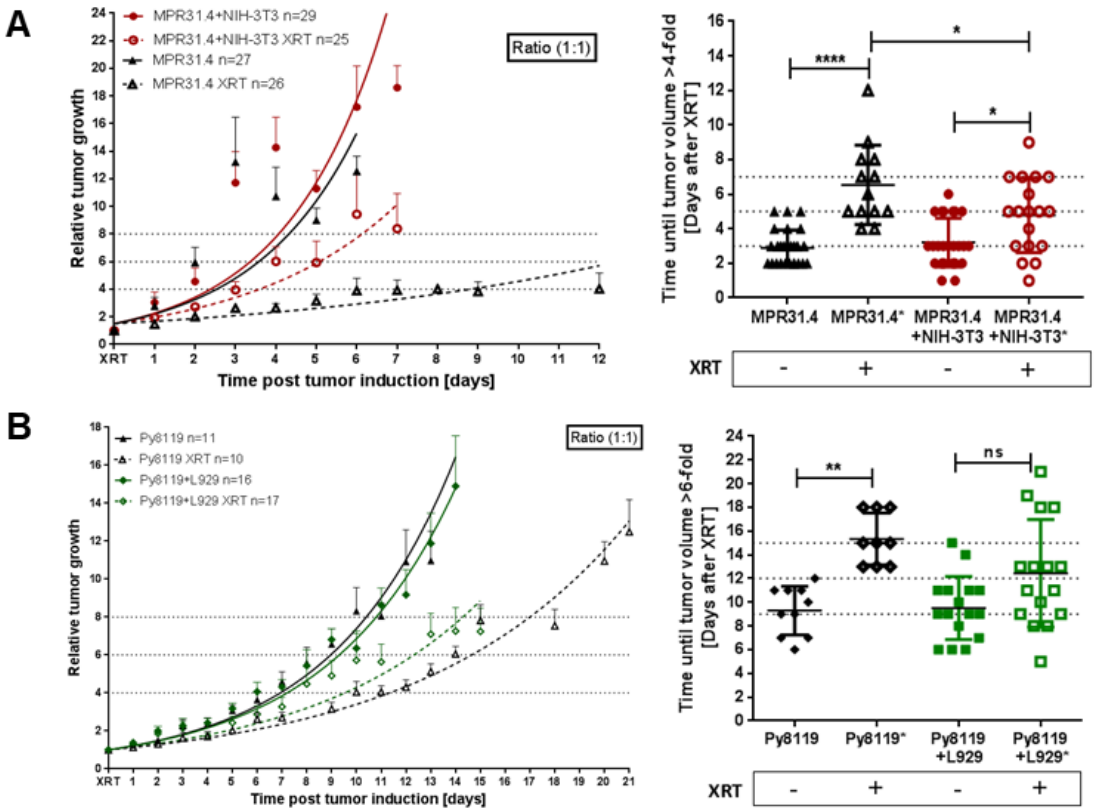

Figure IV.10: **NIH3T3 fibroblasts induced MPR31.4 prostate radio-resistance and tumor growth delay after radiation as well as L929 fibroblasts on Py8119 breast cancer cells.** MPR31.4 prostate **(A)** or Py8119 breast **(B)** cancer cells alone or together with NIH-3T3 **(A)** or L929 **(B)** fibroblasts (ratio of (1:1)) were subcutaneously co-implanted on C57BL/6 mice. When tumor's volumes of ~100 mm³ were reached, one group received a single radiation dose of 10Gy to the tumor. The tumor volume was determined at indicated time points (left diagram). Data were represented as mean ± SEM from 2-3 independent experiments. Tumor growth and respective tumor growth delay were determined as time (days) until the 4 or 6-fold volume was reached (right diagram). "ns" present for no significant, *p<0.05, **p<0.01 and ****p<0.0001 by one-way ANOVA followed by Tukey's test.

Co-implantation of MPR31.4 prostate cancer cells with NIH-3T3 stromal fibroblasts as well as co-implantation of Py8119 prostate cancer cells with L929 stromal fibroblasts led to increased tumor growth and significantly reduced tumor growth delay after IR when compared to tumors generated by cancer cells alone (Figure IV.10A, 10B).

The tumors generated by co-implantation of MPR31.4 and NIH-3T3 cells or MPR31.4 alone reached a 4-fold volume after 3.21±1.41 days and 2.88±1.03 days,

respectively; though the irradiated tumors reached 4-fold volume after 4.78±2.16 and 6.54±2.30 days, respectively (Figure IV.10A). Thus, tumors generated by co-implantation of MPR31.4+NIH-3T3 cells showed a growth delay of only 1.57 days after receiving IR compared to the tumor generated with MPR31.4 alone which had a growth delay of 3.65 days after radiation.

Moreover, tumors generated by co-implantation of Py8119+L929 and Py8119 alone reached a 6-fold volume after 9.5±2.66 and 9.3±2.06 days respectively whereas the same set of irradiated tumors reached their 6-fold volume after 12.44±4.53 days and 15.33±2.18, respectively (Figure IV.10B). The combination of cancer cells and fibroblasts led to a reduction in radiation-induced tumor growth delay of 2.94 days compared to a radiation-induced growth delay of tumors generated from PY8119 cells alone by 6.03 days.

At the end of the experiments, tumors were isolated and subjected to IHC for PCNA. Irradiated MPR31.4 tumors co-implanted with NIH-3T3 fibroblasts and Py8119 tumors co-implanted with L929 fibroblasts were more reactive to PCNA than MPR31.4 and Py8119 tumors generated alone (Figure IV.11). This indicates that these fibroblasts can promote MPR31.4 or Py8119 tumor cell proliferation after radiation *in vivo.*

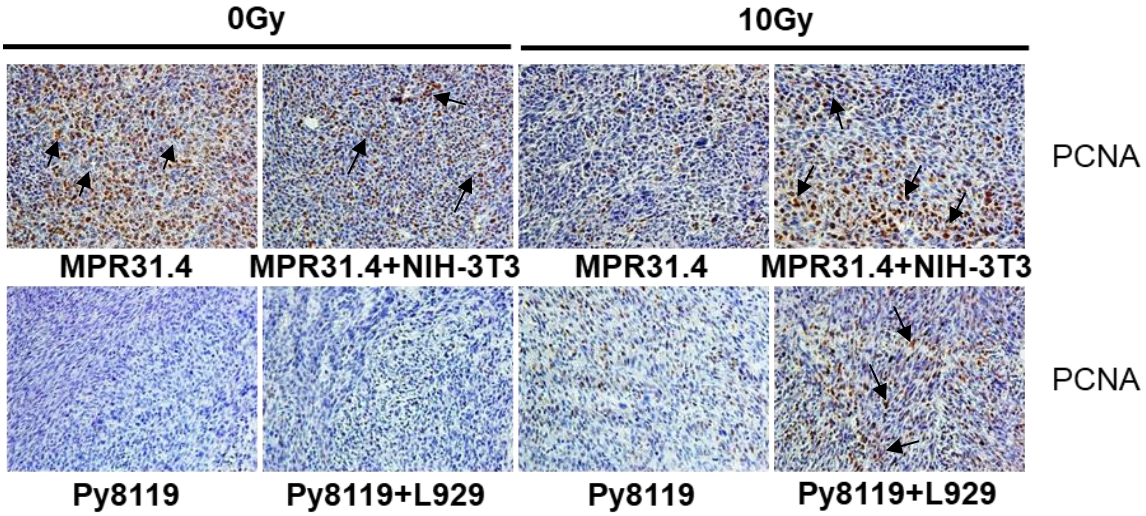

Figure IV.11: **The presence of radio-resistance promoting fibroblasts resulted in increased immunoreactivity for the proliferation markers PCNA.** MPR31.4 prostate alone or together with NIH-3T3 fibroblasts and Py8119 breast cancer cells alone or together with L929 fibroblasts (ratio of (1:1)) were subcutaneously co-implanted onto C57BL/6 mice. When tumor volumes reached a critical size (5–21 days after tumor irradiation) tumors were isolated and subjected to IHC. Sections were stained for Proliferating Cell Nuclear Antigen (PCNA). Representatives' pictures were shown from 2-3 experiments (5 mice total).

Thus, confirming the *in vitro* observation, NIH-3T3 fibroblasts induced MPR31.4 prostate tumor radio-resistance and L929 fibroblasts induced Py8119 breast tumor radio-resistance *in vivo*.

Taken together, fibroblasts-derived signal increased proliferation and reduced cancer cells death in short-term experiments *in vitro*. Fibroblasts-derived signal and direct interaction with cancer cells promoted cancer cells long-term survival after radiation in 2D and 3D experiments *in vitro*. Fibroblasts induced tumor radio-resistance *in vivo* with an increase of tumor proliferation (Table IV.3). Overall, in this set of experiments, fibroblasts exerted a tumor-promoting effect and induced cancer cells radio-resistance.

Cancer cells	Fibroblasts	Indirect co-culture					Direct co-culture	In vivo		Effect
		Short-term				Long-term				
		Proliferation		Cell death		CFA	CFA	Growth delay	Proliferation	
		0Gy	10Gy	0Gy	10Gy					
MPR31.4	NIH-3T3	↗	-	-	↘	↗	↗	↘	↗	Tumor promoting
Py8119	L929	↗	↗	-	↘	↗	n.d.	↘	↗	Tumor promoting

Table IV.3: L929 and NIH-3T3 induced an decrease of MPR31.4 and Py8119 cell death after XRT (↙). L929 were shown to increase Py8119 tumor proliferation after XRT. Fibroblasts induced an increase of survival fraction as well as tumor proliferation. These results suggested a radio-resisting effect of the fibroblasts on the cancer cells. Minus (-) stand for "no effect" and "n.d" for "not determined".

The further investigation of other combinations, e.g. the effect of NIH-3T3 on Py8119, L929 on B16F10, and NIH-3T3 and L929 fibroblasts on TrampC1 prostate cancer cells revealed no influence of fibroblast-derived signals on the proliferation and death of these cells in indirect co-culture (Supplementary figure VII.2). But surprisingly, NIH-3T3 fibroblasts enhanced clonogenic survival of Py8119 cells in direct co-culture (Supplementary figure VII.3) and in indirect co-culture, respectively (only a trend, supplementary figure VII.4). Though the presence of NIH-3T3 fibroblasts in Py8119 tumors had no effect on tumor growth, radiation response (Supplementary figure VII.5) and tumor cell proliferation *in vivo* (Supplementary figure VII.6). Thus, under certain conditions fibroblasts seem to have no clear impact on tumor progression and radiation response.

Taken together, the presented results strongly suggest that the impact of fibroblasts on cancer cell radiation response largely depends on the fibroblast-tumor cell combination. Fibroblasts exerted either a tumor-suppressing effect, a tumor-promoting effect and radio-resistance, or no effect (Table IV.4), which leads to the speculation that the influence of the fibroblasts to alter (i) tumor progression and/or (ii) the therapeutic response may be determined by the cancer cells potential to activate the respective fibroblasts.

Cancer cells	Fibroblasts	Indirect co-culture					Direct co-culture	In vivo		Effect
		Short-term				Long-term	CFA	Growth delay	Proliferation	
		Proliferation		Cell death		CFA				
		0Gy	10Gy	0Gy	10Gy					
MPR31.4	NIH-3T3	↗	-	-	↘	↗	↗	↘	↗	Tumor promoting
MPR31.4	L929	↗	-	↗	↗	-	n.d.	-	↘	Tumor suppressing
Py8119	NIH-3T3	↘	↗	-	-	-	↗	-	-	Controversial /No effect
Py8119	L929	↗	↗	-	↘	↗	n.d.	↘	↗	Tumor promoting
B16F10	NIH-3T3	↘	-	↗	↗	-	n.d.	n.d.	n.d.	Tumor suppressing
B16F10	L929	-	-	-	-	↗	n.d.	n.d.	n.d.	No effect
TrampC1	NIH-3T3	-	-	-	-	n.d.	n.d.	n.d.	n.d.	No effect
TrampC1	L929	-	-	-	-	n.d.	n.d.	n.d.	n.d.	No effect

Table IV.4: Multiple effects of fibroblasts on the radiation response of tumor cells. NIH-3T3 induced a B16F10 radio-sensitizing effect when it induced MPR31.4 radio-resistance. L929 induced MPR31.4 radio-sensitizing effect when it induced Py8119 radio-resistance. Minus (-) stand for “no effect”. The white square stand for “no investigation”.

C. Influence of the cancer cell-fibroblast ratio for the radiation response

Previous studies demonstrated that the percentage of intra-tumoral stroma may vary between tumors; moreover some studies suggested that a high amount of intra-tumoral stroma may predict worse prognosis[100]. In order to investigate the influence of an enhanced relative amount of stromal fibroblasts (increased fibroblast-tumor cell ratio) on the radiation response of cancer cells, similar experiments as before were performed with a two-fold increase in the fibroblast numbers.

1. A two-fold increase in the fibroblast-tumor cell ratio did not impact the tumor cell radiation response *in vitro*.

Therefore, MPR31.4 were plated with NIH-3T3 and Py8119 cancer cells were plated with L929. Cancer cells were plated on the bottom of the well whereas 2 times more fibroblasts were plated in the transwell inserts (Figure IV.12A, 12E) when compared to the experiments depicted in figure IV.6A, 6E, 24h prior irradiation. Then both cell line were irradiated with 0 or 10Gy. The impact of fibroblast-derived signal on cancer cell proliferation and apoptosis were study as described above.

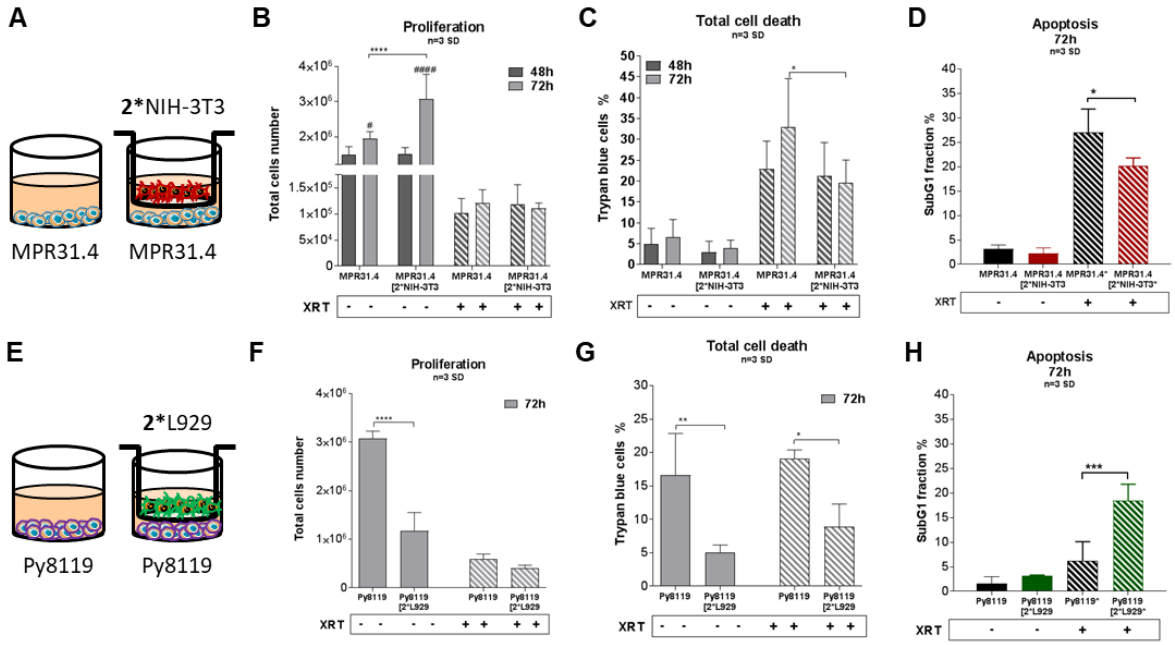

Figure IV.12: **Increasing fibroblast numbers did not affect the cancer cell radiation response promoted by stromal fibroblasts in short term experiments.** MPR31.4 or Py8119 cancer cells were cultured alone or together with stromal fibroblasts (in indirect co-culture) for 24h prior irradiation with 0 or 10Gy (ratio 1-2, **A-E**). After 48h and 72h, total cell numbers as well as dead cells were counted by Trypan blue (**B-F, C-G)**. *p<0.05, **p<0.01, and ****p<0.0001, analyzed by two-way ANOVA test followed by Tukey's test, compared cancer cells with fibroblasts to cancer cells cultured alone. # p<0.5, #### p<0.0001 analyzed by two-way ANOVA test followed by Tukey's test, compared 72h to 48h. SubG1 fractions were measured by Nicoletti staining[85], 72h after irradiation **(D-H).** *p<0.05 and *** p<0.001 analyzed by one-way ANOVA test followed by Tukey's test.

In the indirect co-culture, increasing cell number of NIH-3T3 fibroblasts induced an increase of MPR31.4 total cells number after 72h, raising from 1.9±0.2

$x10^6$ total cells under control conditions to 3.1±0.7 $x10^6$ total cells when co-cultured with NIH-3T3 fibroblasts (Figure IV.12B).

In contrast to the results observed previously, figure IV.6 at 1:1 ratio, increasing the amount of L929 fibroblasts did not induce an increase of Py8119 breast total cells number after IR. L929 fibroblasts derived signal decreased Py8119 total cells number at 0Gy, from 3.1±0.1 $x10^6$ total cells to 1.2±0.04 $x10^6$ total cells when co-culture with L929 fibroblasts (Figure IV.12F).

Increasing the fibroblast-cancer cells ratio in the indirect co-culture appeared to have controversial effects on cancer cell proliferation. Indeed, NIH-3T3 fibroblasts, induced an increase of MPR31.4 total cells numbers at both ratios (ratio (1-1), figure IV.6B and ratio (1-2), figure IV.12B). Instead L929 fibroblasts induced an increase of Py8119 total cells number after IR at a ratio (1-1) (Figure IV.6F) but seemed to have no effect after IR at a ratio (1-2) (Figure IV.12F).

However, increasing NIH-3T3 cells numbers or L929 cells number did not affect the influence of NIH-3T3 and L929 fibroblasts derived signals on cell death or irradiated MPR31.4 and Py8119 cells. After IR, MPR31.4 cancer cells showed 32.9±11.7% and Py8119 19.1±1.3% total cell death. When indirectly co-cultured with NIH-3T3 and L929 fibroblasts, MPR31.4 total cell death was only 19.7±5.4% (Figure IV.12C) and Py8119 total cell death 8.9±3.4% (Figure IV.12G). Moreover, after IR, MPR31.4 showed more apoptosis (27.0±4.8%) when cultured alone compared to indirect co-culture with 2*NIH-3T3 fibroblasts (20.1±1.7%) (Figure IV.12D).

Thus, fibroblasts reduced death of irradiated cancer cells at both ratios (ratio (1-1), figure IV.6C, 6G and ratio (1-2), figure IV.12C,12G).

Besides, other cells set (MPR31.4-L929 and B16F10-NIH-3T3) were plated at a ratio of (1-2). No change was observed on the cancer cell proliferation and cell death after radiation in indirect co-culture between ratio (1-2) compared to ratio (1-1) (Supplementary figure VII.7).

2. Increasing NIH-3T3 fibroblasts amount did not induce MPR31.4 radio-resistance *in vivo*

In order to investigate the influence of the relative amount of stromal fibroblasts (increased fibroblast-tumor cell ratio) on the tumor radiation response, MPR31.4 were co-implanted subcutaneously either alone or together with stromal NIH-3T3 fibroblasts on C57BL/6 mice at a tumor/fibroblast ratio of 1/2 (Figure IV.13).

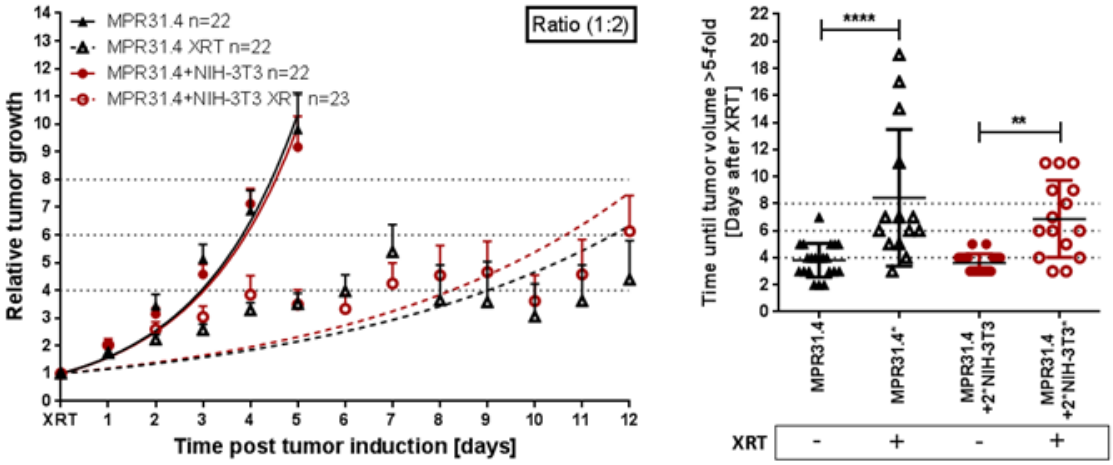

Figure IV.13: **Increasing the fibroblasts numbers resulted in the elimination of stromal fibroblasts-promoted tumor radio-resistance.** MPR31.4 prostate cancer cells alone or together with NIH-3T3 fibroblasts (ratio of (1:2)) were subcutaneously co-implanted in C57BL/6 mice's right leg. When tumor's volumes of ~100 mm³ were reached, one group received a single radiation dose of 10Gy to the tumor. The tumor volume was determined at indicated time points (left diagram). Data were represented as mean ± SEM from 2-3 independent experiments. Tumor growth and respective tumor growth delay were determined as time (days) until the 5-fold volume was reached (right diagram). **p<0.01, ****p<0.0001 by one-way ANOVA followed by Tukey's test.

Tumor generated by co-implantation of MPR31.4 + 2x NIH-3T3 cells and MPR31.4 alone reached respectively a 5-fold volume after 3.81±0.27 days and 3.62±0.67 days while irradiated tumors reached respectively 5-fold volume after 8.43±5.05 and 6.87±2.85 days. Thus, co-implantation with NIH-3T3 stromal fibroblasts had no significant effect on the tumor growth since both tumors generated with MPR31.4 or MPR31.4+NIH-3T3 had a growth delay of respectively 4.62 and 3.25 days (Figure IV.13).

Conclusively, these results demonstrate that the cancer cell/stromal fibroblast proportion in the tumor might impact the outcome of radiotherapy under certain conditions. Thereby these findings implicate that the contribution of stromal fibroblasts to tumor progression and therapy response might depend on the ability of the cancer cells to activate the surrounding stromal fibroblasts. Higher numbers of fibroblasts could thus mean less fibroblast activation by the cancer cells. Cancer cells might need more time to activate a higher number of fibroblasts. Indeed, our results revealed that increasing the fibroblasts/cancer cell ratio had no influence in short-term experiments but had a strong influence in long term and more clinically relevant *in vivo* experiments (Table IV.5).

Cancer cells	Fibroblasts	Ratio	Indirect co-culture				In vivo
			Short-term				Growth delay
			Proliferation		Cell death		
			0Gy	10Gy	0Gy	10Gy	
MPR31.4	NIH-3T3	(1-1)	↗	-	-	↘	↘
MPR31.4	NIH-3T3	(1-2)	↗	-	-	↘	-
Py8119	L929	(1-1)	↗	↗	-	↘	↘
Py8119	L929	(1-2)	↘	-	↘	↘	n.d.
MPR31.4	L929	(1-1)	↗	-	↗	↗	-
MPR31.4	L929	(1-2)	↗	-	-	↗	n.d.
B16F10	NIH-3T3	(1-1)	↘	-	↗	↗	n.d.
B16F10	NIH-3T3	(1-2)	↘	-	↗	↗	n.d.

Table IV.5: Influence of the ratio cancer cells-fibroblasts on the tumor radiation response. Increased number of NIH-3T3 did not induce MPR31.4 tumor growth delay compared to tumors with a smaller number of fibroblasts *in vivo.* However, fibroblasts had the same influence on the cancer cells in short term study in vitro independently of the fibroblasts number. Minus (-) stand for “no effect and n.d. for not determined”.

D. Fibroblasts alter the phenotype of cancer cells: L929 fibroblasts were able to induce epithelial-mesenchymal transition (EMT) in cancer cells after radiation

One well-known mechanism of tumor resistance is EMT[101]. Therefore, it was investigated if fibroblasts may promote cancer cell radio-resistance by inducing cancer cell EMT. Real Time RT PCR analyses were performed for the EMT markers α-SMA, Snai1, Snai2, and TGF-β). Therefore MPR31.4 or Py8119 cancer cells exposed to the same indirect co-culture system as described above (Method 1. Indirect (Transwell) co-culture) and cultured for 72h after XRT.

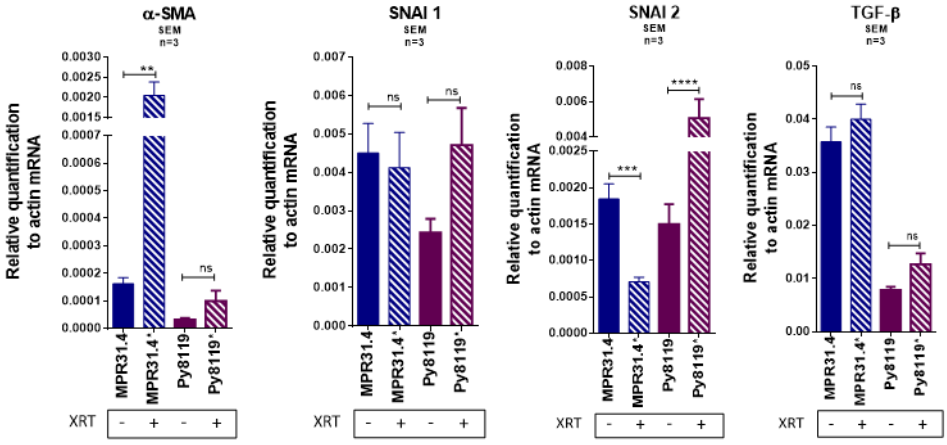

Figure IV.14: **Radiation itself is not sufficient to induce epithelial-mesenchymal transition (EMT) in cancer cells.** MPR31.4 and Py8119 cancer cells were cultured alone for 24h prior to irradiation with 0 or 10Gy (ratio 1-1). 72h after RT, quantitative real time PCR (qRT-PCR) analysis of the reactive EMT markers α-SMA, Snai1, Snai2 and TGF-β were performed in total RNA isolates of cultured cancer cells. Respective expression levels were normalized to β-actin (set at 1). Shown are mean values ± SEM from 3 independent samples per group measured each in triplicate each. "ns" present for no significant, *p<0.5, **p<0.01, *** p<0.001 and ****p<0.0001 analyzed by one-way ANOVA test followed by Tukey's test.

First, the effect of the radiation alone on the cancer cell phenotype was analyzed. In MPR31.4, an approximately 10-fold increase in α-SMA expression could be detected whereas SNAI2 expression decreased to 1/3 and SNAI1 and TGF-β were not modified by XRT compared to non-irradiated controls. In Py8119, an increase of SNAI2 by approximately 2-fold was detected but no change of α-SMA, SNAI1 and TGF-β expression were found (Figure IV.14). In B16F10, a decrease in SNAI1 and TGF-β expression was detected as well as an increase of α-SMA expression but no

change of SNAI2 was found after radiation (Supplementary figure VII.8). Thus, radiation alone is not sufficient to induce a significant change in EMT markers, and thus to induce EMT in cancer cells.

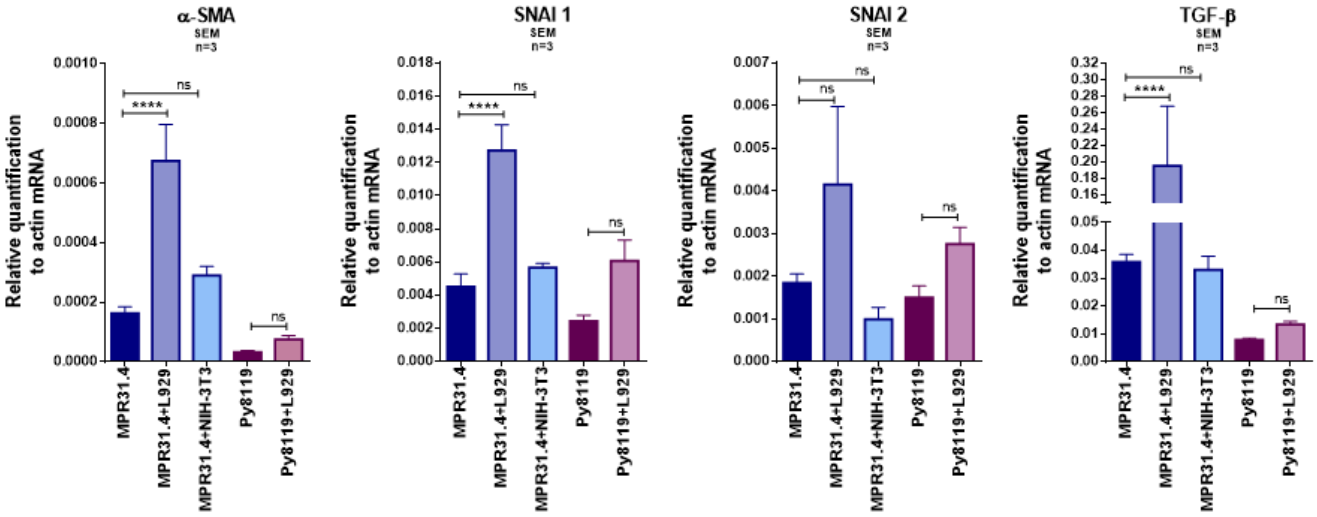

Figure IV.15: **Fibroblasts-derived signals did not induce EMT in cancer cells (except MPR+L929).** MPR31.4 and Py8119 cancer cells were cultured alone or together with stromal fibroblasts NIH-3T3 and L929, (transwell, (ratio 1-1)). After 96h, qRT-PCR analysis of the reactive EMT markers α-SMA (Acta2), Snai1, Snai2 and TGF-β were performed in total RNA isolates of cultured cancer cells. Respective expression levels were normalized to β-actin (set at 1). Shown are mean values ± SEM from 3 independent samples per group measured each in triplicate. "ns" present for no significant, *p<0.5, **p<0.01, and ****p<0.0001 analyzed by one-way ANOVA test followed by Tukey's test.

Secondly, the effect of fibroblasts-derived paracrine signals on the cancer cell phenotype was also analyzed. L929 fibroblasts induced an increase of α-SMA (about 3.5-fold), SNAI1 (about 3-fold) and TGF-β (about 5-fold) expression in MPR31.4 cancer cells but had no influence on SNAI2 expression level. However, NIH-3T3 fibroblasts had no influence on α-SMA, SNAI1, SNAI2 and TGF-β expressions levels in MPR31.4 cancer cells; similarly, L929 fibroblasts had no influence on α-SMA, SNAI1, SNAI2 and TGF-β expressions levels in Py8119 cancer cells after 72h of indirect co-culture (Figure IV.15). NIH-3T3 had neither an influence on EMT marker expression levels in B16F10 (Supplementary figure VII.9). Thus, only co-culture of MPR31.4 cancer cells together with L929 induced an increase of EMT-marker expression in the cancer cells. NIH-3T3 derived paracrine signals neither induced an increase of EMT

marker expression in MPR31.4 nor in B16F10 cells and L929-derived signals failed to induce EMT in Py8119 cancer cells.

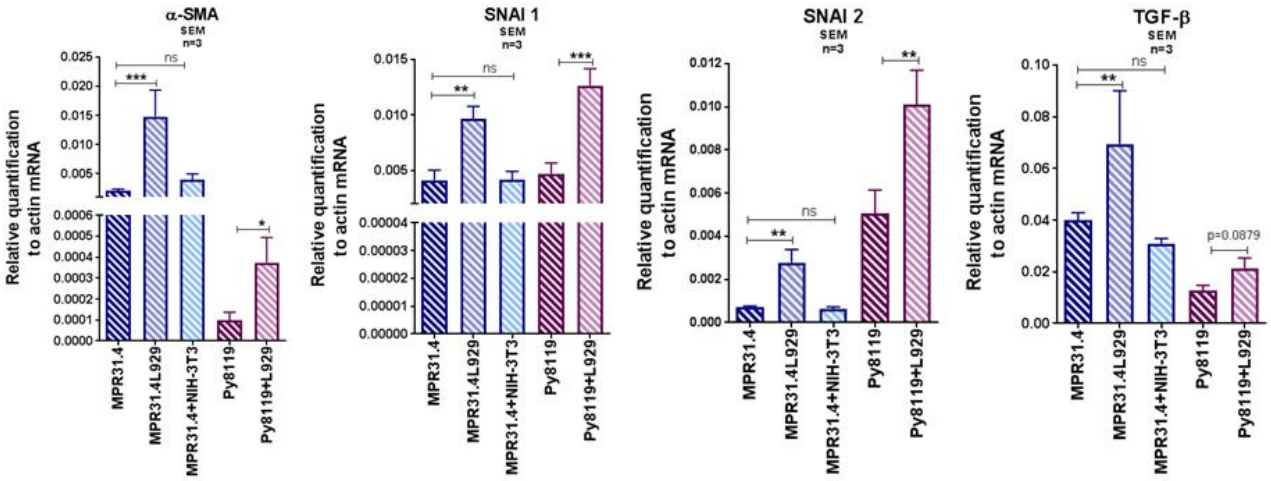

Figure IV.16: **L929 fibroblasts-derived signal induce EMT in cancer cells after IR.** MPR31.4 and Py8119 cancer cells were cultured alone or together with stromal fibroblasts NIH-3T3 and L929 for 24h prior irradiation with 0 or 10Gy (ratio 1-1). After 72h, qRT-PCR analysis of the reactive EMT markers α-SMA (Acta2), Snai1, Snai2 and TGF-β were performed in total RNA isolates of cultured cancer cells. Respective expression levels were normalized to β-actin (set at 1). Shown are mean values ± SEM from 3 independent samples per group measured each in triplicate. "ns" present for no significant, *p<0.5, **p<0.01, and ****p<0.0001 analyzed by one-way ANOVA test followed by Tukey's test.

Next, it was investigated whether the fibroblasts-derived signal influenced the cancer cell phenotype after radiation. Both MPR31.4 and Py8119 cancer cells cultured indirectly 72h with L929 fibroblasts and irradiated, showed a characteristic EMT phenotype (Figure IV.16). L929 fibroblasts induced an increase of α-SMA (about 3-fold), SNAI1 (about 2-fold), SNAI2 (about 3-fold) and TGF-β (about 2-fold) marker expression levels in irradiated MPR31.4 and Py8119 cancer cells. In contrast, NIH-3T3 fibroblasts had no influence on α-SMA, SNAI1, SNAI2 and TGF-β marker levels in irradiated MPR31.4 cancer cells. In addition, NIH-3T3 fibroblasts induced a decrease of TGF-β expression and had no influence on α-SMA, SNAI1, SNAI2 in irradiated B16F10 cancer cells (Supplementary figure VII.10).

Therefore, only L929 fibroblasts induced an EMT phenotype in MPR31.4 and Py8119 cancer cells after radiation. While NIH-3T3 fibroblasts induced radiation resistance of MPR31.4, they did not induce EMT in MPR31.4 after radiation. In

addition, L929 fibroblasts had no influence on the radiation response of MPR31.4, but induced MP31.4's EMT. Therefore, the differential effects of fibroblasts on the cancer cell radiation response cannot be simply explained by EMT induction in cancer cells.

E. Fibroblasts' activation into CAFs by cancer cells

The communication between stromal cells and cancer cells was shown to be bidirectional[23]. Concerning the hypothesis that cancer cells were able to activate fibroblasts into pro-tumorigenic CAFs we quantified typical CAFs markers (α-SMA, PDGFR-β, and NG2) in mRNA isolated from fibroblasts via qRT-PCR. NIH-3T3 and L929 fibroblasts were generated in the same indirect co-culture system as described above and cultured with cancer cells for 72h after XRT (of both cell lines).

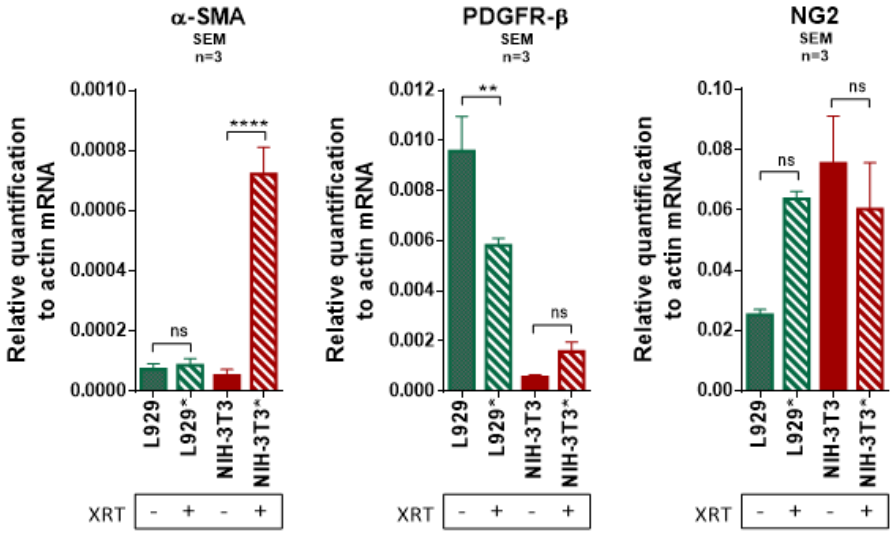

Figure IV.17: **Radiation alone was not sufficient to induce a CAFs phenotype in short-term indirect co-culture.** L929 or NIH-3T3 stromal fibroblasts alone were cultured alone 24h prior irradiation with 0 or 10Gy. After 72h, qRT-PCR analysis of the CAFs markers α-SMA, PDGFR-β and NG2 were performed in total RNA isolates of cultured fibroblasts. Respective expression levels were normalized to β-actin (set at 1). Shown are mean values ± SEM from 3 independent samples per group measured each in triplicate. "ns" present for no significant, **p<0.01, ****p<0.0001 analyzed by one-way ANOVA test followed by Tukey's test.

First, the effect of the radiation alone on the fibroblast activation phenotype was analyzed. Fibroblasts L929 and NIH-3T3 were plated and cultured for 72h after radiation (Figure IV.17). Radiation alone was not able to induce a CAFs phenotype into L929 and NIH-3T3 fibroblasts. Radiation induced a decrease of PDGFR-β of

approximately 1.5-fold and no change of α-SMA and NG2 in L929 fibroblasts. Instead radiation induced an increase of α-SMA expression by about 7-fold in NIH-3T3 fibroblasts when compared to non-irradiated controls, whereas NG2 and PDGFR-β expression was not significantly changed. Thus, radiation alone is not sufficient to induce a significant change in the fibroblast phenotype.

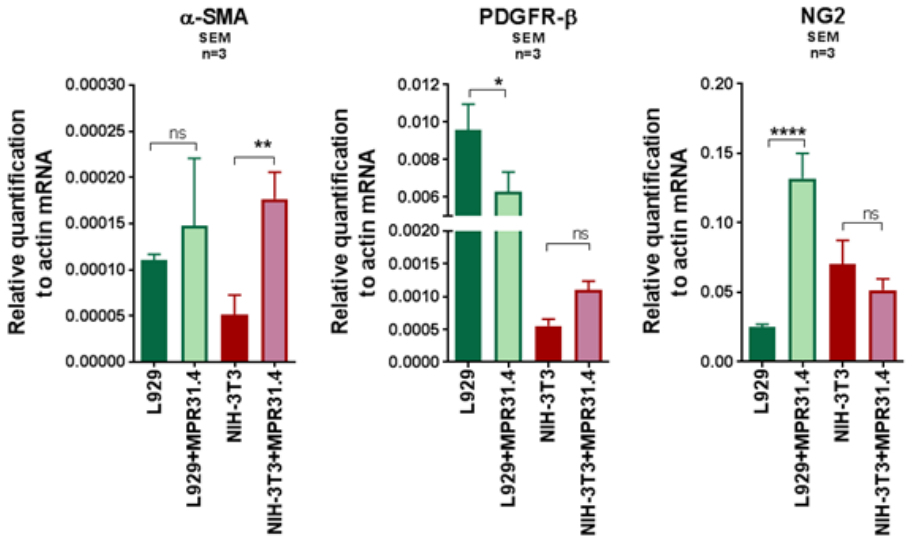

Figure IV.18: **Cancer cells didn't induce a CAF phenotype in fibroblasts in short-term indirect co-culture**. L929 or NIH-3T3 stromal fibroblasts were cultured alone or together with MPR31.4 (transwell, ratio1-1). After 72h, qRT-PCR analysis of the CAFs markers α-SMA, PDGFR-β and NG2 were performed in total RNA isolates of cultured fibroblasts. Respective expression levels were normalized to β-actin (set at 1). Shown are mean values ± SEM from 3 independent samples per group measured each in triplicate. "ns" present for no significant, *p<0.5, **p<0.01 and ****p<0.0001 analyzed by one-way ANOVA test followed by Tukey's test.

Next, the effect of the cancer cells on the fibroblast's phenotype was analyzed (Figure IV.18). MPR31.4 induced a decrease in PDGFR-β expression by about 1.5-fold, an increase in NG2 of about 5-fold and did not change the expression of α-SMA in L929 when compared to L929 cultured alone. Surprisingly, MPR31.4 did not influence PDGFR-β and NG2 levels in NIH-3T3 although it increased α-SMA expression levels by about 3.5-fold in NIH-3T3. Even though, NIH-3T3 was shown to induce MPR31.4 radio-resistance in previous experiments. In addition, B16F10 did not influence α-SMA and PDGFR-β levels, however it decreased NG2 levels in NIH-3T3 fibroblasts (Supplementary figure VII.11). Thus, in contrast to our expectation

cancer cells did not induced CAFs-like phenotypes in fibroblasts in indirect co-culture, at least under the experimental conditions of the present thesis.

Finally, the effect of the cancer cells on the fibroblasts' phenotype after radiation was determined by measuring the RNA expression level of CAF markers after irradiation of cancer cells and fibroblasts into the indirect co-culture model.

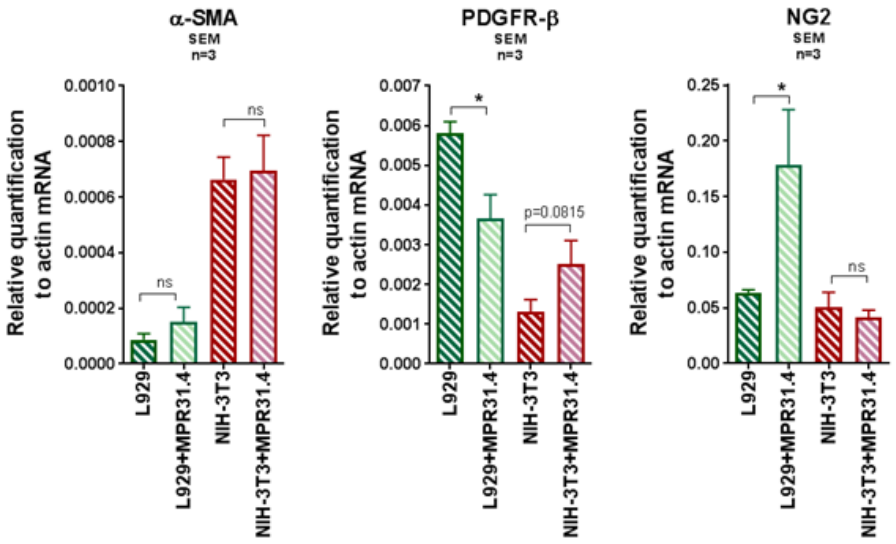

Figure IV.19: **Fibroblasts did not express a CAFs-like phenotype 72h after radiation in indirect co-culture with cancer cells**. L929 or NIH-3T3 stromal fibroblasts alone or together with MPR31.4 or B16F10 cancer cells (transwell, (ratio 1-1)) were cultured 24h prior irradiation with 0 or 10Gy. After 72h, qRT-PCR analysis of the CAFs markers α-SMA (Acta2), PDGFR-β and NG2 were performed in total RNA isolates of cultured fibroblasts. Respective expression levels were normalized to β-actin (set at 1). Shown are mean values ± SEM from 3 independent samples per group measured each in triplicate each. "ns" present for no significant and *p<0.5 analyzed by one-way ANOVA test followed by Tukey's test.

MPR31.4 did not influence α-SMA, PDGFR-β and NG2 levels in NIH-3T3 fibroblasts after IR. In L929 fibroblasts, after IR, MPR31.4 induced an increase of NG2 about 3.5-fold, a decrease of approximately 1.5-fold and did not influence α-SMA levels (Figure IV.19).

In conclusion, NIH-3T3 fibroblasts co-cultured indirectly with MPR31.4 cancer cells did not undergo a significant up-regulation of known CAFs markers except for α-SMA before or after radiation. This might indicate that an indirect co-culture with cancer cells is not sufficient to induce a CAF-like phenotype or that a larger number of CAFs markers needs to be investigated.

F. Fibroblasts phenotype in tumors

As the indirect co-culture of NIH-3T3 (or L929) and MPR31.4 or L929 and Py8119 did not reveal a clear CAF-like phenotype, α-SMA expression levels were analyzed in isolated tumor tissues of tumors raised from co-implantation of cancer cells (MPR31.4 and Py8119) and fibroblasts (NIH-3T3 and L9292), compared to the tumors generated from cancer cells alone. Tissue morphology and the composition of the tumors were evaluated by trichrome (TC) and Hematoxylin and Eosin (H&E) staining. TC is commonly used to selectively identify connective tissue (green), muscle and collagen fibers. Hematoxylin stains cell nuclei purplish blue. Eosin stains cell cytoplasm protein and connective tissue fibers in different shades of pink and red.

1. L929 skin fibroblasts

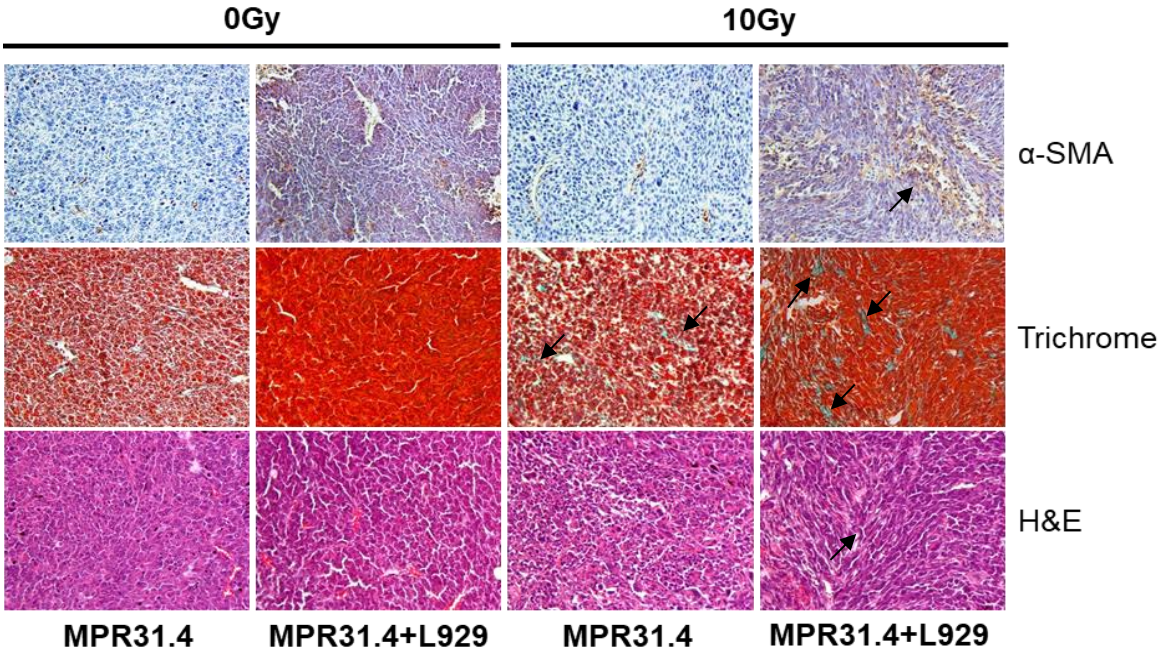

Figure IV.20 : **Stromal L929 fibroblasts induced a slight increase of the CAF marker, α-SMA as well as fibrotic compartment in irradiated tumors.** MPR31.4 prostate cancer cells alone or together with L929 fibroblasts (ratio of (1:1)) were subcutaneously co-implanted in C57BL/6 mice. At the end of the experiment, when tumor volumes reached a critical size (5–12 days after tumor irradiation) tumors were isolated and subjected to IHC using an α-SMA antibody. Masson Goldner trichrome and Hematoxylin and Eosin (HE) staining were performed in addition. Photomicrographs depict representative pictures of 2-3 experiments (5 mice in total) at 200x magnification.

A slight increase of α-SMA was observed by IHC staining in the tumors generated by co-implantation of MPR31.4 cells and L929 fibroblasts (which had no influence on the radiation response) compared to tumors generated from MPR31.4 cells alone, as indicated by the increase in the brown color (Figure IV.20). An increase in connective tissue fractions (in green, TC staining) and in fibrotic morphology (H&E) was also observed in the MPR31.4+L929 tumors after radiation when compared to MPR31.4 tumors.

These results suggested that MPR31.4 tumor generated with L929 fibroblasts have a more fibrotic phenotype. The low SMA levels might indicate that the fibroblasts present in the tumors were not reactive tumor-promoting CAFs.

Besides, similar results as MPR31.4+L929 were observed in Py8119+NIH-3T3 tumors compared to Py8119 tumors (Supplementary figure VII.8).

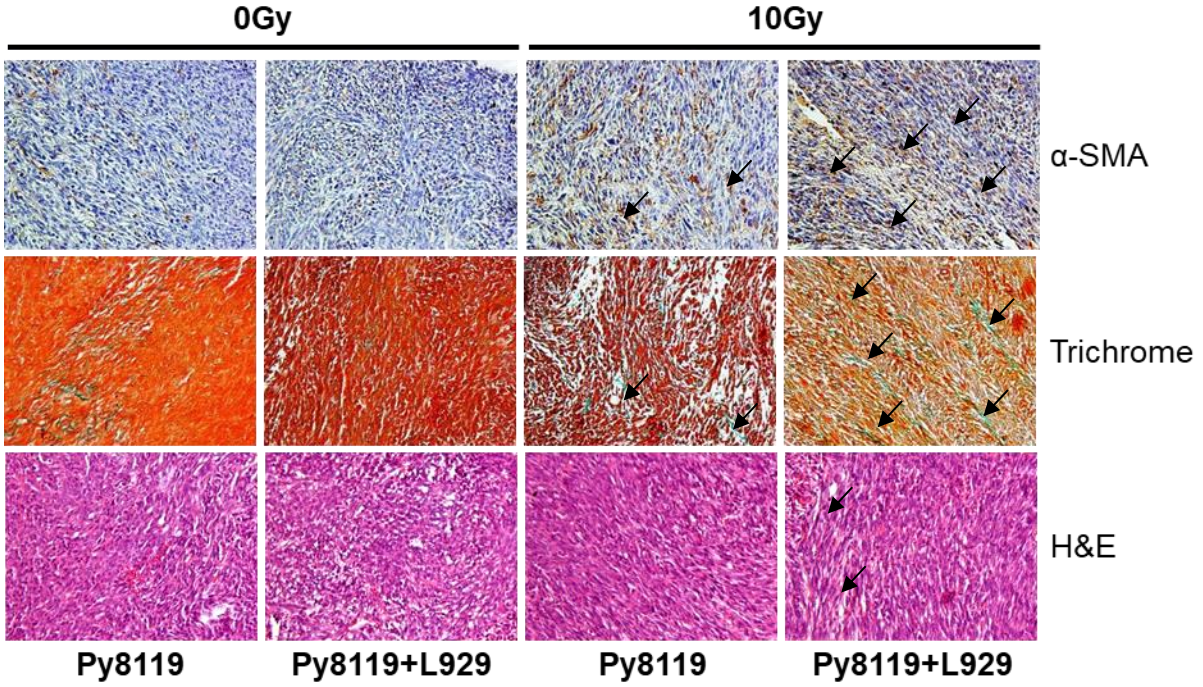

Figure IV.21 : **L929 stromal fibroblasts led to a strong increase in the expression of the CAF marker, α-SMA and enhanced levels of fibrotic compartments in the tumor after irradiation.** Py8119 breast cancer cells alone or together with L929 fibroblasts (ratio of (1:1)) were subcutaneously co-implanted onto C57BL/6 mice. At the end of the experiment, when tumor volumes reached a critical size (5–12 days after tumor irradiation) tumors were isolated and subjected for IHC using an α-SMA antibody. Masson Goldner trichrome and HE stains were performed in addition. Representatives' pictures were shown from 2-3 experiments (5 mice in total) at 200x magnification.

On the contrary, Py8119+L929 (which were shown to induce a tumor radio-resistance) showed a strong increase in α-SMA expression after radiation compared to the Py8119 tumor alone and a large increased in connective tissue expression (in green, TC staining) as well as in fibrotic areas (figure IV.21).

2. NIH-3T3 fibroblasts

Tumors generated with co-implantation of MPR31.4+NIH-3T3 (which were shown to induce a tumor radio-resistance) showed a strong increase in α-SMA expression after radiation compared to the MPR31.4 tumor alone and a large increase of connective tissue and of fibrotic areas (figure IV.22).

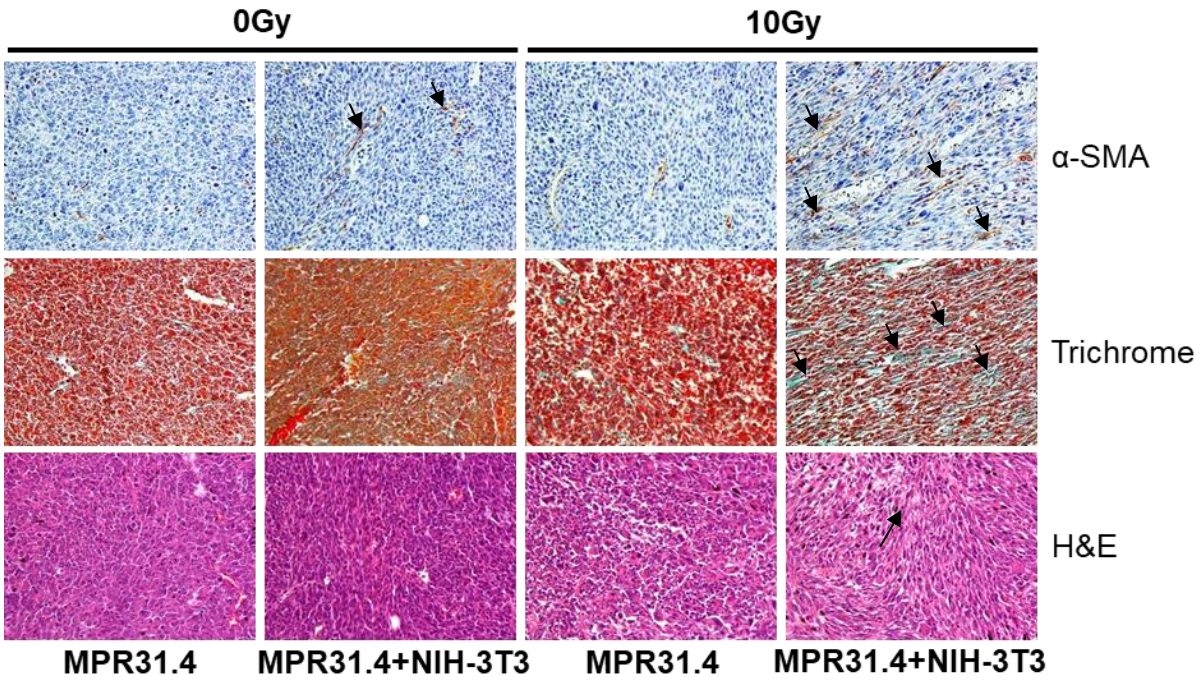

Figure IV.22: **NIH-3T3 stromal fibroblasts led to a strong increase of CAFs marker, α-SMA as well as fibrotic compartment in the tumor after irradiation.** MPR31.4 prostate cancer cells alone or together with NIH-3T3 fibroblasts (ratio of (1:1)) were subcutaneously co-implanted onto C57BL/6 mice. When tumor volumes reached a critical size (5–12 days after tumor irradiation) tumors were isolated and subjected for α-SMA IHC, Masson Goldner trichrome and HE stains. Representatives' pictures were shown from 2-3 experiments (5 mice total).

These results suggested that MPR31.4+NIH-3T3 and Py8119+L929 tumors might contain more reactive stroma and activated pro-tumorigenic CAFs which are illustrated by strong α-SMA expression levels, whereas MPR31.4+L929 might contain less activated CAFs. These activated pro-tumorigenic CAFs might contribute to increased radio-resistance of the tumors.

V. DISCUSSION

A. Tumor promoting effect of Cancer-associated fibroblasts

1. Pro-tumorigenic activities of CAFs

Research during the last decade revealed that CAFs play an essential role in the tumor development[102,103]. Direct stimulation of cancer cells by CAFs-derived signals promote cancer cells proliferation[104,105]. Indeed, in the present study, it was confirmed that fibroblasts-derived signal increased proliferation and reduced cancer cells death in short-term experiments *in vitro*. NIH-3T3 fibroblasts were shown to promote MPR31.4 prostate cancer cells proliferation and L929 fibroblasts were shown to promote Py8119 breast cancer cells proliferation in indirect co-culture through paracrine derived signals. Consistent with the observations of the present study, direct stimulation of cancer cells by CAF-derived signals enhanced also migration and invasion[106,107] as described by Owens *et al*. and Pena *et al*. CAFs-derived signals (e.g. MMP) also promoted the adoption of cancer stem cells phenotype via EMT induction which led to a higher cancer aggressiveness[101,108]. Indeed, breast and prostate cancer cells undergoing EMT were shown to lose cell-cell contacts and acquire a mesenchymal phenotype developing invasive and migratory abilities thereby escaping the primary tumor and allowing dissemination of metastases at distance, as well as developing stem-like properties[109]. However, in contrast with these findings, in the present study, EMT was only induced in MPR31.4 prostate cancer cells by L929 skin fibroblasts after 96h of indirect co-culture. The time of indirect co-culture were suspected to be insufficient for fibroblasts to definitively act on cancer cells.

The pro-tumorigenic functions of CAFs are generally determined by their transformed secretome[67,110,111]. CAFs up-regulate genes as chemokines like CXCL2, CXCL1, CXCL5 or CCL3, cytokines like IL-6, IL-1β or IL-1F9, IL-11 and ECM components like MMP12 or MMP3 as well as serglycin or cyclooxygenase (Cox-2) compared to normal fibroblasts[111]. Pro-tumorigenic activities of CAFs induce strong paracrine effects impacting on different cell types present in the tumor like platelet, endothelial or immune cells and involved host cells recruitment[112–114]. For example, platelet protect circulating tumor cells from immune system, as well as assist them during extravasation[115]. It is a rich source of TGF-β[116]. Calon *et al.*, showed that

colorectal tumor-derived TGF-β promote IL-11 production from CAFs to increase platelet activation which may further enhance stromal TGF-β response[113]. Moreover, *Jia et al*. show that isolated CAFs from hepatocellular carcinoma (HCC) promote the growth of HCC via the secretion of HGF[104]. Thus, determination of specific CAF secretome is important to better understand CAF pro-tumorigenic activities.

2. CAFs induce radio-resistance

Radiotherapy plays a central part in curing cancer. For decades, most research on improving treatment outcomes has focused on modulating radiation-induced biological effects on cancer cells, ignoring complex biological exchanges between the tumor and its surroundings[117]. The TME start to be recognized as a pivotal importance in cancer radiation response[84]. Factually, in the present study, fibroblasts-derived signal and direct interaction with cancer cells promoted cancer cells long-term survival after radiation in 2D and 3D experiments *in vitro*. Fibroblasts induced tumor radio-resistance *in vivo* with an increase of tumor proliferation. NIH-3T3 embryonic fibroblasts were shown to promote better clonogenic MPR31.4 prostate cancer cells survival after radiation in direct 3D and indirect 2D co-culture as well as to induce tumor growth delay and radio-resistance *in vivo*. In addition, L929 skin fibroblasts were shown to promote clonogenic Py8119 breast cancer cells survival in indirect co-culture and to induce tumor growth delay and radio-resistance *in vivo*. In this context, the CAFs showed the ability to promote tumor radio-resistance and tumor proliferation after IR. Overall, in this set of experiments, fibroblasts exerted a tumor-promoting and radio-resistance effect. It would be interesting to characterize the change in those CAFs secretome which lead to cancer cells radio-resistance.

Precisely, IR leads to a quick, total and persistent activation of the TME[118]. Damage from ionizing radiation leads to effects on numerous cell types within the TME. Tumor endothelial cells are sensitive to radiation, and the death of these cells initiates the inflammation cascade. Radiation-induced vascular damage potentiates tumor hypoxia and triggers immune responses through the increased production of cytokines and chemokines that induce immune cells recruitment. CAF activation (illustrating by a strong α-SMA expression in the tumor after IR) following radiation

leads to altered growth factor secretion and to the release of numerous modulators of the extracellular matrix (ECM) and cytokines[84].

It has been shown that exposure of fibroblasts to growth factors (TGF-β, PDGF), cytokine (e.g. IL-1, IL-6) and ROS or a rigid matrix can induce a CAFs phenotype[119,120]. Many cytokines are induced by IR (e.g. epidermal growth factor[121], pro-inflammatory cytokines[122], fibroblasts growth factor). Additionally, irradiated lung and pancreatic CAFs have been reported to show changes in secretory signal with consequence for tumor growth and invasion[123,124]. Hellevick *et al*. showed that CAFs isolated from lung tumors and exposed to IR result in downregulation of angiogenic molecules secretions such as stromal cell-derived factor-1 (SCDF-1), angiopoietin, and thrombospondin-2 and in up- regulation of basic fibroblast growth factor (FGF) released. Besides, it was also shown that breast cancer cell grown in association with chronic irradiated fibroblasts in a three dimensional co-culture increase malignant behavior and progression[125]. Moreover, high abundance of CAFs, leukocytes and endothelial cells in rectal tumor predict RT resistance[126].

In addition, pro-tumorigenic CAFs secrete variety of pro-inflammatory factors[110,127] leading to the recruitment and promotion of immunosuppressive[128] and tumor promoting immune cells[129] which contribute to a tumor permissive environment. Tumor progression requires the cancer cells to develop resistance to immune attack. Thus, immune cells may play a role in the CAFs-induced tumor radio-resistance phenotype.

In accordance with this knowledge, tumor tissues were isolated and subjected for IHC for CD45 specifics markers of immune cells (Figure V.1). Preliminary data indicate that tumors generated by co-implantation of MPR31.4+NIH-3T3 and Py8119+L929 were more reactive to CD45 (brown staining, arrow) after IR compared to the tumor generated with cancer cells alone or with co-implantation of MPR31.4+L929. Tumors MPR31.4+NIH-3T3 and Py8119+L929 which showed tumor radio-resistance before, had a stronger immune cells infiltration after IR. These data suggested that immune infiltration induced by radiation and CAFs may play a role in the tumor radiation response.

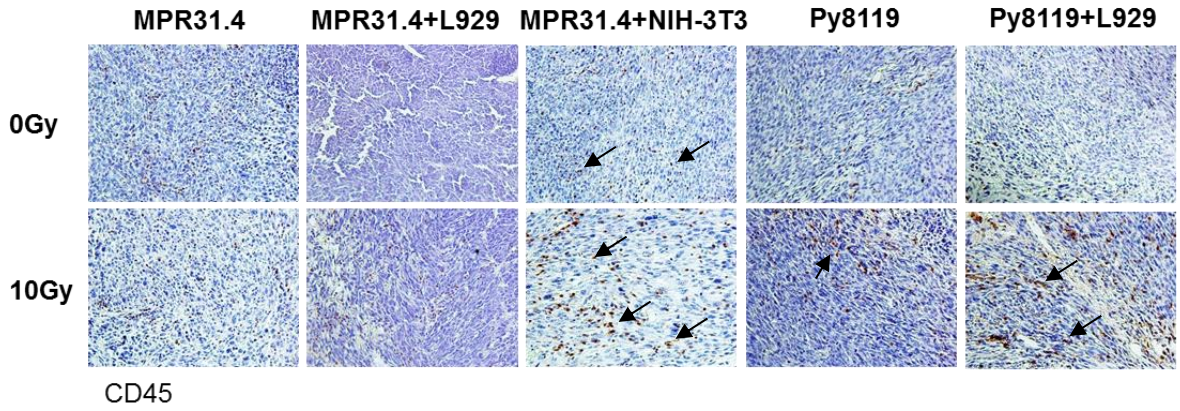

Figure V.1: **NIH-3T3 fibroblasts led to an increase of immune infiltration into MPR31.4 tumors as well as L929 fibroblasts into Py8119 tumors after irradiation.** MPR31.4 prostate or Py8119 breast cancer cells alone or together with NIH-3T3 or L929 fibroblasts (ratio of (1:1)) were subcutaneously co-implanted onto C57BL/6 mice. When tumor volumes reached a critical size (5–21 days after tumor irradiation) tumors were isolated and subjected for CD45 IHC staining. Representatives' pictures were shown from 2-3 experiments (5 mice total).

It would be interesting to characterize which type of immune cells infiltrated the tumor in this context. Tumor phenotype can be separated into two main groups, based on rich or poor infiltration of T lymphocytes, often referred to as "hot" and "cold" tumors, respectively[130,131]. In hot tumors the relative proportion of T CD8 effector cells and T regulatory cells differs, reflecting different degrees of immunosuppression and influencing the tendency of a tumor to progress[132]. IL-6 produced by CAFs constrains the maturation of dendritic cells and redirects monocytes toward macrophage differentiation[133]. In addition, CAFs producing CXCL12 and CCL2 chemokines can recruit macrophage into the TME and support their differentiation into the tumor-associated macrophage type 2 (TAM-2) activated phenotype[129]. Moreover, Comito *et al* already showed that CAFs support the differentiation of macrophage into tumor-promoting TAM-2 in prostate tumors. Furthermore, myeloid derived suppressor cells can also be recruited by CAFs secreted chemokines and inhibit the activity of natural killer (NK) and T cells in the TME as well as induce agiogenesis[75].

Thus, it can only be speculated that hereby, CAFs promote the recruitment of immunosuppressive and tumor-promoting immune cells in the prostate and breast tumors after radiation which lead to the protection of the tumor from radiation.

3. Importance of stoma/tumor cells ratio

The present study demonstrates the cancer cell/stromal fibroblast proportion in the tumor might impact the outcome of radiotherapy under certain conditions. Thereby these findings implicate that the contribution of stromal fibroblasts to tumor progression and therapy response might depend on the ability of the cancer cells to activate the surrounding stromal fibroblasts. Higher numbers of fibroblasts could thus mean less fibroblast activation by the cancer cells. Cancer cells might need more time to activate a higher number of fibroblasts. Indeed, our results revealed that increasing the fibroblasts/cancer cell ratio had no influence in short-term experiments but had a strong influence in long term and more clinically relevant *in vivo* experiments. As described previously, normal fibroblasts have a tumor-inhibiting effect[43]. Then, fibroblasts are activated into CAFs by the cancer cells. But, the pro-tumorigenic activity of CAFs evolves gradually depending of the amount of signal they receive from the cancer cells and the TME. Tumors were isolated 7 to 15 days after implantation due to the legal and ethical tumor size limitation. Cancer cells might not have the time to transform the fibroblasts into pro-tumorigenic CAFs in this model when a higher number of fibroblasts was implanted. However, clinical studies revealed that patients with high stromal/carcinoma ratios have a poor prognosis. E.g. In colorectal cancer[134] and in oral squamous cell carcinoma[135], high tumor/stroma ratios led to treatment resistance and worse outcome. To study more in detail the impact of stroma/cancer cells ratio on tumor radiation response, it would be interesting to establish long-term *in vivo* experiments (weeks) with low cancer cells amount implantation and/or with patient derived CAFs. Organoids implantations composed of different cancer cells/fibroblasts ratio could be also another possibility. Different and higher ratio of cancer cells/fibroblasts could be study to determine more precisely how and when the cancer cells success to transform fibroblasts into pro-tumorigenic CAFs. Proportion of fibroblasts/cancer cells and normal fibroblasts/CAFs at the time of radiation would be also interesting to investigate for a better understanding of how tumor become radio-resistant. However, the difficulty to characterize a specific CAF phenotype with specific markers limit the possible investigation.

B. Tumor suppressive effect of cancer-associated fibroblasts

In the present study, fibroblasts were also shown to have tumor-suppressive phenotype. Fibroblast-derived signals increased cancer cell death in short-term experiments *in vitro* and reduced tumor cell proliferation *in vivo*. Even though, fibroblasts did not impact cancer cell long-term survival, tumor growth and radiation response. Indeed, NIH-3T3 embryonic fibroblasts revealed to have inhibitory effect on B16F10 melanoma cells and L929 skin fibroblasts were shown to have an inhibitory effect on MPR31.4 prostate cancer cells. However, NIH-3T3 were shown to support MPR31.4 tumor and L929 revealed to support Py8119 breast cancer cells. Thus, the inhibitory effect of fibroblasts was also dependent of the tissue origin and the tumor cells type.

Consistent with this findings, recent data obtained from *in vitro* co-culture and *in vivo* xenograft models[53,136] suggest a tumor inhibitory role of CAFs. E.g. Sonic hedgehod (Shh), a soluble ligand overexpressed in pancreatic cancer, drives formation of a fibroblasts-rich desmoplastic stroma. To better understand its role in malignant progression, Rhim *et al*, deleted Shh in a mouse model. Shh-deficient tumors showed a reduced stromal content but tumors were more aggressive[137]. In addition, Özdemir *et al*, revealed that depletion of myofibroblasts in mouse pancreas cancer by targeting α-SMA+ cells led to invasive tumors associated with decrease of survival[136]. Some components of the stroma can act to restrain tumor growth. Fibroblasts from normal and cancer tissue can inhibit growth of a panel of co-cultured cancer cells[138]. Flaberg *et al*, showed *in vitro* that the proliferation inhibiting effect of the fibroblasts differed depending on their site of origin and the age of the donor[138]. The fibroblasts panel (up to 107) included both adult and pediatric sample from skin and from internal sites such as the inguinal hernia sac and the prostate. 6 human tumor cell lines (LnCap, DU-145, IB4, H1299, PC-3 and A549) were used. Pediatric fibroblasts were shown to have significantly stronger inhibitory effect on LnCap than adult fibroblasts. The opposite was true for PC3 where fibroblasts from adult donors could better inhibit proliferation of PC3. In overall, skin fibroblasts showed a better inhibitory capacity than fibroblast derived from internal sites. In addition, the majority of the analyzed fibroblast samples inhibited the proliferation of the slowly growing cells line as LnCap, Du-145 and IB-4. The co-culture of the fast-

growing tumor cells (H1299, PC-3 and A549) revealed a full spectrum of growth ranging from strong inhibition to no inhibition or to support of growth.

CAFs express a variety of different factors that contribute to shaping the tumor environment. CAFs derived factors act in a cell type and/or tumor stage-dependent manner. E.g. TGF-β (which CAFs is an important source) suppresses tumor initiation and early tumor growth[139] but promotes tumor progression and metastasis[140]. In general TGF-β is early express in irradiated tissue due to the fact that the ECM is a reservoir for TGF-β[141]. Determination of TGF-β status in our tumor tissues would be interesting.

The molecular mechanisms underlying the differential action of CAFs from promoting to inhibiting tumors, still needs to be elucidated. One mechanism known so far was provided by Chang *et al.:* herein primary fibroblasts (CAFs or normal breast-associated fibroblasts (NAFs)) were isolated from breast cancer patients. MDA-MB-231 and SKBR3 breast cancer cells were co-cultured with those primary fibroblasts. By cDNA microarrays Robo1 was found as an interesting candidate which might explain the contrasting phenotypes of the fibroblast-suppressing cell lines versus the fibroblast-promoting cancer cell lines. Normal fibroblasts and CAFs expressing the Robo1 ligand, Slit2 were shown to inhibit the tumor-promoting potential of breast cancer cells[142]. The tumorigenic inhibition of breast cancer cells is determined by an interaction between the Robo1 receptor and its ligand Slit2, which is secreted by stromal fibroblasts. Clinically, high Robo1 expression in the breast cancer cells was associated with better breast cancer patients' survival, and low Slit2 expression in the breast stromal fibroblasts was related to lymph node metastasis. However, tumor-inhibiting functions of CAFs are poorly investigated.

Tumor promoting or tumor inhibiting activities of CAFs is determined by their intrinsic properties like the immune or ECM modulation, and how the signals are processed by the TME[102,143]. Anti-tumor properties are predominantly associated with their function as regulators of anti-tumor immunity[49]. Indeed, tumors generated with fibroblasts sensitive to radiation showed a low level of immune infiltration (MPR31.4+L929, Figure IV.1). This suggests that fibroblasts may not be able to recruit and promote tumor-promoting immune cells as TAM-2 or T regulatory cells.

C. Heterogeneity of CAFs lead to CAFs subtype

Different cellular origins and tumor-derived factors shape the CAF phenotype. Identification and characterization of a CAF phenotype remains challenging. Several intracellular and plasma membranes associated proteins are used as CAF markers[49,144]. The markers that are the most commonly used to identify CAFs *in vivo* in pre-clinical and in clinical studies[54] include (i) ECM components such as collagen I, collagen II, fibrobnectin, TN-C and periostin, and remodeling enzymes, such as LOX, LOXL1, MMPs and TIMPs[145,146]; (ii) growth factors and cytokines, such as TGF-β, VAGF, PDGF, EGF, FGF, PGE2, CTGF, SDF-1 and WNTs[67,110,145]; (iii) receptors and other membrane-bound proteins, such as PDGFRα/β, VCAM1, DDR2, TGFβRI/II, EGFR, FGFRs, BMPRI, podolanin and FAP[23,147,148]; (iv) cytoskeleton components and other cytoplasmic proteins, such as desmin, vimentin, α-SMA and FSP1/S100A4[65,147]. Orr *et al* revealed additional markers such as ASPN, ZEB1 and OGN that distinguish prostate CAFs from their normal counterpart[149]. The established CAFs markers are not unique for fibroblasts cell type and are expressed by other cell types of the tumor (e.g smooth muscle cells, epithelial cells) which shows the plasticity of stromal cells.

In addition, within the same type of tissue, CAFs markers are not uniformly expressed on every CAFs[150,151]. Tchou *et al*, revealed that CAFs isolated from the three main subtype of breast cancer Her2+, ER+ and triple negative (TNBC) expressed different gene profiles. CAFs derived from Her2+ breast cancer were shown to up-regulate pathways associated with cytoskeleton and integrin signaling compare to CAFs derived from TNBC and ER+ cancer[150]. Sugimoto *et al* were first to describe different CAFs-subtypes base on expression analysis of FSP-1, PDGRβ, NG2 and α-SMA in pancreatic and breast cancer mouse model[65]. This study revealed that one CAFs-subtype expressed α-SMA, PDGRβ and NG2, another expressed FSP-1. However, it is not clear how many subtypes exists. In the present study, it was decided to characterize the different CAFs depending of their action on the tumor response. It was hypothesized that NIH-3T3 which induced MPR31.4 prostate tumor radio-resistance and L929 which induced Py8119 breast tumors radio-resistance were expressing different CAFs markers profile than NIH-3T3 which induced B16F10 melanoma inhibition and L929 which induced MPR31.4 prostate cancer cells inhibition. PDGFR-β, NG2 and α-SMA are the most characterized and used CAFs

markers in the literature, it is why they were chosen in this study. However, a clear and specific phenotype was not observed between the different fibroblasts. Those markers were differentially expressed from one fibroblast to another and were not linked to a specific function. Furthermore, like described previously, CAFs markers are strongly heterogeneous and not yet well determined. Other CAFs markers expression or gene expression profiles between the different fibroblasts generated need to be examined.

However, it is conceivable that different subtypes exert different functions even in the same tumor[145,152]. E.g. in pancreatic cancer different subtypes of CAFs can exert distinct paracrine actions that impact tumor-enhancing inflammation[153]. The pro-tumorigenic functions of CAFs could be attributed to their role in reprogramming and shaping the metabolic microenvironment of tumors[49,154]. In addition, the CAFs can act on stimulation with other stromal cells like immune cells or platelets leading to a dynamic microenvironment. A complex stimulating microenvironment of CAFs and tumor explain the differences observed in experiments between *in vitro* (2D versus 3D) and *in vivo* and their limitations. A tri co-culture cancer cells, fibroblasts and immune cells would be interesting to develop to mimic at its maximum the tumor complexity and its role on CAFs function. Isolation of CAFs directly from generated tumors which exerted a radio-resistance phenotype (MPR32.4+NIH-3T3 and Py8119+L929) or which exerted radio-sensitivity phenotype (MPR31.4+L929) could be used *in vitro* to better determine or characterize CAFs sub-populations with a specific function and radiation response. In addition, these CAFs isolated could be reimplanted in mice in combination of another cancer cells types to determine whether this CAFs still induce the same tumor radiation response as before or whether the new tumor entities change *de novo* the CAFs phenotype.

D. CAFs as another polarized cell type

Taken together, the presented results strongly suggest that the impact of fibroblasts on cancer cell radiation response largely depends on the fibroblast-tumor cell combination. Fibroblasts exerted either a tumor-suppressing effect, a tumor-promoting effect, or no effect, which leads to the speculation that the influence of the fibroblasts to alter (i) tumor progression and/or (ii) the therapeutic response may be determined by the cancer cells potential to activate the respective fibroblasts. In contrast to this observation, CAFs are currently defined by their tumor-promoting activities and their association with cancer cells within the tumor. However, the initial definition of CAFs is challenged by CAFs' functional diversity. As discuss previously, different elements like the diverse secretome of CAFs, their expression of signaling receptors together with epigenetic reprograming likely contribute to the plasticity and diverse phenotype of CAFs. To better express the dynamics state of fibroblasts, Mader *et al.* introduced the term "CAFs state" to describe the marker-based heterogeneity of these cells[54]. Moreover, Augsten *et al*, extend the concept of "polarization" used in the context of immune cells into CAFs[66]. CAFs type 1 and type 2 would mark the end of polarization spectrum and represent distinct cellular lineage associated with different markers and opposing activities in the tumor. CAFs1 would be shown to promote tumor growth and radiation resistance by secreting survival signal, remodeling ECM to favor invasion and reshape tumor immunity to favor immunosuppressive environment, when CAFs2 would induce tumor-suppressive effect and radio-sensitivity, restrain growth by remodeling the ECM and eliciting an anti-tumor immune response.

Polarization appears to be a more general phenomenon[155]. Indeed, different tumor associated cells types actively regulate the polarization status of each other. For example, it is known that CAFs-derived signals can promote the polarization of T CD4+ lymphocytes to adopt a tumor-suppressive phenotype[156]. Main of the research studying the impact of CAFs on cancer cells and CAFs characterization use co-culture of CAFs and cancer cells. However, in human tumors every stromal cell influence activation state and phenotype of each other.

However, considering the tumor heterogeneity, a certain CAF subtype might display suppressive effect in a particular tumor microenvironment while having stimulatory effect in another[157].

Nevertheless, genetically engineered mouse models (GEMMS) are offering new insight on functional heterogeneity[136]. For example, the study of GEMMS designed to delete the pro-angiogenic growth factor VEGFs in breast CAFs revealed that there are distinct functional subtype of CAFs[145]. O'connell *and al* showed that FSP positive (S100A4+) stromal fibroblasts are important for metastatic colonization of breast tumors.

The most challenging aspect in the study of CAFs is to characterize heterogeneous CAFs subpopulation markers that inform on their functions at distinct stages of cancer progression. This would be beneficial for cancer treatment.

E. Conclusion

The impact of fibroblasts on tumor cells radiation response largely depends on the fibroblast and tumor cell type, the culture conditions (direct/indirect co-culture) and the respective endpoint (short-term versus long-term; *in vitro* versus *in vivo*).

In indirect co-culture, MPR31.4+NIH-3T3 and Py8119+L929 were shown to have less cell death and a better proliferation in indirect short-term co-culture. They expressed a better clonogenic survival after radiation in indirect 2D co-culture and in direct 3D co-culture. They were also shown to increase tumor proliferation and to be radio-resistant *in vivo*. On the contrary, MPR31.4+L929 and B16F10+NIH-3T3 were shown to increase cell death in short term after radiation and to express no difference in clonogenic survival in indirect 2D co-culture. They were also shown to have less proliferation *in vivo* and no impact on the tumor radiation response.

Thus, fibroblasts exerted either a tumor-promoting and radioresistant effect, a tumor-suppressing effect or no effect. This observation may be explained by the fact that tumor-residing fibroblasts exhibit a certain degree of plasticity as other stromal cells types and that the same type of CAFs can exert a broader spectrum of activities ranging from tumor stimulation to tumor inhibition[66,158] (Figure V.2). However, deeper CAFs phenotype characterization would be necessary to determine which

type of CAFs is involve in tumor radiation response. Identification of better and more specific CAFs markers are needed as well as the mechanism underlying the influence of the CAFs on the tumor cells. Which type of CAFs induce radio-resistance and how.

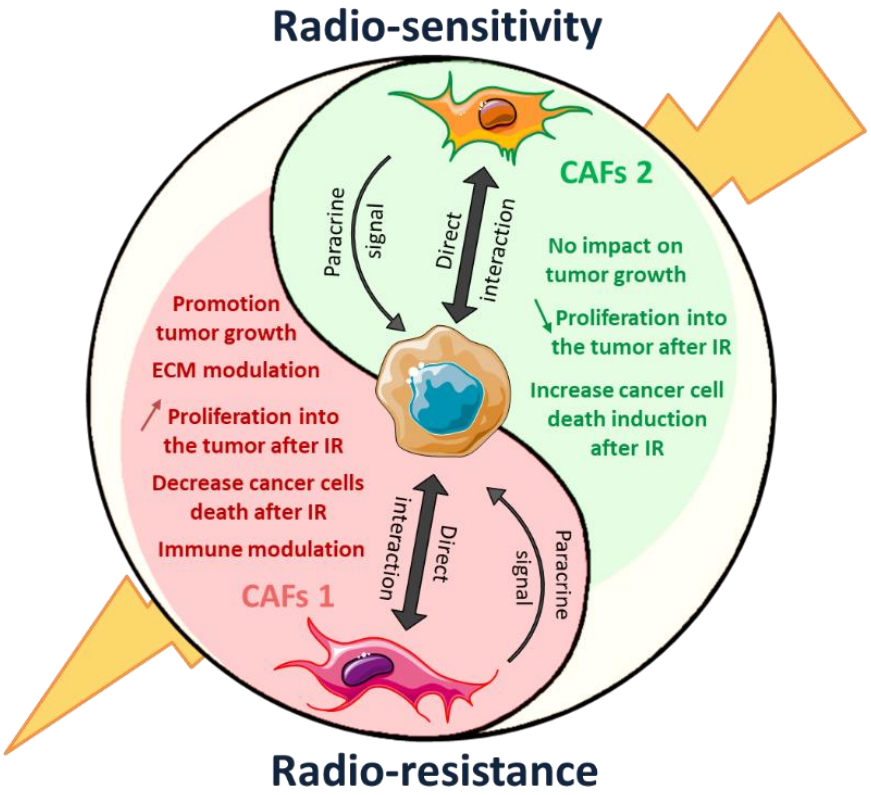

Figure V.2: **Dual role of CAFs on radiation response of solid tumor: another polarized cell type of the tumor microenvironment.** CAFs 1 and 2 mark the end of the polarization spectrum, represent distinct cellular lineage associated with different markers and opposing activities in the tumor. CAFs1 (in red) shown promotion of tumor growth and radiation resistance. When CAFs2, another type of CAFs, induced tumor-suppressive effect.

VI. REFERENCES

1. WHO | Global status report on noncommunicable diseases 2014. *WHO* (2015).
2. Bray, F. *et al.* Global cancer statistics 2018: GLOBOCAN estimates of incidence and mortality worldwide for 36 cancers in 185 countries. *CA. Cancer J. Clin.* (2018). doi:10.3322/caac.21492
3. Pietras, K. & Östman, A. Hallmarks of cancer: Interactions with the tumor stroma. *Exp. Cell Res.* **316**, 1324–1331 (2010).
4. Hanahan, D. & Weinberg, R. A. The hallmarks of cancer. *Cell* **100**, 57–70 (2000).
5. Hanahan, D. & Weinberg, R. A. Hallmarks of Cancer: The Next Generation. *Cell* **144**, 646–674 (2011).
6. Bissell, M. J. & Radisky, D. Putting tumours in context. *Nat. Rev. Cancer* **1**, 46–54 (2001).
7. Furuta, S., Ghajar, C. M. & Bissell, M. J. Caveolin-1: Would-be Achilles' heel of tumor microenvironment? *Cell Cycle* **10**, 3431 (2011).
8. Takahashi, H. *et al.* Cancer-associated fibroblasts promote an immunosuppressive microenvironment through the induction and accumulation of protumoral macrophages. *Oncotarget* **8**, 8633–8647 (2017).
9. Turley, S. J., Cremasco, V. & Astarita, J. L. Immunological hallmarks of stromal cells in the tumour microenvironment. *Nat. Rev. Immunol.* **15**, 669–682 (2015).
10. De Wever, O. & Mareel, M. Role of tissue stroma in cancer cell invasion. *J. Pathol.* **200**, 429–447 (2003).
11. Leef, G. & Thomas, S. M. Molecular communication between tumor-associated fibroblasts and head and neck squamous cell carcinoma. *Oral Oncol.* **49**, 381–386 (2013).
12. Kalluri, R. & Zeisberg, M. Fibroblasts in cancer. *Nat. Rev. Cancer* **6**, 392–401 (2006).
13. Franco, O. E., Shaw, A. K., Strand, D. W. & Hayward, S. W. Cancer associated fibroblasts in cancer pathogenesis. *Semin. Cell Dev. Biol.* **21**, 33–39 (2010).
14. Lewis, M. P. *et al.* Tumour-derived TGF-β1 modulates myofibroblast differentiation and promotes HGF/SF-dependent invasion of squamous carcinoma cells. *Br. J. Cancer* **90**, 822–832 (2004).
15. Dudás, J. *et al.* Tumor-produced, active Interleukin-1 β regulates gene expression in carcinoma-associated fibroblasts. *Exp. Cell Res.* **317**, 2222–2229 (2011).
16. Neesse, A. *et al.* Stromal biology and therapy in pancreatic cancer. *Gut* **60**, 861–8 (2011).
17. Smith, N. R. *et al.* Tumor stromal architecture can define the intrinsic tumor response to VEGF-targeted therapy. *Clin. Cancer Res.* **19**, 6943–56 (2013).
18. Östman, A. & Augsten, M. Cancer-associated fibroblasts and tumor growth – bystanders turning into key players. *Curr. Opin. Genet. Dev.* **19**, 67–73 (2009).
19. Neesse, A. *et al.* Stromal biology and therapy in pancreatic cancer. *Gut* **60**, 861–8 (2011).
20. Smith, N. R. *et al.* Tumor stromal architecture can define the intrinsic tumor response to VEGF-targeted therapy. *Clin. Cancer Res.* **19**, 6943–56 (2013).
21. Leyva-Illades, D., McMillin, M., Quinn, M. & Demorrow, S. Cholangiocarcinoma pathogenesis: Role of the tumor microenvironment. *Transl. Gastrointest. Cancer* **1**, 71–80 (2012).
22. Onimaru, M. & Yonemitsu, Y. Angiogenic and lymphangiogenic cascades in the tumor microenvironment. *Front. Biosci. (Schol. Ed).* **3**, 216–25 (2011).
23. Räsänen, K. & Vaheri, A. Activation of fibroblasts in cancer stroma. *Exp. Cell Res.* **316**, 2713–2722 (2010).
24. Rojas, A., Figueroa, H. & Morales, E. Fueling inflammation at tumor microenvironment: the role of multiligand/rage axis. *Carcinogenesis* **31**, 334–341 (2010).

25. Bhowmick, N. A., Neilson, E. G. & Moses, H. L. Stromal fibroblasts in cancer initiation and progression. *Nature* **432**, 332–7 (2004).

26. Bhowmick, N. A. *et al.* TGF-beta signaling in fibroblasts modulates the oncogenic potential of adjacent epithelia. *Science* **303**, 848–51 (2004).

27. Strnad, H. *et al.* Head and neck squamous cancer stromal fibroblasts produce growth factors influencing phenotype of normal human keratinocytes. *Histochem. Cell Biol.* **133**, 201–211 (2010).

28. LeBedis, C., Chen, K., Fallavollita, L., Boutros, T. & Brodt, P. Peripheral lymph node stromal cells can promote growth and tumorigenicity of breast carcinoma cells through the release of IGF-I and EGF. *Int. J. Cancer* **100**, 2–8 (2002).

29. Thijssen, V. L. J. L., Brandwijk, R. J. M. G. E., Dings, R. P. M. & Griffioen, A. W. Angiogenesis gene expression profiling in xenograft models to study cellular interactions. *Exp. Cell Res.* **299**, 286–293 (2004).

30. Pietras, K., Pahler, J., Bergers, G. & Hanahan, D. Functions of paracrine PDGF signaling in the proangiogenic tumor stroma revealed by pharmacological targeting. *PLoS Med.* **5**, e19 (2008).

31. Sung, S.-Y. *et al.* Coevolution of prostate cancer and bone stroma in three-dimensional coculture: implications for cancer growth and metastasis. *Cancer Res.* **68**, 9996–10003 (2008).

32. Duvall, M. *Atlas d'Embryologie*. (1879).

33. Virchow, R. *Die Cellularpathologie in lhrer Begruendung auf Physiologische und Pathologische Gewebelehre*. (1858).

34. Tarin, D. & Croft, C. B. Ultrastructural features of wound healing in mouse skin. *J. Anat.* **105**, 189–90 (1969).

35. Gabbiani, G., Ryan, G. B. & Majno, G. Presence of modified fibroblasts in granulation tissue and their possible role in wound contraction. *Experientia* **27**, 549–550 (1971).

36. Lajiness, J. D. & Conway, S. J. The Dynamic Role of Cardiac Fibroblasts in Development and Disease. *J. Cardiovasc. Transl. Res.* **5**, 739–748 (2012).

37. WERNER, S. & GROSE, R. Regulation of Wound Healing by Growth Factors and Cytokines. *Physiol. Rev.* **83**, 835–870 (2003).

38. Hinz, B. Formation and Function of the Myofibroblast during Tissue Repair. *J. Invest. Dermatol.* **127**, 526–537 (2007).

39. Desmoulière, A., Darby, I. A. & Gabbiani, G. Normal and Pathologic Soft Tissue Remodeling: Role of the Myofibroblast, with Special Emphasis on Liver and Kidney Fibrosis. *Lab. Investig.* **83**, 1689–1707 (2003).

40. Tomasek, J. J., Gabbiani, G., Hinz, B., Chaponnier, C. & Brown, R. A. Myofibroblasts and mechano: Regulation of connective tissue remodelling. *Nat. Rev. Mol. Cell Biol.* **3**, 349–363 (2002).

41. Bartok, B. & Firestein, G. S. Fibroblast-like synoviocytes: key effector cells in rheumatoid arthritis. *Immunol. Rev.* **233**, 233–255 (2010).

42. Martin, W., Zempel, G., Hülser, D. & Willecke, K. Growth inhibition of oncogene-transformed rat fibroblasts by cocultured normal cells: relevance of metabolic cooperation mediated by gap junctions. *Cancer Res.* **51**, 5348–51 (1991).

43. Klein, G. Evolutionary aspects of cancer resistance. *Semin. Cancer Biol.* **25**, 10–14 (2014).

44. Alkasalias, T. *et al.* Fibroblasts in the Tumor Microenvironment: Shield or Spear? *Int. J. Mol. Sci.* **19**, 1532 (2018).

45. Dvorak, H. F. Tumors: wounds that do not heal-redux. *Cancer Immunol. Res.* **3**, 1–11 (2015).

46. Berdiel-Acer, M. *et al.* Differences between CAFs and their paired NCF from adjacent colonic mucosa reveal functional heterogeneity of CAFs, providing prognostic information. *Mol. Oncol.* **8**, 1290–1305 (2014).

47. Desmoulière, A., Geinoz, A., Gabbiani, F. & Gabbiani, G. Transforming growth factor-beta 1 induces alpha-smooth muscle actin expression in granulation tissue myofibroblasts and in quiescent and growing cultured fibroblasts. *J. Cell Biol.* **122**, 103–11 (1993).

48. Kojima, Y. *et al.* Autocrine TGF-beta and stromal cell-derived factor-1 (SDF-1) signaling drives the evolution of tumor-promoting mammary stromal myofibroblasts. *Proc. Natl. Acad. Sci. U. S. A.* **107**, 20009–14 (2010).

49. Kalluri, R. The biology and function of fibroblasts in cancer. *Nat. Rev. Cancer* **16**, 582–598 (2016).

50. Qiu, W. *et al.* No evidence of clonal somatic genetic alterations in cancer-associated fibroblasts from human breast and ovarian carcinomas. *Nat. Genet.* **40**, 650–655 (2008).

51. Walter, K., Omura, N., Hong, S.-M., Griffith, M. & Goggins, M. Pancreatic cancer associated fibroblasts display normal allelotypes. *Cancer Biol. Ther.* **7**, 882–8 (2008).

52. Hosein, A. N. *et al.* Breast carcinoma-associated fibroblasts rarely contain p53 mutations or chromosomal aberrations. *Cancer Res.* **70**, 5770–7 (2010).

53. Öhlund, D., Elyada, E. & Tuveson, D. Fibroblast heterogeneity in the cancer wound. *J. Exp. Med.* **211**, 1503–23 (2014).

54. Madar, S., Goldstein, I. & Rotter, V. 'Cancer associated fibroblasts' – more than meets the eye. *Trends Mol. Med.* **19**, 447–453 (2013).

55. Albrengues, J. *et al.* Epigenetic switch drives the conversion of fibroblasts into proinvasive cancer-associated fibroblasts. *Nat. Commun.* **6**, 10204 (2015).

56. Zeisberg, E. M. & Zeisberg, M. The role of promoter hypermethylation in fibroblast activation and fibrogenesis. *J. Pathol.* **229**, 264–273 (2013).

57. Li, P. *et al.* Epigenetic silencing of microRNA-149 in cancer-associated fibroblasts mediates prostaglandin E2/interleukin-6 signaling in the tumor microenvironment. *Cell Res.* **25**, 588–603 (2015).

58. Mrazek, A. A. *et al.* Colorectal Cancer-Associated Fibroblasts are Genotypically Distinct. *Curr. Cancer Ther. Rev.* **10**, 97–218 (2014).

59. LeBleu, V. S. & Kalluri, R. A peek into cancer-associated fibroblasts: origins, functions and translational impact. *Dis. Model. Mech.* **11**, dmm029447 (2018).

60. Hinz, B. *et al.* The myofibroblast: One function, multiple origins. *Am. J. Pathol.* **170**, 1807–1816 (2007).

61. LeBleu, V. S. *et al.* Origin and function of myofibroblasts in kidney fibrosis. *Nat. Med.* **19**, 1047–53 (2013).

62. Zeisberg, E. M., Potenta, S., Xie, L., Zeisberg, M. & Kalluri, R. Discovery of endothelial to mesenchymal transition as a source for carcinoma-associated fibroblasts. *Cancer Res.* **67**, 10123–8 (2007).

63. Iwano, M. *et al.* Evidence that fibroblasts derive from epithelium during tissue fibrosis. *J. Clin. Invest.* **110**, 341–50 (2002).

64. Ziani, L., Chouaib, S. & Thiery, J. Alteration of the Antitumor Immune Response by Cancer-Associated Fibroblasts. *Front. Immunol.* **9**, 414 (2018).

65. Sugimoto, H., Mundel, T. M., Kieran, M. W. & Kalluri, R. Identification of fibroblast heterogeneity in the tumor microenvironment. *Cancer Biol. Ther.* **5**, 1640–1646 (2006).

66. Augsten, M. Cancer-associated fibroblasts as another polarized cell type of the tumor microenvironment. *Front. Oncol.* **4**, 62 (2014).

67. Orimo, A. *et al.* Stromal Fibroblasts Present in Invasive Human Breast Carcinomas Promote Tumor Growth and Angiogenesis through Elevated SDF-1/CXCL12 Secretion. *Cell* **121**, 335–348 (2005).

68. Su, S. *et al.* CD10+GPR77+ Cancer-Associated Fibroblasts Promote Cancer Formation and Chemoresistance by Sustaining Cancer Stemness. *Cell* **172**, 841–856.e16 (2018).

69. Zhuang, J. *et al.* TGFβ1 secreted by cancer-associated fibroblasts induces epithelial-mesenchymal

transition of bladder cancer cells through lncRNA-ZEB2NAT. *Sci. Rep.* **5**, 11924 (2015).

70. Hawinkels, L. J. A. C. *et al.* Interaction with colon cancer cells hyperactivates TGF-β signaling in cancer-associated fibroblasts. *Oncogene* **33**, 97–107 (2014).

71. Kaler, P., Owusu, B. Y., Augenlicht, L. & Klampfer, L. The Role of STAT1 for Crosstalk between Fibroblasts and Colon Cancer Cells. *Front. Oncol.* **4**, 88 (2014).

72. Alexander, J. & Cukierman, E. Stromal dynamic reciprocity in cancer: intricacies of fibroblastic-ECM interactions. *Curr. Opin. Cell Biol.* **42**, 80–93 (2016).

73. De Wever, O., Van Bockstal, M., Mareel, M., Hendrix, A. & Bracke, M. Carcinoma-associated fibroblasts provide operational flexibility in metastasis. *Semin. Cancer Biol.* **25**, 33–46 (2014).

74. Cirri, P. & Chiarugi, P. Cancer associated fibroblasts: the dark side of the coin. *Am. J. Cancer Res.* **1**, 482–97 (2011).

75. Tommelein, J. *et al.* Cancer-Associated Fibroblasts Connect Metastasis-Promoting Communication in Colorectal Cancer. *Front. Oncol.* **5**, 63 (2015).

76. Types of Cancer Treatment - National Cancer Institute. Available at: https://www.cancer.gov/about-cancer/treatment/types. (Accessed: 21st November 2018)

77. Ito, E. *et al.* Uroporphyrinogen decarboxylase is a radiosensitizing target for head and neck cancer. *Sci. Transl. Med.* **3**, 67ra7 (2011).

78. Jaffray, D. A. & Gospodarowicz, M. K. *Radiation Therapy for Cancer*. *Cancer: Disease Control Priorities, Third Edition (Volume 3)* (The International Bank for Reconstruction and Development / The World Bank, 2015). doi:10.1596/978-1-4648-0349-9_CH14

79. Bray, F., Jemal, A., Grey, N., Ferlay, J. & Forman, D. Global cancer transitions according to the Human Development Index (2008–2030): a population-based study. *Lancet Oncol.* **13**, 790–801 (2012).

80. Eric J. Hall, A. J. G. *Radiobiology for the radiologist*. (2012).

81. Liauw, S. L., Connell, P. P. & Weichselbaum, R. R. New Paradigms and Future Challenges in Radiation Oncology: An Update of Biological Targets and Technology. *Sci. Transl. Med.* **5**, 173sr2-173sr2 (2013).

82. Desouky, O., Ding, N. & Zhou, G. Targeted and non-targeted effects of ionizing radiation. *J. Radiat. Res. Appl. Sci.* **8**, 247–254 (2015).

83. Mladenov, E., Magin, S., Soni, A. & Iliakis, G. DNA Double-Strand Break Repair as Determinant of Cellular Radiosensitivity to Killing and Target in Radiation Therapy. *Front. Oncol.* **3**, 113 (2013).

84. Barcellos-Hoff, M. H., Park, C. & Wright, E. G. Radiation and the microenvironment – tumorigenesis and therapy. *Nat. Rev. Cancer* **5**, 867–875 (2005).

85. Demaria, S., Bhardwaj, N., McBride, W. H. & Formenti, S. C. Combining radiotherapy and immunotherapy: A revived partnership. *Int. J. Radiat. Oncol.* **63**, 655–666 (2005).

86. Durand, R. E. The influence of microenvironmental factors during cancer therapy. *In Vivo* **8**, 691–702

87. Duluc, C. *et al.* Pharmacological targeting of the protein synthesis mTOR/4E-BP1 pathway in cancer-associated fibroblasts abrogates pancreatic tumour chemoresistance. *EMBO Mol. Med.* **7**, 735–53 (2015).

88. Zhang, H. *et al.* Paracrine SDF-1α signaling mediates the effects of PSCs on GEM chemoresistance through an IL-6 autocrine loop in pancreatic cancer cells. *Oncotarget* **6**, 3085–3097 (2015).

89. Hesler, R. A. *et al.* TGF-β-induced stromal CYR61 promotes resistance to gemcitabine in pancreatic ductal adenocarcinoma through downregulation of the nucleoside transporters hENT1 and hCNT3. *Carcinogenesis* **37**, 1041–1051 (2016).

90. Bonomi, A. *et al.* Gemcitabine-releasing mesenchymal stromal cells inhibit in vitro proliferation of human pancreatic carcinoma cells. *Cytotherapy* **17**, 1687–1695 (2015).

91. Dauer, P. *et al.* Inactivation of Cancer-Associated-Fibroblasts Disrupts Oncogenic Signaling in Pancreatic

Cancer Cells and Promotes Its Regression. *Cancer Res.* **78**, 1321–1333 (2018).

92. Scott, A. M. *et al.* A Phase I dose-escalation study of sibrotuzumab in patients with advanced or metastatic fibroblast activation protein-positive cancer. *Clin. Cancer Res.* **9**, 1639–47 (2003).

93. Jiang, G.-M. *et al.* The application of the fibroblast activation protein α-targeted immunotherapy strategy. *Oncotarget* **7**, 33472–33482 (2016).

94. Shaker, M. R. *et al.* Dietary 4-HPR suppresses the development of bone metastasis in vivo in a mouse model of prostate cancer progression. *Clin. Exp. Metastasis* **18**, 429–38 (2000).

95. Thompson, T. C. *et al.* Genetic predisposition and mesenchymal-epithelial interactions in ras + myc—induced carcinogenesis in reconstituted mouse prostate. *Mol. Carcinog.* **7**, 165–179 (1993).

96. Klein, D. *et al.* Endothelial Caveolin-1 regulates the radiation response of epithelial prostate tumors. *Oncogenesis* **4**, e148–e148 (2015).

97. Riccardi, C. & Nicoletti, I. Analysis of apoptosis by propidium iodide staining and flow cytometry. *Nat. Protoc.* **1**, 1458–1461 (2006).

98. Cordes, N. & van Beuningen, D. Cell adhesion to the extracellular matrix protein fibronectin modulates radiation-dependent G2 phase arrest involving integrin-linked kinase (ILK) and glycogen synthase kinase-3β (GSK-3β) in vitro. *Br. J. Cancer* **88**, 1470–1479 (2003).

99. Matschke, J. *et al.* Targeted Inhibition of Glutamine-Dependent Glutathione Metabolism Overcomes Death Resistance Induced by Chronic Cycling Hypoxia. *Antioxid. Redox Signal.* **25**, 89–107 (2016).

100. Huijbers, A. *et al.* The proportion of tumor-stroma as a strong prognosticator for stage II and III colon cancer patients: validation in the VICTOR trial. *Ann. Oncol.* **24**, 179–185 (2013).

101. Giannoni, E. *et al.* Reciprocal Activation of Prostate Cancer Cells and Cancer-Associated Fibroblasts Stimulates Epithelial-Mesenchymal Transition and Cancer Stemness. *Cancer Res.* **70**, 6945–6956 (2010).

102. Picard, O. *et al.* Fibroblast-dependent tumorigenicity of cells in nude mice: implication for implantation of metastases. *Cancer Res.* **46**, 3290–4 (1986).

103. Trimboli, A. J. *et al.* Pten in stromal fibroblasts suppresses mammary epithelial tumours. *Nature* **461**, 1084–1091 (2009).

104. Jia, C.-C. *et al.* Cancer-Associated Fibroblasts from Hepatocellular Carcinoma Promote Malignant Cell Proliferation by HGF Secretion. *PLoS One* **8**, e63243 (2013).

105. Subramaniam, K. S. *et al.* Cancer-Associated Fibroblasts Promote Proliferation of Endometrial Cancer Cells. *PLoS One* **8**, e68923 (2013).

106. Owens, P. *et al.* Bone Morphogenetic Proteins Stimulate Mammary Fibroblasts to Promote Mammary Carcinoma Cell Invasion. *PLoS One* **8**, e67533 (2013).

107. Pena, C. *et al.* STC1 Expression By Cancer-Associated Fibroblasts Drives Metastasis of Colorectal Cancer. *Cancer Res.* **73**, 1287–1297 (2013).

108. Fiaschi, T. *et al.* Carbonic anhydrase IX from cancer-associated fibroblasts drives epithelial-mesenchymal transition in prostate carcinoma cells. *Cell Cycle* **12**, 1791–1801 (2013).

109. Kalluri, R. & Weinberg, R. A. The basics of epithelial-mesenchymal transition. *J. Clin. Invest.* **119**, 1420–8 (2009).

110. Erez, N., Truitt, M., Olson, P. & Hanahan, D. Cancer-Associated Fibroblasts Are Activated in Incipient Neoplasia to Orchestrate Tumor-Promoting Inflammation in an NF-κB-Dependent Manner. *Cancer Cell* **17**, 135–147 (2010).

111. Mezawa, Y. & Orimo, A. The roles of tumor- and metastasis-promoting carcinoma-associated fibroblasts in human carcinomas. *Cell Tissue Res.* **365**, 675–689 (2016).

112. Quante, M. *et al.* Bone Marrow-Derived Myofibroblasts Contribute to the Mesenchymal Stem Cell Niche and Promote Tumor Growth. *Cancer Cell* **19**, 257–272 (2011).

113. Calon, A. *et al.* Dependency of Colorectal Cancer on a TGF-β-Driven Program in Stromal Cells for Metastasis Initiation. *Cancer Cell* **22**, 571–584 (2012).

114. Yauch, R. L. *et al.* A paracrine requirement for hedgehog signalling in cancer. *Nature* **455**, 406–410 (2008).

115. Gay, L. J. & Felding-Habermann, B. Contribution of platelets to tumour metastasis. *Nat. Rev. Cancer* **11**, 123–134 (2011).

116. Labelle, M., Begum, S. & Hynes, R. O. Direct signaling between platelets and cancer cells induces an epithelial-mesenchymal-like transition and promotes metastasis. *Cancer Cell* **20**, 576–90 (2011).

117. Barker, H. E., Paget, J. T. E., Khan, A. A. & Harrington, K. J. The tumour microenvironment after radiotherapy: mechanisms of resistance and recurrence. *Nat. Rev. Cancer* **15**, 409–425 (2015).

118. Barcellos-Hoff, M. H. The Potential Influence of Radiation-Induced Microenvironments in Neoplastic Progression. *J. Mammary Gland Biol. Neoplasia* **3**, 165–175 (1998).

119. Calvo, F. *et al.* Mechanotransduction and YAP-dependent matrix remodelling is required for the generation and maintenance of cancer-associated fibroblasts. *Nat. Cell Biol.* **15**, 637–46 (2013).

120. Giannoni, E., Bianchini, F., Calorini, L. & Chiarugi, P. Cancer Associated Fibroblasts Exploit Reactive Oxygen Species Through a Proinflammatory Signature Leading to Epithelial Mesenchymal Transition and Stemness. *Antioxid. Redox Signal.* **14**, 2361–2371 (2011).

121. Dent, P., Yacoub, A., Fisher, P. B., Hagan, M. P. & Grant, S. MAPK pathways in radiation responses. *Oncogene* **22**, 5885–5896 (2003).

122. McBride, W. H. *et al.* A Sense of Danger from Radiation [1]. *Radiat. Res.* **162**, 1–19 (2004).

123. Hellevik, T. *et al.* Changes in the Secretory Profile of NSCLC-Associated Fibroblasts after Ablative Radiotherapy: Potential Impact on Angiogenesis and Tumor Growth. *Transl. Oncol.* **6**, 66–74 (2013).

124. Milas, L. *et al.* Effect of radiation-induced injury of tumor bed stroma on metastatic spread of murine sarcomas and carcinomas. *Cancer Res.* **48**, 2116–20 (1988).

125. Rudolph-Owen, L. A., Chan, R., Muller, W. J. & Matrisian, L. M. The matrix metalloproteinase matrilysin influences early-stage mammary tumorigenesis. *Cancer Res.* **58**, 5500–6 (1998).

126. Isella, C. *et al.* Stromal contribution to the colorectal cancer transcriptome. *Nat. Genet.* **47**, 312–319 (2015).

127. Erez, N., Glanz, S., Raz, Y., Avivi, C. & Barshack, I. Cancer Associated Fibroblasts express pro-inflammatory factors in human breast and ovarian tumors. *Biochem. Biophys. Res. Commun.* **437**, 397–402 (2013).

128. Mace, T. A. *et al.* Pancreatic Cancer-Associated Stellate Cells Promote Differentiation of Myeloid-Derived Suppressor Cells in a STAT3-Dependent Manner. *Cancer Res.* **73**, 3007–3018 (2013).

129. Comito, G. *et al.* Cancer-associated fibroblasts and M2-polarized macrophages synergize during prostate carcinoma progression. *Oncogene* **33**, 2423–2431 (2014).

130. Sharma, P. & Allison, J. P. The future of immune checkpoint therapy. *Science* **348**, 56–61 (2015).

131. Demaria, S., Coleman, C. N. & Formenti, S. C. Radiotherapy: Changing the Game in Immunotherapy. *Trends in cancer* **2**, 286–294 (2016).

132. Fridman, W. H., Pagès, F., Sautès-Fridman, C. & Galon, J. The immune contexture in human tumours: impact on clinical outcome. *Nat. Rev. Cancer* **12**, 298–306 (2012).

133. Park, S.-J. *et al.* IL-6 regulates in vivo dendritic cell differentiation through STAT3 activation. *J. Immunol.* **173**, 3844–54 (2004).

134. Mesker, W. E. *et al.* Presence of a high amount of stroma and downregulation of SMAD4 predict for worse survival for stage I-II colon cancer patients. *Cell. Oncol.* **31**, 169–78 (2009).

135. Niranjan, K. C. & Sarathy, N. A. Prognostic impact of tumor-stroma ratio in oral squamous cell carcinoma

- A pilot study. *Ann. Diagn. Pathol.* **35**, 56–61 (2018).

136. Özdemir, B. C. *et al.* Depletion of Carcinoma-Associated Fibroblasts and Fibrosis Induces Immunosuppression and Accelerates Pancreas Cancer with Reduced Survival. *Cancer Cell* **28**, 831–833 (2015).

137. Rhim, A. D. *et al.* Stromal elements act to restrain, rather than support, pancreatic ductal adenocarcinoma. *Cancer Cell* **25**, 735–47 (2014).

138. Flaberg, E. *et al.* High-throughput live-cell imaging reveals differential inhibition of tumor cell proliferation by human fibroblasts. *Int. J. Cancer* **128**, 2793–2802 (2011).

139. Bhowmick, N. A. *et al.* TGF-beta signaling in fibroblasts modulates the oncogenic potential of adjacent epithelia. *Science* **303**, 848–51 (2004).

140. Stuelten, C. H. *et al.* Transient Tumor-Fibroblast Interactions Increase Tumor Cell Malignancy by a TGF-β Mediated Mechanism in a Mouse Xenograft Model of Breast Cancer. *PLoS One* **5**, e9832 (2010).

141. Annes, J. P., Munger, J. S. & Rifkin, D. B. Making sense of latent TGFβ activation. *J. Cell Sci.* **116**, 217–224 (2003).

142. Samowitz, W. S. *et al.* Beta-catenin mutations are more frequent in small colorectal adenomas than in larger adenomas and invasive carcinomas. *Cancer Res.* **59**, 1442–4 (1999).

143. Bissell, M. J. & Hines, W. C. Why don't we get more cancer? A proposed role of the microenvironment in restraining cancer progression. *Nat. Med.* **17**, 320–329 (2011).

144. Ochiai, A. & Neri, S. Phenotypic and functional heterogeneity of cancer-associated fibroblast within the tumor microenvironment. *Adv. Drug Deliv. Rev.* **99**, 186–196 (2016).

145. O'Connell, J. T. *et al.* VEGF-A and Tenascin-C produced by S100A4+ stromal cells are important for metastatic colonization. *Proc. Natl. Acad. Sci. U. S. A.* **108**, 16002–7 (2011).

146. DE WEVER, O. *et al.* Tenascin-C and SF/HGF produced by myofibroblasts in vitro provide convergent pro-invasive signals to human colon cancer cells through RhoA and Rac. *FASEB J.* **18**, 1016–1018 (2004).

147. Quail, D. F. & Joyce, J. A. Microenvironmental regulation of tumor progression and metastasis. *Nat. Med.* **19**, 1423–37 (2013).

148. Sotgia, F. *et al.* Caveolin-1-/- null mammary stromal fibroblasts share characteristics with human breast cancer-associated fibroblasts. *Am. J. Pathol.* **174**, 746–61 (2009).

149. Orr, B. *et al.* Identification of stromally expressed molecules in the prostate by tag-profiling of cancer-associated fibroblasts, normal fibroblasts and fetal prostate. *Oncogene* **31**, 1130–42 (2012).

150. Tchou, J. *et al.* Human breast cancer associated fibroblasts exhibit subtype specific gene expression profiles. *BMC Med. Genomics* **5**, 39 (2012).

151. Cortez, E., Roswall, P. & Pietras, K. Functional subsets of mesenchymal cell types in the tumor microenvironment. *Semin. Cancer Biol.* **25**, 3–9 (2014).

152. Lee, H.-O. *et al.* FAP-overexpressing fibroblasts produce an extracellular matrix that enhances invasive velocity and directionality of pancreatic cancer cells. *BMC Cancer* **11**, 245 (2011).

153. Öhlund, D. *et al.* Distinct populations of inflammatory fibroblasts and myofibroblasts in pancreatic cancer. *J. Exp. Med.* **214**, 579–596 (2017).

154. Lisanti, M. P., Martinez-Outschoorn, U. E. & Sotgia, F. Oncogenes induce the cancer-associated fibroblast phenotype: Metabolic symbiosis and "fibroblast addiction" are new therapeutic targets for drug discovery. *Cell Cycle* **12**, 2723–2732 (2013).

155. Fridlender, Z. G. *et al.* Polarization of tumor-associated neutrophil phenotype by TGF-beta: "N1" versus "N2" TAN. *Cancer Cell* **16**, 183–94 (2009).

156. Liao, D., Luo, Y., Markowitz, D., Xiang, R. & Reisfeld, R. A. Cancer associated fibroblasts promote tumor growth and metastasis by modulating the tumor immune microenvironment in a 4T1 murine breast cancer model. *PLoS One* **4**, e7965 (2009).

157. Marusyk, A., Almendro, V. & Polyak, K. Intra-tumour heterogeneity: a looking glass for cancer? *Nat. Rev. Cancer* **12**, 323–334 (2012).

158. Ronca, R., Van Ginderachter, J. A. & Turtoi, A. Paracrine interactions of cancer-associated fibroblasts, macrophages and endothelial cells: tumor allies and foes. (2017). doi:10.1097/CCO.0000000000000420

VII. APPENDIX

A. Supplementary figures

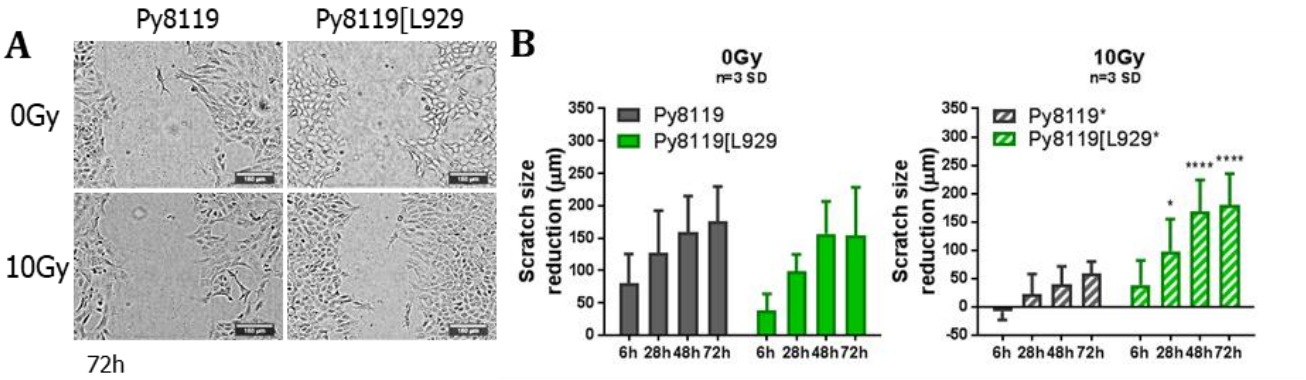

Supplementary figure VII.1: **Impact of fibroblasts on cancer cells' migration after radiation.** Py8119 cancer cells alone or together with L929 stromal fibroblasts were cultured 96h prior irradiation with or 10Gy (Transwell ratio 1/1). Wound healing scratch assay was performed 72h after IR (0Gy and 10Gy) on confluent Py8119 by drawing a line across the bottom of the dish **(A)**. Migrations were measured until 72h **(B)**. *p<0.5, and ****p<0.0001 were analyzed by two-way ANOVA test followed by Tukey's test.

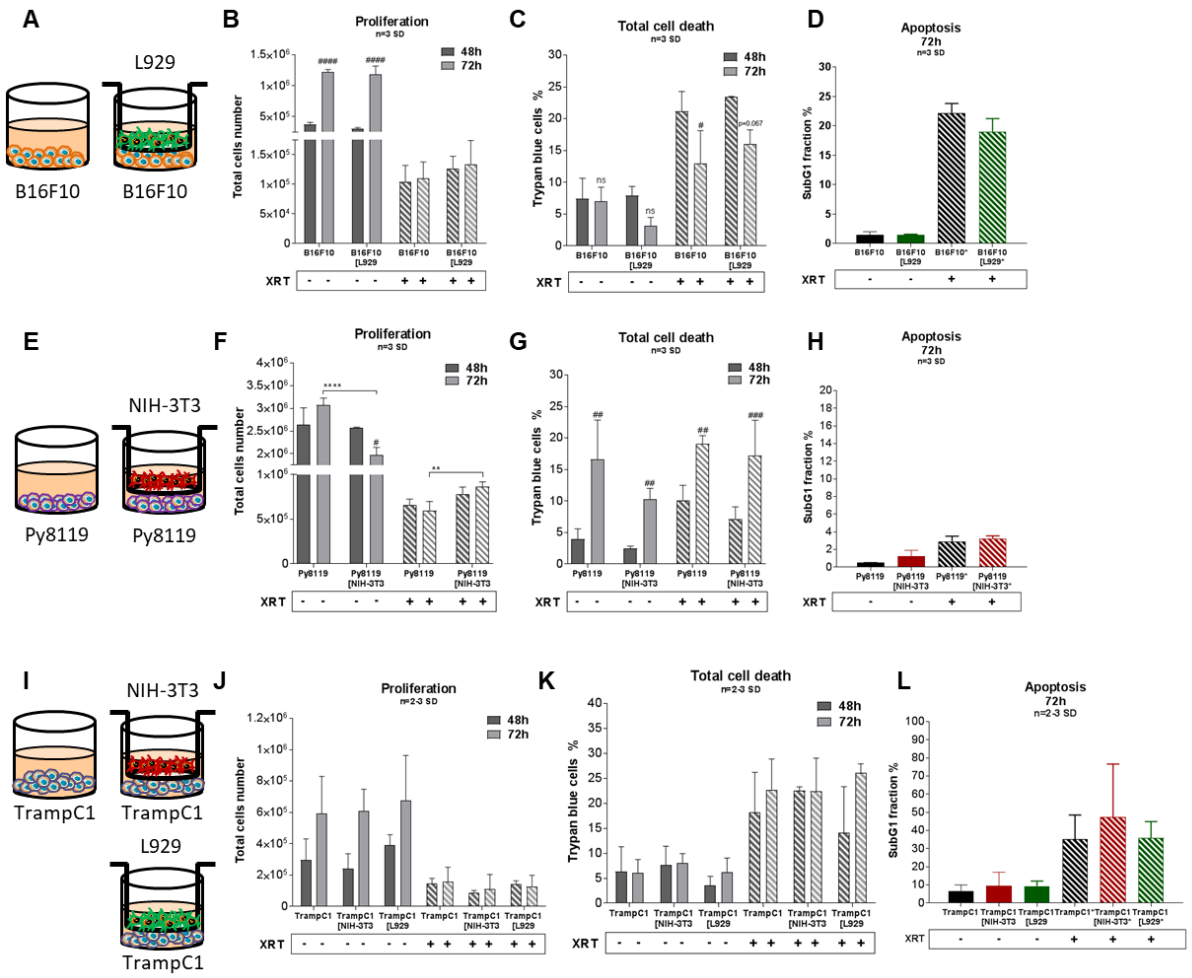

Supplementary figure VII.2: **Fibroblasts had no impact on cancer cells proliferation and death after radiation.** B16F10 melanoma **(A),** Py8119 breast **(E)** or TrampC1 prostate **(I)** cancer cells alone or together with stromal fibroblasts (in indirect co-culture) were cultured for 24h prior irradiation with 0 or 10Gy (ratio 1-1). After 48h and 72h, total cell numbers as well as dead cells were counted by trypan blue (**B-F-J, C-G-K)**. **p<0.01, ****p<0.0001 analyzed by two-way ANOVA test followed by Tukey's test, compared cancer cells with fibroblasts to cancer cells cultured alone. "ns" present for no significant, $^{\#}$p<0.5, $^{\#\#}$p<0.01, $^{\#\#\#}$p<0.001 and $^{\#\#\#\#}$p<0.0001 analyzed by two-way ANOVA test followed by Tukey's test, compared 72h to 48h. SubG1 fractions were measured by Nicoletti staining[85], 72h after irradiation **(D-H-L).** SubG1 data were analyzed by one-way ANOVA test followed by Tukey's test.

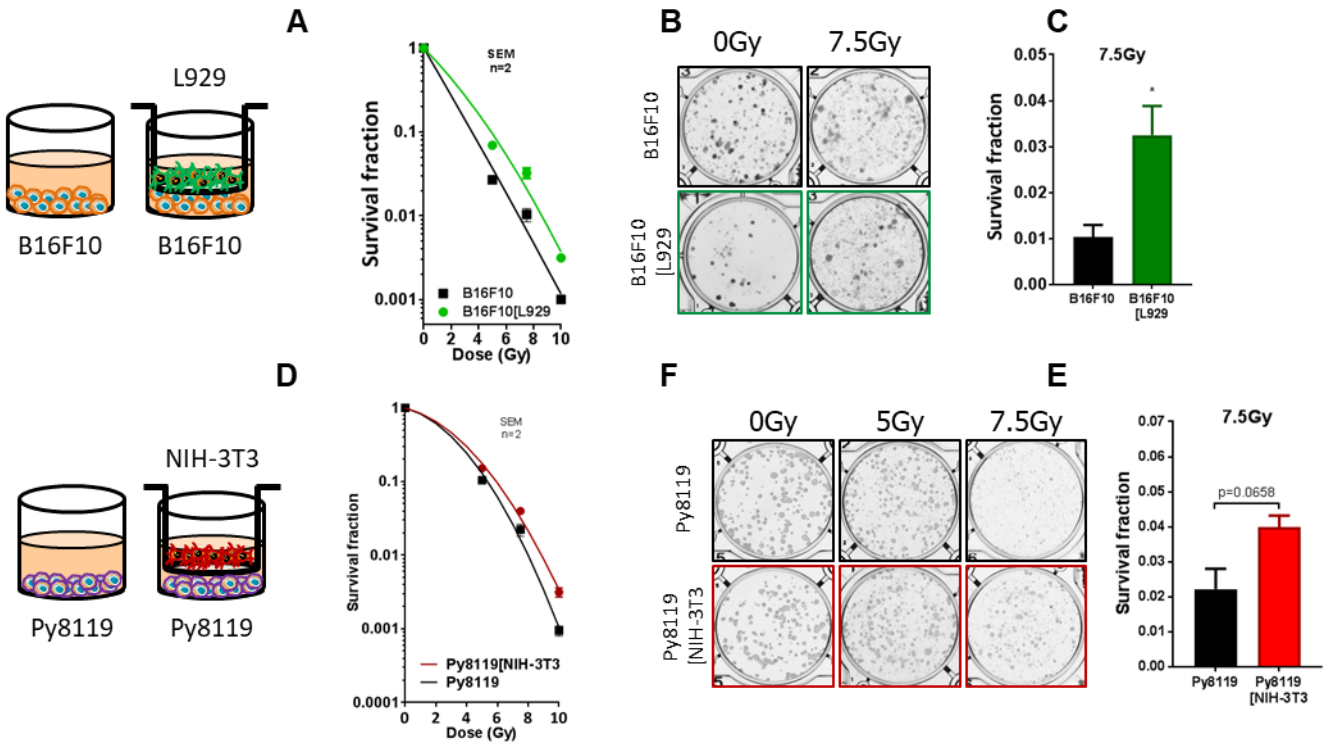

Supplementary figure VII.3: **L929 fibroblasts increased long-term survival of B16F10 cancer but NIH-3T3 had no influence on Py8119 clonogenic survival after XRT** B16F10 or Py8119, cancer cells alone or together with stromal fibroblasts were plated 24h prior irradiation with 0 or 10Gy (ratio 1-1) and subsequently further incubated for additional 7 days. Graphs depict the surviving fractions from two independent experiments measured in sextuplet each (means ± SEM) **(A-D, C-E)**. Plates were scanned, colonies were counted, and survival fraction was calculated **(B-F)**. *p<0.05 analyzed by one-way ANOVA test followed by Tukey's test.

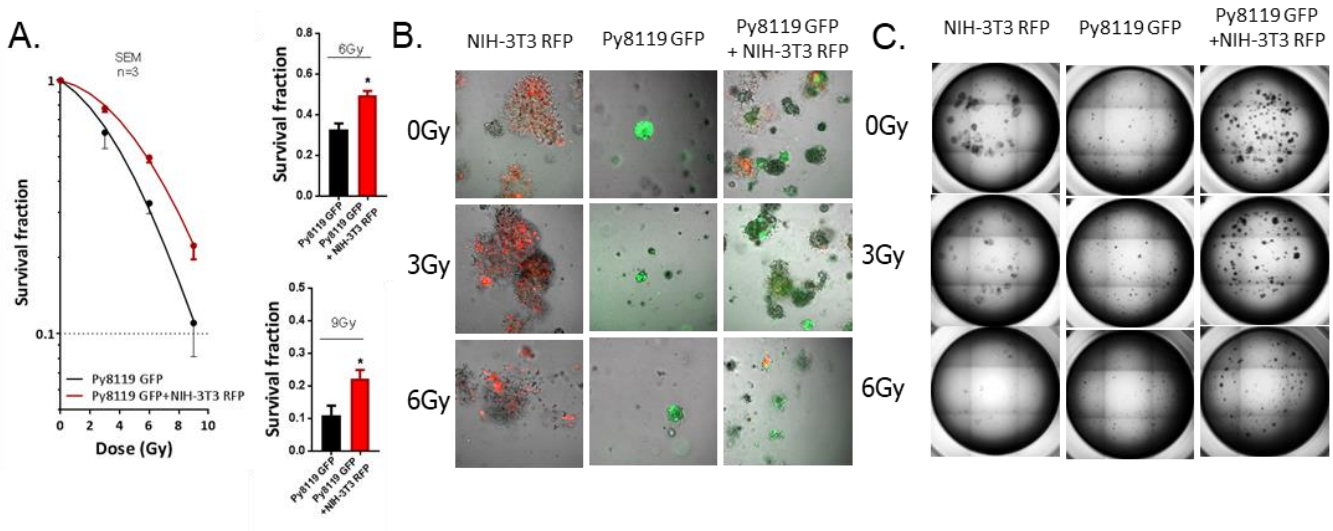

Supplementary figure VII.4: **Stromal fibroblasts NIH-3T3 increased long term survival after radiation of the Py8119 breast cancer cells in direct 3D culture.** Py8119 cancer cells were plated for colony formation assay alone or together with NIH-3T3 fibroblasts (ratio (1/1)) in a 3D Matrigel system, irradiated with indicated doses (0–9Gy) and subsequently further incubated for additional 7 days. Surviving fractions from three experiments measured in quintuplet each were shown (means ± SEM). **A-C** the colonies were counted, and the survival fraction calculated. **B-D** Picture of the well taken in bright light at 2.5 magnifications. **E-F** Representative pictures of the well taken by fluorescence microscopy at 10 magnifications. Fibroblasts were transiently transfected with RFP (red) and cancer cells with GFP (green). *p<0.5, by two-way ANOVA test followed by Tukey's test.

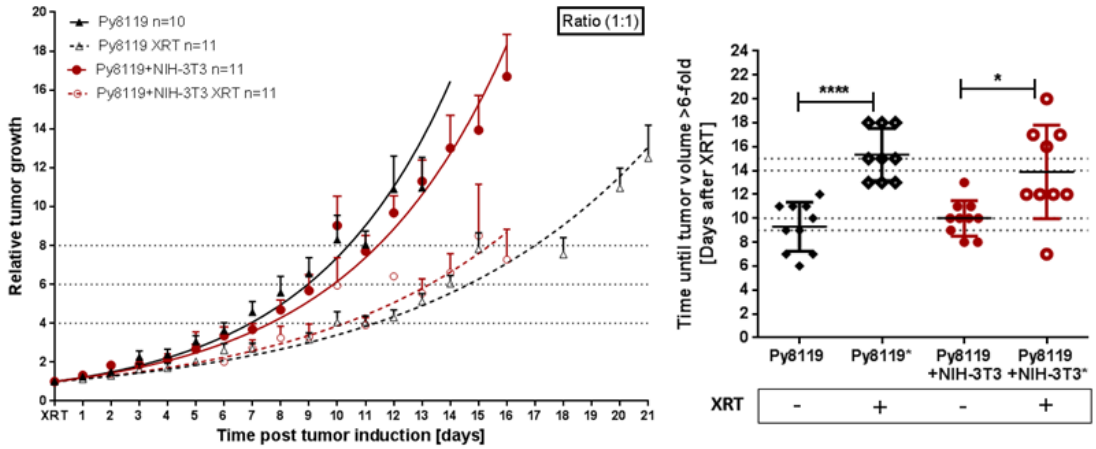

Supplementary figure VII.5: **Stromal NIH-3T3 fibroblasts did not affect tumor growth and radiation response of Py8119 xenograft tumors.** Py8119 breast cancer cells alone or together with NIH-3T3 fibroblasts (ratio of (1:1)) were subcutaneously co-implanted onto C57BL/6 mice When tumor's volumes of ~100 mm^3 were reached, one group received a single radiation dose of 10Gy to the tumor. The tumor volume was determined at indicated time points (left diagram). Data were represented as mean ± SEM from 2-3 independent experiments. Tumor growth and respective tumor growth delay were determined as time (days) until the 6-fold volume was reached (right diagram). ***p<0.001, ****p<0.0001 by one-way ANOVA followed by Tukey's test.

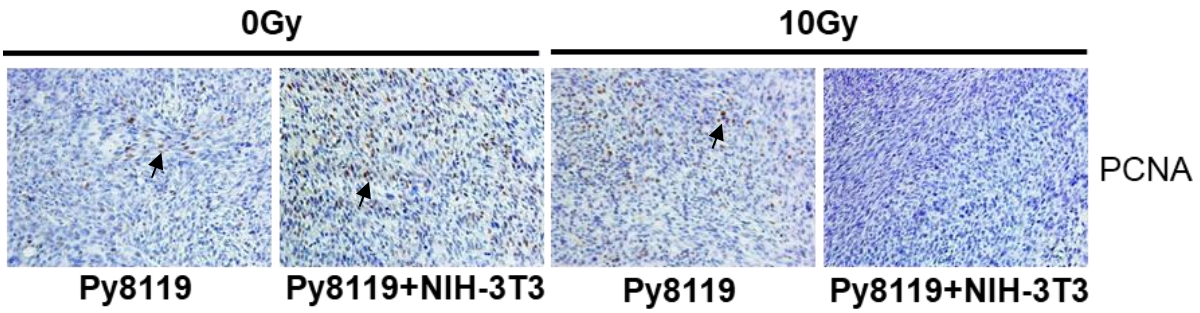

Supplementary figure VII.6: **Stromal NIH-3T3 fibroblasts did not influence the proliferation of Py8119 xenograft tumors.** Py8119 breast cancer cells alone or together with NIH-3T3 fibroblasts (ratio of (1:1)) were subcutaneously co-implanted onto C57BL/6 mice. When tumor volumes reached a critical size (5–21 days after tumor irradiation) tumors were isolated and subjected for IHC. Sections were stained for PCNA. Representatives' pictures were shown from 2-3 experiments (5 mice in total).

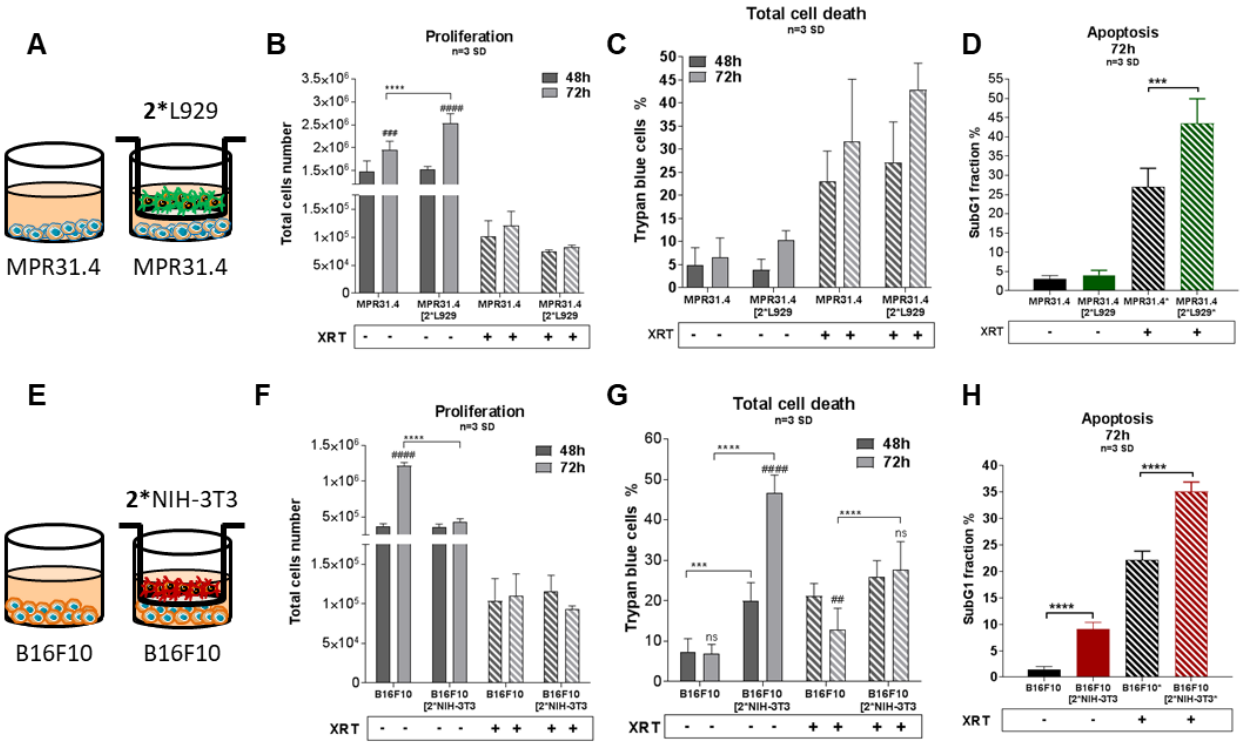

Supplementary figure VII.7: **Increasing fibroblasts numbers did not affect the cancer cells radiation response promoted by stromal fibroblasts in short-term study.** MPR31.4 or B16F10 cancer cells were cultured alone or together with stromal fibroblasts (in indirect co-culture) for 24h prior irradiation with 0 or 10Gy (ratio 1-2, **A-E**). After 48h and 72h, total cell numbers as well as dead cells were counted by trypan blue (**B-F, C-G)**. ***p<0.001, and ****p<0.0001, analyzed by two-way ANOVA test followed by Tukey's test, compared cancer cells with fibroblasts to cancer cells cultured alone. $^{\#\#}$p<0.01, $^{\#\#\#}$p<0.0001 and $^{\#\#\#\#}$p<0.0001 analyzed by two-way ANOVA test followed by Tukey's test, compared 72h to 48h. SubG1 fractions were measured by Nicoletti staining[85], 72h after irradiation **(D-H).** ***p<0.001 and ****p<0.0001 were analyzed by one-way ANOVA test followed by Tukey's test.

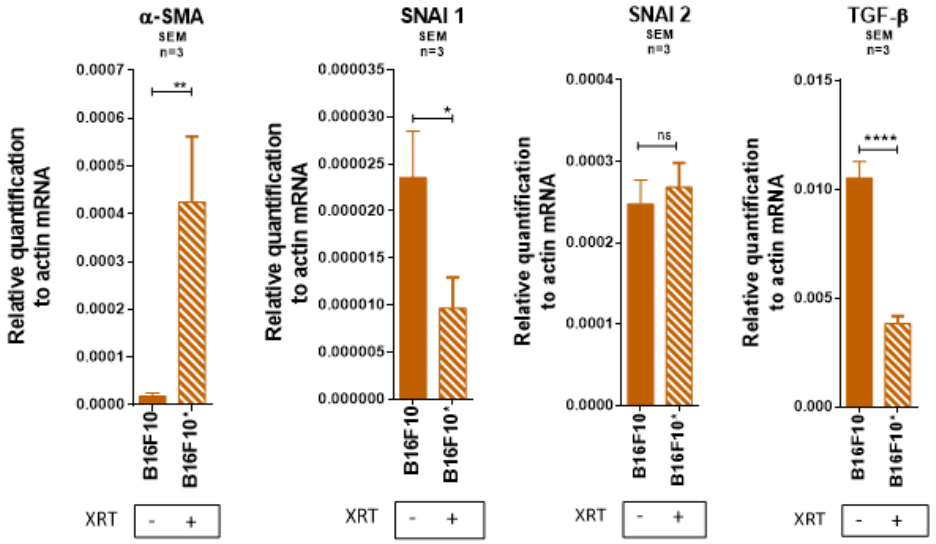

Supplementary figure VII.8: **Radiation itself is not sufficient to induce cancer cells' epithelial-mesenchymal transition (EMT).** B16F10 cancer cells, were cultured alone for 24h prior irradiation with 0 or 10Gy (ratio 1-1). After 72h, qRT-PCR analysis of the reactive EMT markers α-SMA, Snai1, Snai2 and TGF-β were performed in total RNA isolates of cultured cancer cells. Respective expression levels were normalized to β-actin (set at 1). Shown are mean values ± SEM from 3 independent samples per group measured each in triplicate each. "ns" present for no significant, *p<0.5, **p<0.01, *** p<0.001 and ****p<0.0001 analyzed by one-way ANOVA test followed by Tukey's test.

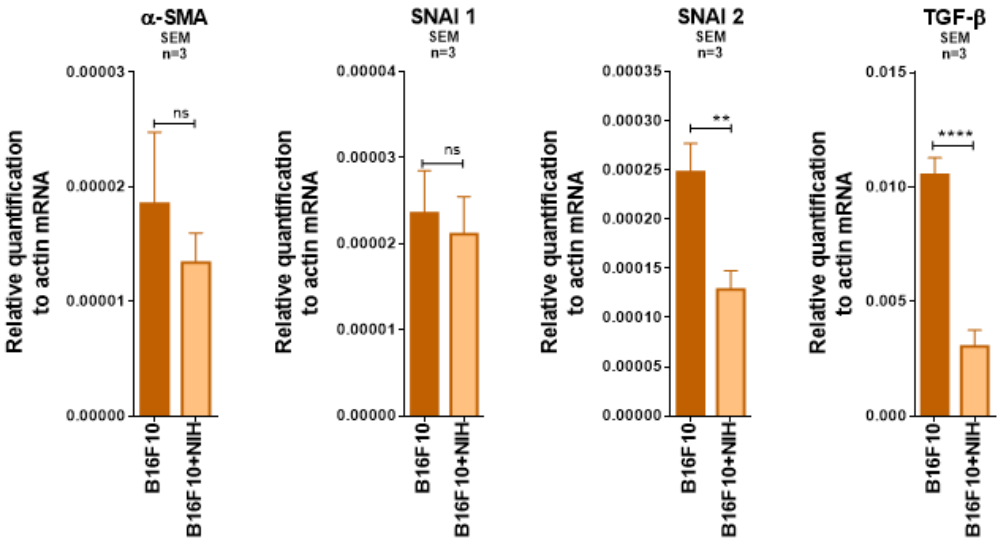

Supplementary figure VII.9: **NIH-3T3 fibroblast did not induce B16F10 EMT.** B16F10 cancer cells, were cultured alone or together with NIH-3T3 (ratio 1-1). After 96h, qRT-PCR analysis of the reactive EMT markers α-SMA, Snai1, Snai2 and TGF-β were performed in total RNA isolates of cultured cancer cells. Respective expression levels were normalized to β-actin (set at 1). Shown are mean values ± SEM from 3 independent samples per group measured each in triplicate each. “ns” present for no significant, *p<0.5, **p<0.01, *** p<0.001 and ****p<0.0001 analyzed by one-way ANOVA test followed by Tukey’s test.

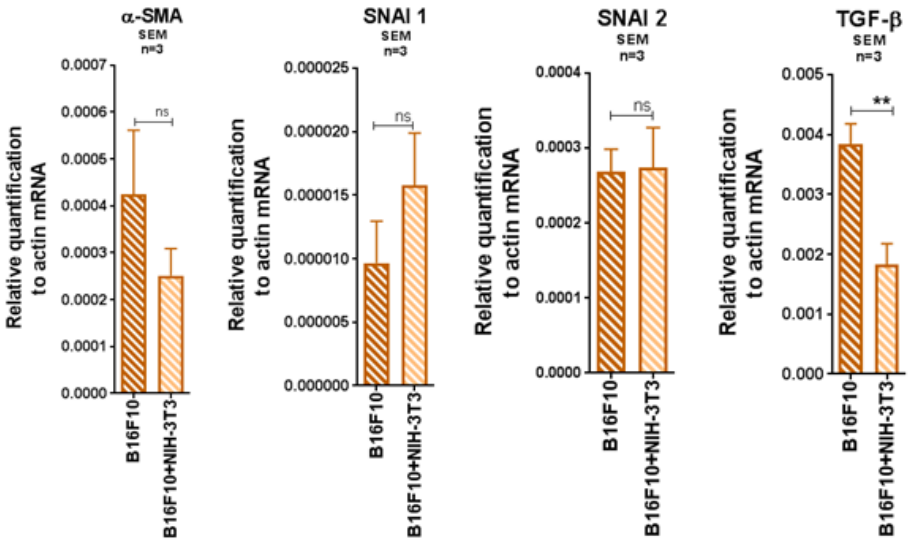

Supplementary figure VII.10: **NIH-3T3 fibroblast did not induce B16F10 EMT after XR.** B16F10 cancer cells, were cultured alone or together with NIH-3T3 for 24h prior irradiation with 0 or 10Gy (ratio 1-1). After 72h, qRT-PCR analysis of the reactive EMT markers α-SMA, Snai1, Snai2 and TGF-β were performed in total RNA isolates of cultured cancer cells. Respective expression levels were normalized to β-actin (set at 1). Shown are mean values ± SEM from 3 independent samples per group measured each in triplicate each. “ns” present for no significant, *p<0.5, **p<0.01, *** p<0.001 and ****p<0.0001 analyzed by one-way ANOVA test followed by Tukey’s test.

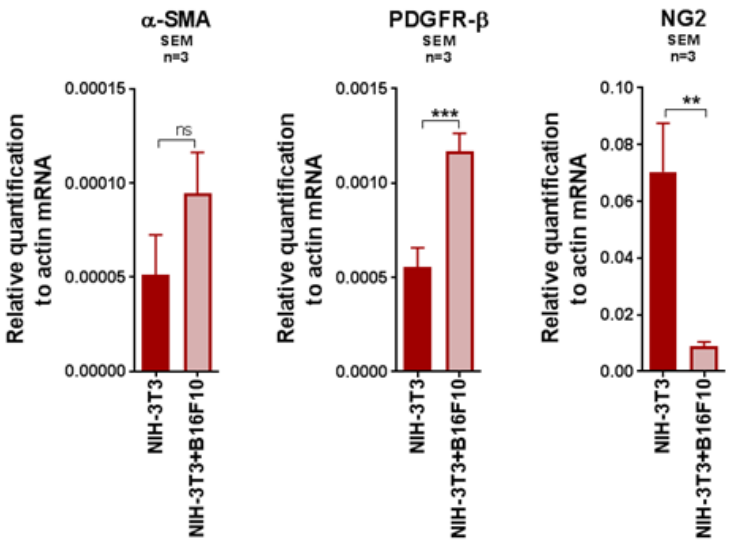

Supplementary figure VII.11: **B16F10 did not induce NIH-3T3 fibroblast activation into CAFs-like phenotype.** NIH-3T3 fibroblasts, were cultured alone or together with B16F10 cancer cells (ratio 1-1). After 96h, qRT-PCR analysis of the reactive EMT markers α-SMA, NG2, and PDGFR-β were performed in total RNA isolates of cultured fibroblasts. Respective expression levels were normalized to β-actin (set at 1). Shown are mean values ± SEM from 3 independent samples per group measured each in triplicate each. “ns” present for no significant, *p<0.5, **p<0.01, *** p<0.001 and ****p<0.0001 analyzed by one-way ANOVA test followed by Tukey’s test

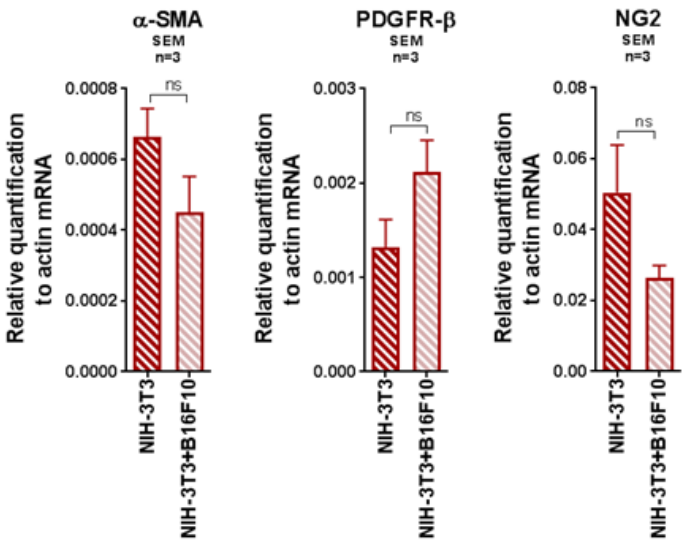

Supplementary figure VII.12: **B16F10 did not induce NIH-3T3 fibroblast activation into CAFs-like phenotype after IR.** NIH-3T3 fibroblasts, were cultured alone or together with B16F10 cancer cells for 24h prior irradiation with 0 or 10Gy (ratio 1-1). After 72h, qRT-PCR analysis of the reactive EMT markers α-SMA, NG2, and PDGFR-β were performed in total RNA isolates of cultured fibroblasts. Respective expression levels were normalized to β-actin (set at 1). Shown are mean values ± SEM from 3 independent samples per group measured each in triplicate each. “ns” present for no significant, *p<0.5, **p<0.01, *** p<0.001 and ****p<0.0001 analyzed by one-way ANOVA test followed by Tukey’s test

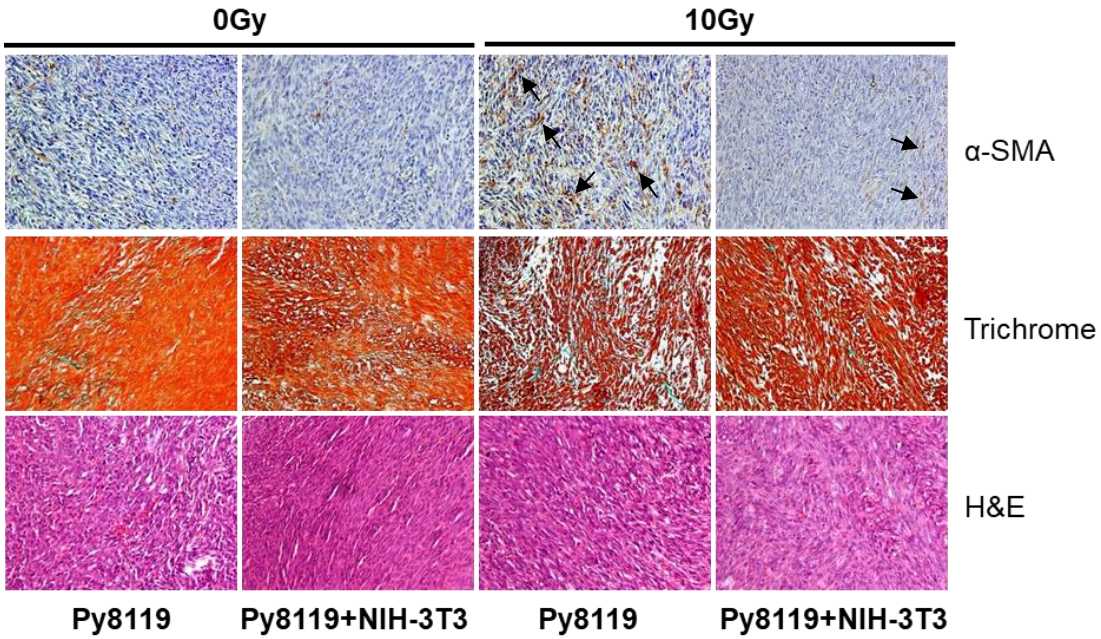

Supplementary figure VII.13: **NIH-3T3 stromal fibroblasts decreased α-SMA expression, the main CAFs marker, in the Py8119 breast tumor after irradiation.** Py8119 prostate cancer cells alone or together with NIH-3T3 fibroblasts (ratio of (1:1)) were subcutaneously co-implanted in C57BL/6 mice's right leg. When tumor volumes reached a critical size (5–21 days after tumor irradiation) tumors were isolated and subjected for α-SMA IHC, Masson Goldner trichrome and Hematoxylin and Eosin (HE) staining. Representatives' pictures were shown from 2-3 experiments (5 mice).

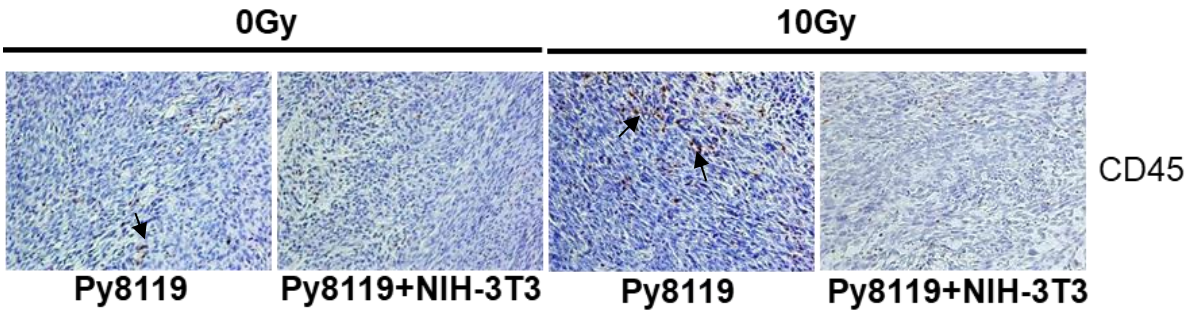

Supplementary figure VII.14: **NIH-3T3 stromal fibroblasts did not influence Py8119 breast tumor immune infiltration.** Py8119 breast cancer cells alone or together with NIH-3T3 fibroblasts (ratio of (1:1)) were subcutaneously co-implanted on C57BL/6 mice. When tumor volumes reached a critical size (5–21 days after tumor irradiation) tumors were isolated and subjected for IHC. Sections were stained CD45. Representatives' pictures were shown from 2-3 experiments (5 mice total).

B. Abbreviations

%	Percent
% v/v	Percent volume
% w/v	Percent weight per volume
°C	Degrees celsius
µl	Microliter
µm	Micrometer
2D	Two dimensions
3D	Three dimensions
ANOVA	Analysis of variance
CAF	Cancer-associated fibroblast
Cav1	Caveolin-1
CD	Cluster of differentiation
cDNA	Complementary deoxyribonucleic acid
ECM	Extracellular matrix
EDTA	Ethylenediaminetetraacetic acid
EMT	Epithelial mesenchymal transition
EndoMT	Endothelial mesenchymal transition
FACS	Fluorescence activated cell sorting
FAP	Fibroblast activated protein
FGF	Fibroblast growth factor
FSP-1	Fibroblast specific protein-1
GFP	Green fluorescent protein
Gy	Gray
h	Hour
HGF	Hepatocyte growth factor
IGF	Insulin-like growth factor
IHC	Immunohistochemistry
IL	Interleukin
IR	Ionizing radiation
kDa	Kilodalton
kV	Kilovolt

mA	Millimeter
min	Minute
MPR	Mouse prostate reconstitution
NG2	Neuron glial antigen-2
PBS	Phosphate buffered saline
PCNA	Proliferating cell nuclear antigen
PDGFR-β	Platelet-derived growth factor receptor beta
PFA	Paraformaldehyde
PGE	Prostaglandin
PI	Propidium iodide
qRT-PCR	Quantitative Real Time polymerase chain reaction
RADIATE	Radiation innovations for therapy and education
RFP	Red fluorescent protein
RNA	Ribonucleic acid
RT	Radiotherapy
SDF-1	Stromal cell-derived factor 1
SNAI	Zinc finger protein
TGF-β	Transforming growth factor beta
TN-C	Tenascin-C
TNF-α	Tumor necrosis factor alpha
α-SMA	Alpha-smooth muscle actin

C. Figures index

D. Tables index

E. Acknowledgement

First, I would like to thank Prof. Dr. Verena Jendrossek, who gave me the opportunity to work on such an exciting project. Thank you for letting me be independent in my research. Thank you for your outstanding support and your understanding. These 3 years allowed me to develop my personal and scientific strengths.

Thanks to Prof. Dr. med. Jens Siveke who kindly accepted to be the second reviewer of this thesis.

A special thanks goes to PD Dr. Diana Klein for her supervision and support during hard times. Thank you for your help and patience during the writing process.

Furthermore, I want to thank Prof. Dr. med Nils Cordes who hosted me for 2 months in his institute, Oncoray at Dresden. There, I got the chance to learn three-dimensional cell culture model. I want to thank Prof. Dr. George Iliakis and Prof. Dr. med Martin Stuschke as well for the permission to carry out irradiation experiments in their institutes.

I am also grateful for Dr. Johann Matschke who came to irradiate the mice with me when no one else was available. Special thanks to Mohamed Benchellal for his help and guidance with the *in vivo* experiments and for his kindness and moral support.

I would like to give a deep and special acknowledgement to Dr. Nagma Khan and the RADIATE-ITN for these wonderful meetings and discussions. Every time, I came back full of energy, motivation and a reminder of why I love research. Being part of this European consortium was the best.

I am also grateful for my RADIATE partner and friend, Adam Krysztofiak, who supported me during these 3.5 years. Being next to me all the time may not have been easy. Thank you for the funny and nice time spent together.

Thank you also to Klaudia Szymonowicz for crazy, enjoyable and funny times spent together.

Big thanks to all members of AG1 for the nice atmosphere. Thanks to the GRK1739 training group and all its members.

Finally, I want to thank my family for being at my side whatever happens, even so far away. At last, I feel lucky to have a special person in my life. You kept me sane and gave me smile all along. Without you nothing would have been possible.

F. Curriculum Vitae

Aus datenschutzrechtlichen Gründen ist der Lebenslauf in der Online-Version nicht enthalten

G. Declarations

Erklärung:

Hiermit erkläre ich, gem. § 6 Abs. (2) g) der Promotionsordnung der Fakultät für Biologie zur Erlangung der Dr. rer. nat., dass ich das Arbeitsgebiet, dem das Thema „**Role of the cancer-associated fibroblasts on the radiation response of solid tumors**" zuzuordnen ist, in Forschung und Lehre vertrete und den Antrag von **Alizée Steer** befürworte und die Betreuung auch im Falle eines Weggangs, wenn nicht wichtige Gründe dem entgegenstehen, weiterführen werde.

Essen, den _____ _____

Unterschrift des Betreuers (Prof. oder PD) an der Universität Duisburg-Essen

Erklärung:

Hiermit erkläre ich, gem. § 7 Abs. (2) d) + f) der Promotionsordnung der Fakultät für Biologie zur Erlangung des Dr. rer. nat., dass ich die vorliegende Dissertation selbständig verfasst und mich keiner anderen als der angegebenen Hilfsmittel bedient, bei der Abfassung der Dissertation nur die angegeben Hilfsmittel benutzt und alle wörtlich oder inhaltlich übernommenen Stellen als solche gekennzeichnet habe.

Essen, den _____ _____

Unterschrift des/r Doktoranden/in

Erklärung:

Hiermit erkläre ich, gem. § 7 Abs. (2) e) + g) der Promotionsordnung der Fakultät für Biologie zur Erlangung des Dr. rer. nat., dass ich keine anderen Promotionen bzw. Promotionsversuche in der Vergangenheit durchgeführt habe und dass diese Arbeit von keiner anderen Fakultät/Fachbereich abgelehnt worden ist.

Essen, den _____ _____

Unterschrift des/r Doktoranden/in